Università degli Studi di Milano
Scuola di Dottorato in Medicina Molecolare

Curriculum di Genomica, Proteomica e Tecniche Correlate

Ciclo XXV

Anno Accademico 2011-2012

Dottorando: Simona MRAKIC-SPOSTA

Matricola: R08674

Reactive Oxygen Species, Oxidative Damage, and Antioxidant Defense Mechanisms: in humans and in vitro Electron Paramagnetic Resonance spin-trapping studies

Direttore della Scuola: Ch.mo Prof. Mario Clerici

Tutore: Prof. Maristella Gussoni

Correlatore: Dott.ssa Alessandra Vezzoli

SOMMARIO

Scopo della ricerca sviluppata durante questi tre anni di Dottorato è quello di spiegare i meccanismi sottesi alla risposta allo stress ossidativo nell'uomo a livello integrativo e molecolare.
Per questo fine, nel primo anno di Dottorato, si è innanzi tutto implementato un metodo quantitativo assoluto atto a valutare la produzione dei radicali liberi.
Come è noto ciò che importa è l'equilibrio tra produzione di Specie Reattive dell'Ossigeno (ROS) e la disponibilità di difese antiossidanti. Quando questo equilibrio viene meno, si parla di Stress Ossidativo, con conseguenze a carico degli acidi nucleici, dei lipidi e delle proteine, compromettendo il metabolismo e la vitalità cellulare, fino a indurre apoptosi o necrosi. Questo è un fenomeno ricorrente in molte malattie acute e croniche oltre che nel fisiologico processo di invecchiamento.
Allo scopo si è utilizzata la tecnica di Risonanza Paramagnetica Elettronica (EPR) accoppiata a specifiche sonde molecolari (spin trapping) per sviluppare un metodo quantitativo "in vivo" in grado di monitorare la produzione di ROS in campioni biologici quale il sangue e sue frazioni.
Gli inizi del mio periodo di Dottorato sono fortunatamente coincisi con l'acquisizione da parte dell'Istituto di Bioimmagini e Fisiologia Molecolare (IBFM) del CNR (Lita di Segrate), di uno strumento EPR che risponde alle esigenze di maneggevolezza e portabilità (e-scan Bruker BioSpin, Germania), di recente immissione sul mercato, che opera in onda continua (CW), nella banda X delle μW, in grado di rilevare concentrazioni molto basse (nM) in piccoli campioni (50 μl), utilizzando una cavità risonante le cui proprietà ottimizzano il fattore di riempimento, conferendo un'elevata sensibilità allo strumento.
L'attendibilità dell'efficacia del metodo sviluppato è stata verificata con correlazioni tra metodi classici enzimatici e misure EPR in vari stati: fisiologici e parafisiologici.
Trattandosi della messa a punto di un metodo di misura completamente innovativo e mancando pertanto dati di letteratura cui fare riferimento, si sono rese necessarie molte prove sperimentali da campioni ematici, in un vasto gruppo di soggetti, con tantissime acquisizioni modificando e ottimizzando di volta in volta i parametri e le condizioni (T, pO_2) Questo procedimento è stato lento e laborioso; una volta superate le difficoltà tecniche, si è avuto a disposizione un piccolo catalogo di misurazioni che è servito ad ottenere i primi dati sperimentali che saranno illustrati nei primi paragrafi di questa tesi.
Si è inoltre cercata una correlazione statistica tra la produzione di ROS determinata con tecnica EPR ed i marcatori dello stress ossidativo ottenuti dai vari test convenzionali enzimatici riportati in letteratura quali il dosaggio da sostanze reattive all'acido tiobarbiturico (TBARS) e carbonili proteici (PC) in grado di quantizzare il danno "a posteriori" prodotto dai ROS su lipidi e proteine rispettivamente. Una correlazione sistematica tra i dati EPR e i dati enzimatici non era certa, in quanto questi ultimi rivelano un danno conclamato. Tuttavia, è stata trovata una significativa correlazione (ANOVA, $p<0.05$) in soggetti a riposo, tra la produzione di ROS/TBARS e PC (rispettivamente: $r^2=0.74$ e $r^2=0.60$).

Per rispondere allo scopo della ricerca, abbiamo assunto come modello l'ipossia studiata 1) come situazione che induce uno sbilanciamento tra Stress Ossidativo e capacità antiossidante e 2) nel tentativo di identificare i possibili meccanismi di

ripristino dell'equilibrio.
Dall'insieme dei dati raccolti, al di là dei risultati specifici, possiamo evincere che anche se la misura quantitativa assoluta della produzione di ROS (umol . mim^{-1}) non può essere un parametro generalizzato, perché funzione di variabili fisico-chimiche (pO_2, Temperatura, concentrazione della sonda), acquisizione ed elaborazione dei parametri vanno comunque prese in considerazione. Dal calcolo dei limiti di detenzione (LOD): 30 · 10^{-3} mM, e quantificazione (LOQ): 100 · 10^{-3} mM, lo strumento si è rilevato sensibile e affidabile.
Allo stesso tempo, va tenuto presente che il dato ottenuto rappresenta la produzione di ROS non tamponati dal sistema antiossidante. Per questo, si è ritenuto che la misura su campione ematico fosse rappresentativa della risposta sistemica integrativa. In particolare, il sangue capillare, oltre alla sua elevata sensibilità e riproducibilità (0,5% di differenza tra misure ripetute), ci ha permesso di disegnare un protocollo agile mini-invasivo. Da quanto fin qui esposto, possiamo ricavare che, al di là della ricerca di un dato assoluto da riportare in letteratura, è una valida procedura che ogni soggetto, monitorato nel tempo risulti controllo di se stesso, ovvero che a indice della risposta equilibrio/squilibrio vengano quantizzate le variazioni.
Nel tentativo di identificare i possibili meccanismi di ripristino dell'equilibrio dello stress ossidativo, gli esperimenti sono stati condotti su: A) soggetti sani, che come tali sono caratterizzati da una condizione di equilibrio tra ROS e difese antiossidanti, B) soggetti affetti da patologie neurodegenerative, per i quali era logico attendersi, come confermato dalla realtà, che fossero caratterizzati da una condizione di conclamato squilibrio, rivelabile da un significativo incremento di ROS prodotti in condizioni di riposo.
In soggetti sani, si sono disegnati, messi a punto e applicati differenti protocolli sperimentali, per testare l'effetto: a) dell'esercizio fisico (stato ipossico transitorio) di breve (hockeisti e nuotatori) e lunga durata (atleti di triathlon); b) dell'allenamento (nuotatori); c) dell'ipossia normobarica e ipobarica acuta e prolungata (giovani soggetti sedentari); d) dell'assunzione di molecole antiossidanti sulla produzione di ROS.
In patologie neurodegenerative (pazienti affetti da: Neuropatia Diabetica (tipo II DN), decadimento cognitivo lieve (MCI) e Sclerosi Laterale Amiotrofica sporadica (sSLA)) dopo aver rilevato uno squilibrio in condizioni basali, è stato studiato l'effetto dell'esercizio/allenamento (SLA) o dell'assunzione di antiossidanti (tipo II DN) sulla possibilità di un potenziale ripristino a valori di equilibrio. Importanti risultati sono emersi dall'analisi dei dati registrati nelle varie condizioni sperimentali e sono illustrati in questa tesi. Il tema comune di tutti i test, oltre all'evidente studio sulla produzione dei ROS, è stato quello dell'ipossia.

Infatti l'Ipossia, nelle sue varie espressioni (intese come deficienze parziali o totali di O_2 nel nostro organismo), è stato elemento caratterizzante in tutti i protocolli che abbiamo testato.
I protocolli di studio su pazienti sono tuttora in corso; pertanto i dati illustrati devono intendersi come preliminari. Nei soggetti patologici si è costatata una differente produzione di ROS in condizioni di riposo, mostrando un valore significativamente ($p<0,05$) più alto nei pazienti affetti da SLA (+20%) rispetto ai soggetti sani. L'allenamento, in questi pazienti, sembra giocare un ruolo favorevole nel diminuire la produzione di ROS: un decremento del 7% è stato calcolato nei

valori a riposo pre e post allenamento. Un sicuro effetto positivo dell'allenamento controllato, dopo otto settimane, è stato osservato nei nuotatori (-25%) sulla produzione di ROS (2.24 ± 0.14 µmol · min^{-1}).

Tutti questi esperimenti sono stati condotti e i risultati ottenuti durante il secondo e terzo anno della mia Scuola di Dottorato. A parte gli specifici risultati ottenuti dal set di dati raccolti, osservazioni generali possono essere riassunte come segue:

1) Non vi è alcun modo per ottenere dati per quantificare il volume totale di ROS prodotta da un soggetto in qualsiasi condizione. Il dato EPR ricavato dalle misurazioni rappresenta l'eccesso di ROS che il sistema ha prodotto (µmol · min^{-1}) in una determinata condizione, ed è quindi un tasso di produzione di ROS Inoltre si è scelto di effettuare la misura da sangue invece che da campioni di tessuto in modo da ottenere dati il più possibile sistematici. In particolare, il sangue capillare (rispetto al sangue venoso o plasma) ha dato la possibilità di sviluppare un metodo di misurazione affidabile, relativamente semplice e mini-invasivo. Tuttavia quando si passa da misurazioni di sangue capillare a venoso, bisogna prendere in considerazione la differente pO_2. (la produzione di ROS in sangue venoso è stata trovata circa il 18% inferiore a quella nel sangue capillare: 1.79 ± 0.12 vs 1.48 ± 0.29 µmol·min^{-1} rispettivamente).

2) I dati non possono essere presi come parametri generali, poiché dipendono strettamente da variabili fisico-chimiche (T, pO_2) Da tutti questi punti, si può evincere che, al di là della ricerca di un dato assoluto da riportare in letteratura, è una valida procedura che ogni soggetto, monitorato nel tempo risulti controllo di se stesso, ovvero che a indice della risposta equilibrio/squilibrio vengano quantizzate le variazioni.

3) Tuttavia si è consapevoli che il dato fornito da EPR deve essere integrato con dati sistemici quali: analisi ematochimiche di laboratorio (ematocrito, ferro, colesterolo, piastrine, neutrofili, linfociti, monociti), saturazione dell'ossigeno, cinetica degli scambi gassosi (VO_2max).

Si ritiene che il metodo possa trovare applicazione i) medicina dello sport offrendo un valido aiuto nei centri sportivi per monitorare l'efficacia dell'allenamento e gli eventuali effetti dello stress provocato ed eventualmente migliorare i protocolli; ii) alla medicina di montagna per lo studio delle patologie da alta quota, poiché l'ipossia è il primo e più delicato problema dell'altitudine sin dalla quota media (1800m); iii) ai centri clinici/diagnostici per monitorare gli effetti delle terapie/trattamenti sulla progressione di patologia.

Seconda parte della mia attività di ricerca, è stato lo studio in vitro dell'ipossia da un punto di vista molecolare mediante misurazioni spettroscopiche EPR. Partendo da una visione molecolare, l'ipossia orchestra una moltitudine di processi e di pathway molecolari. Nel tradizionale meccanismo dell'ipossia si ha la presenza di una proteina eme in grado di rilevare il legame reversibile di O_2 il quale causa un cambiamento allosterico nell'emo-proteina: da inattivo (forma ossigenata) ad attivo (forma de-ossigenata). Quindi l'attività di una proteina emo è determinata dalla presenza o assenza dell'ossigeno legato.

Nella presente ricerca, la rilevanza di stati ipossici, dal punto di vista molecolare, atti ad essere rilevati sia in condizioni fisiologiche che patologiche è stato attribuito all'Ossido Nitrico (NO) e al ruolo della Mioglobina (Mb). E' noto, infatti, che l'NO è un radicale libero particolarmente espresso in condizioni ipossiche in quanto è in grado di regolare la vasodilatazione, quindi aumenta l'afflusso di sangue e al

tempo stesso può essere però dannoso andando ad inibire la catena respiratoria a livello del complesso IV.
In letteratura sono riportate cinque isoforme di Mb umana (Mb I-V) presenti nel muscolo scheletrico in percentuali diverse (Mb I: 75%; Mb II: 20%; Mb III-V: 5%) le cui funzioni non sono ancora state chiarite. Prendendo a riferimento Mb II, queste proteine differiscono solo per un singolo residuo aminoacidico: E54K (Mb I), K133N(Mb III), R139Q (Mb IV) a R139W (Mb V).
Inoltre popolazioni tibetane, native dell'alta quota, presentano come risposta all'ipossia alte capacità antiossidanti, alto flusso ematico sistemico, metabolismo ed efficienza meccanica migliore, alti livelli di metaboliti circolanti biologicamente attivi all'NO e sono caratterizzate da un significativo aumento della concentrazione di Mb a livello muscolare con particolare riferimento all' isoforma 54E (Mb II).
Il presente studio, grazie all'analisi combinata EPR e simulazioni di Dinamica Molecolare (MD), contribuisce ulteriormente a sottolineare il ruolo importante svolto dalla Mb in condizioni di ipossia; inoltre segna un primo passo verso l'identificazione dei diversi ruoli svolti dalle isoforme della Mb
Importanti risultati funzionali si sono ottenuti dallo studio EPR: l'NO ha capacità di legame significativamente maggiore con l'isoforma 54E rispetto all'isoforma 54K; questa è più circoscritta alla struttura dello stato de-ossigenato e la capacità di legame diventa significativamente inferiore ($p<0.01$) e quasi identica per le due proteine in presenza di O_2 anche a differenti livelli di pO_2 (40 e 100 mmHg).
Concludendo, osservazioni e prospettive future possono essere condensate nella convinzione, che confidiamo saranno condivise e verificate anche dal lettore, della validità del nuovo del metodo sviluppato e dei dati raccolti.
Alcuni risultati, in particolar modo quelli concernenti gli stati patologici, sono da considerarsi preliminari; tuttavia la strada da percorrere è estremamente interessante e richiede ulteriori indagini.

ABSTRACT

The aim of the research developed in the time course of the three years of my Doctoral course in Molecular Medicine was to shed light into the mechanisms involved in Oxidative Stress responses in man at both integrative and molecular levels. To reach this general and high-level purpose we firstly focused our attention towards developing a method capable of returning an absolute quantitative estimation of Free Radicals production level. This particular aim was the subject of the first year of my researching activity. As a matter of fact, as is well known, in any physiological and/or pathological condition a subject could be involved, 'oxidative stress' results from the imbalance between Reactive Oxygen Species (ROS) production and his antioxidant capacity. Electron Paramagnetic Technique (EPR) resulted the method of choice since, as is well known, it is the only technique capable of returning, in a non-invasive way, the 'intrinsic' quantitative information (the signal is proportional to the number of excited electron spins).

Indeed the beginning of my Doctoral period fortunately coincided with the acquisition by the Molecular Bioimaging and Physiology (IBFM) Institute of CNR (Lita Segrate) of an EPR instrument (e-scan Bruker BioSpin, Germany) of recent design, responding to the innovative characteristics of easy portability and handling. The spectrometer operates at the common X-Band microwave frequency and deals with very low concentration levels (nM) even in small sample volumes (50 µl). Aware of the novelty of the method, we first looked for a correlation between the attained EPR experimental data and those returned when adopting the classical enzymatic methods (e.g. ThioBarbituric Acid Reactive Substances (TBARS) and Protein Carbonyls (PC) data collected from the same subject). Indeed, a correlation could not, by principle, be expected, since, compared to the EPR data, enzymatic methods give a quantitative "a posteriori" evaluation of the damage produced by ROS, on lipids and cellular proteins. As a matter of fact, a positive correlation (ANOVA, $p<0.05$) was found between EPR ROS production data and TBARS ($r^2 \sim 0.7$) as well as PC concentration ($r^2 \sim 0.6$), which was found in resting subjects.

Then, in order to achieve the overall objective of the research, we assumed 'hypoxia' as the 'particular' condition to be investigated, since it was viewed as a peculiar state capable of: 1) producing un imbalance between oxidative stress and anti-oxidant capacity; 2) offering the possibility of the identification of mechanisms involved in the perturbed balance restoring.

To attain this 'secondary' aim, the experiments were carried out on: A) healthy subjects, that as such, were expected to start from a balance equilibrium condition; B) subjects affected by neurodegenerative pathologies, for whom, on the contrary, a sure imbalance condition was expected, that would be confirmed by a significant increment of ROS production, even at rest.

However a fully innovative method had been developed, so that we lacked of referring literature data: a series of preliminary measurements on a homogeneous group of healthy subjects had to be firstly carried out, not only to optimize the acquisition and environmental conditions (T, pO_2 that have to be carefully defined since they greatly affect EPR data), but also to reach reliable resting physiological values and range of variability. A great reproducibility of the data (µmol · min^{-1}) *was found on blood capillary samples taken from the same healthy subject six hours apart ($r^2 = 0.99$, ~ 0.5%* discrepancy) and was calculated; *limit of detection (LOD)*

and quantification (LOQ) of 30 · 10^{-3} mM and 100 · 10^{-3} mM were calculated respectively.
In healthy subjects, the experimental protocols were designed in order to study the effects of: a) exercise (as inducing a transitory hypoxic state) of both short (in hockey players, swimmers) and long duration (in triathletes); b) training (as inducing a balance restore, in swimmers); c) hypoxia, both hypo- and normobaric (to study the effect of the assumed model condition itself, in young sedentary subjects); d) antioxidant molecules administration as an external way helping to restore the balance.
In neurodegenerative pathologies (patients affected by: type II Diabetic Neuropathy (type II DN), Mild Cognitive Impairment (MCI) and sporadic Amyotrophic Lateral Sclerosis (sALS)) after checking the expected unbalance throughout a significant increase of ROS production (sALS versus healthy subjects: +20%, $p<0.05$) under resting conditions, the effect of training on the possibility of approaching a normal ROS production level was investigated. The collected data thus far, that have to be nevertheless considered as preliminary results, of the training effect in sALS patients showed a beneficial effects; an decrease ROS production resting value (about -7%) was calculated after twelve weeks of training by the patients. in swimmers a significantly lower (about -25%) basal ROS production value (2.24 ± 0.14 µmol · min^{-1}) after eight weeks training period was calculated.
All these experiments were carried out and results obtained during my second and third year of my Doctoral School. Besides and beyond the specific results obtained from the collected data set, pointed out throughout my thesis, general observations can be summarized as follows:
1) There is no way to obtain data quantifying the total amount of ROS produced by a subject under any condition. Rather, EPR data return amount of ROS there were not scavenged by the antioxidant system. In other words, under a given condition, they represent the excess of the ROS produced in a given time, that is ROS production rate (µmol · min^{-1}). Moreover we chose to carry out the measurement on blood instead of tissue samples to obtain most possible integrative data. In particular capillary blood (with respect to venous blood or plasma) gave us the opportunity of developing a mini-invasive, reliable and easy measurement method. Nevertheless when going from capillary to venous data, the different blood pO_2 must be taken into account. (ROS production in venous was found about 18% lower than in capillary blood: e.g. 1.79 ± 0.12 vs 1.48 ± 0.29 µmol · min^{-1} respectively).
2) The obtained data cannot be taken as general parameters, since they strictly depend on the physic-chemical variables (T, pO_2) assumed for the measurement that must be taken into great account. From all these considerations, we can therefore conclude that beyond the possibility of obtaining absolute data to report for the first time in literature, this method was found as quite a sensitive and reliable mean to monitor the changes of each subject during time progression, therefore making each subject the control.
3) Despite the reliability and high reproducibility of the afore-developed method, we are anyway aware that EPR data have to be compared and integrated by collecting systemic data: hematochemical parameters (e.g. hematocrit, iron, cholesterol, platelets, neutrophils, lymphocytes, monocytes), oxygen saturation, maximal oxygen consumption (VO_2max).
Finally we are confident that our method will be in the near future considered

suitable to be applied into different medical fields: i) sport medicine, as an effective available help in sports centers to set up and adjusts training protocols by monitoring training effects on oxidative stress. ii) mountain medicine, in studying pathologies induced by hypoxia following high altitude acute and chronic staying; iii) clinic and diagnostic centers, helping in monitoring progression of pathologies and/or effects of therapies.

On the other side, second part of my researching activity, the study of hypoxia throughout EPR measurements, was carried out in vitro at a molecular level. In fact, hypoxia orchestrates a multitude of processes of molecular pathway responses. Nevertheless the traditional mechanism of sensing hypoxia involves the presence of a heme protein so that hypoxia can be detected by a reversible binding of O_2 at the heme site, which causes an allosteric shift in the hemoprotein from inactive (oxyform) to active (deoxy) form. The activity of a hemoprotein is therefore determined by the presence or absence of bound oxygen.

Among heme proteins, the relevance of hypoxic states, suitable to be encountered in both physiological and pathological conditions was, in the present research, made in conjunction with the supporting role recently attributed to deoxy-Myoglobin (Mb) as a ROS scavenger, with particular attention to a peculiar reactive species molecule, that is nitric oxide (NO). NO is a highly diffusive and reactive molecule, produced, in the cells, by the NO synthases enzymes (NOS), using L-arginine and O_2 as substrates. Under normoxic conditions, if NO concentration becomes too high, oxy-Mb is able to scavenge and oxidize it into NO^{3-}, maintaining mitochondrial O_2 consumption, thus cellular respiration, at the optimum. On the contrary, under hypoxia, the low O_2 availability leads to NOS inactivation (being substrate limited). The NO produced by Mb down-regulates mitochondria O_2 consumption, contributing to elongate the intracellular oxygen gradient and limiting the formation of deleterious reactive oxygen species. In addition, Mb-produced NO might contribute to hypoxic vasodilatation. Thus, Mb's nitrite reductase activity (very low pO_2 level) might participate both in the modulation of tissue mitochondrial respiration and in the limitation of ischemia-reperfusion injury, under hypoxic.

The relevance of hypoxic states, in conjunction with the supporting role recently attributed to deoxy-Myoglobin throughout its scavenging and vasodilatory properties was the rational basis for this study.

As regard as Mb, in human's skeletal muscle, up to five different Mb isoforms are reported in the literature (Mb I-V). Also different Mb percentages are present in the muscle: Mb I 75%, Mb II 29%, Mb III-V 5%.

Taking Mb-II as a reference, these proteins differ only for one external amino acid and, namely, they can be seen as the E54K (Mb I), K133N (Mb III), R139Q (Mb IV) and R139W (Mb V) mutants, whose specific functions, if any, are completely unknown. In addition, these general observations were supported by specific findings on populations born and living in extreme hypoxic conditions possibly explaining their better metabolic and mechanic efficiency by the increase of Mb concentration, with particular reference to the 54E isoform (Mb II). Throughout a combined EPR and MD simulations analysis, the present study aimed to give experimental evidenced able to further underline the relevant role played by Mb under hypoxic conditions, then marking a first step towards the identification of different roles played by Mb isoforms, whose presence, among mammals, is a distinct feature of human Mb.

Functional results obtained by the EPR study showed up not only a significantly greater NO binding capacity (more than double; $p<0.01$) of the 54E with respect to the 54K isoform was calculated from the EPR spectra integrated areas but even more circumscribed this property to the deoxygenate state, the binding capacity becoming significantly lower and almost the same for the two proteins in the presence of O_2 at the two analyzed pO_2 levels (40 and 100 mmHg). This novel and quite intriguing result was supported by structural considerations emerged by the MD simulation analysis and in turn mutually supported by structural EPR results.

Concluding remarks and future perspectives can be summarized in our firm belief, which we are confident will be verified and accorded by the reader as well, of the novelty of the developed method and of the reported data. Indeed some of them, especially when concerning pathological subjects, have to considered 'in fieri', nevertheless the road to take is extremely interesting, and calls for further investigations.

INDEX

INDEX OF FIGURES

INDEX OF TABLES

LIST OF ABBREVIATIONS

%	percent
µl	microliter
µmol	micromole
µW	microWave
AD	Alzheimer Disease
ALS	Amyotrophic Lateral Sclerosis
AMS	Altitude Mountain Sickness
a.u.	arbitrary unit
ATP	Adenosine TriphosPhate
CAT	Catalase
CMH	1-hydroxy-3-methoxycarbonyl-2,2,5,5tetramethylpyrrolidine
CP*	3-carboxy-2,2,5,5- tetramethyl-1-pyrrolidinyloxy
CW	Continuous Wave
DETC	Sodium Diethyldithio-Carbamate Trihydrate
DF	Deferroxamine Methane-sulfonate Salt
d-ROM	Reactive Oxygen Metabolites
EPR	Electron Paramagnetic Resonance
FORT	Free Radical Oxygen Test
FR	Free Radical
G	Gauss
GSH	Glutathione
h	hour(s)
Hb	Hemoglobin
HD	Huntington Disease
HHb	deoxy Haemoglobin
HIF-1	Hypoxia Inducibile Factor -1
HMb	deoxy Myoglobin
HO-1	Heme Oxygenase-1
KHB	Krebs-Hepes buffer
HPLC	High Performance Liquid Chromatography

K	Kelvin
LOD	Limit of Detection
LOQ	Limit of Quantification
MAPK	Mutagen Activate Protein Kinase
Mb	Myoglobin
MCH	Mean Corpuscolar Hemoglobin
MCHC	Mean Corpuscolar Hemoglobin Concentration
MCI	Mild Cognitive Impairment
min	minute(s)
mmHg	millimeters of mercury
MRI	Magnetic Resonance Imaging
MS	Mass Spectrometry
NADPH	Nicotinamide Adenine Dinucleotide Phosphate
nM	nanoMolar
NO	Nitric Oxide
NOS	Nitric Oxide Synthase
NOX	Oxygen-sensitive probe Oxyethidium
OXPHOS	Oxidative Phoshorylation
PC	Protein Carbonyls
PD	Parkinson Disease
pO_2	O_2 pressure
NQO-1	Quinone Oxidoreductase-1
RBC	Red Blood Cell
ROS	Reactive Oxygen Species
RNS	Reactive Nitrogen Species
SNR	Signal-Noise Ratios
SO_2	Oxygen Saturation
SOD	SuperOxide Dismutase
T	Temperature
TBARS	ThioBarbituric Acid Reactive Substances
Type II DN	Type II Diabetic Neuropathy
VEGF	Vascular Endothelial Growth Factors
VO_2max	maximal Oxygen consumption

1 INTRODUCTION

Setting the scene: How did redox biology begin?
Nowadays the redox biology is probably the most rapidly expanding field in biology; indeed the number of conferences, books, journals and special issues in this area, books are increasing significantly [1]. All animals need O_2 for an efficient production of energy by mitochondria. This need for O_2 obscures the fact that it is a toxic mutagenic gas; aerobes survive only because they have evolved antioxidant defenses [2]. Thus antioxidants and free radicals permeate the whole of life, creating the field of redox biology. Free radicals are not all bad as well as antioxidants are not all not good. Life is a balance between the two: antioxidants serve to keep down the levels of free radicals, allowing them to perform useful biological functions without too much damage [2]. This is true in humans as in plants. Yet some damage is inevitable, requiring repair systems to maintain cell viability.

1.1 Free radicals: what's about? Where they come from?

1.1.1 Discovery of Free Radicals

In the late 1950 terms like Free Radicals (FR) and antioxidants, were almost unknown in biological and clinical sciences, the presence of radicals in biological materials being demonstrated only in 1954. For the first time in 1956, Denham Harman, has established a link between the toxic effects of high levels of oxygen in aerobic organisms and ionizing radiation, suggesting the idea that oxygen toxicity was due to formation of FR [3].
Free Radicals are highly reactive molecules or fragments of them carrying one or more unpaired electrons in the outer shell.
In **Table 1** the classification of FR (oxygen radicals, non-oxygen radicals and nitrogen radicals), symbol and intracellular half life (s) [4]. Among them reactive oxygen species (ROS) can be classified into two groups of compounds, radicals and non-radicals. The specimens in **Table 1** belong to the radical group, often incorrectly called Free-Radicals (the term is not accurate, because, due to the presence of the e^-, a radical can be always considered 'free') and are capable of independent existence. The occurrence of one unpaired electron results in high reactivity by their tendency to give or subtract electrons to attain stability.
By contrast, a large variety of substances belong to the non-radical compounds group, some of which, although not radical by definition, are extremely reactive. Among them, produced in high concentrations in living cells, hypo-chlorous acid (HClO), hydrogen peroxide (H_2O_2), organic peroxides, aldehydes, ozone (O_3), and O_2 can be found. Indeed, by definition, the oxygen molecule itself can be considered a bi-radical, because it contains two unpaired electrons in two different orbitals. Nevertheless, ROS are paramagnetic oxygen molecules, produced in cells as by-products of oxidation–reduction (REDOX) reactions, which can in turn be

stabilized by subtracting electrons to neighboring molecules (e.g. lipids, proteins, DNA).

Name	Symbol	Half life t1/2 (s)
OXYGEN RADICALS		
Oxygen (bi-radical)	**O_2••**	**10^{-6}**
Superoxide	**O_2•-**	**10^{-4}**
Hydroxyl	**OH•**	**10^{-9}**
Peroxyl	**RO_2•**	**0.1**
Alkoxyl	**RO•**	**10^{-6}**
Nitric oxide	**NO•**	**0.4**
NON RADICALS OXYGEN		
Singlet	**O_2**	**10^{-3}**
Hydrogen peroxide	**H_2O_2**	**1**
Ozone	**O_3**	**sec/min/h/day (T° dependent)**
NITROGEN REACTIVE SPECIES		
Nitrogen dioxide	**NO_2•**	**s**
Nitrate	**NO_3•**	**s**

***Table 1**: Radicals and non-radicals oxygen and nitrogen metabolites*

1.1.2 Exogenous and endogenous sources

Cells are exposed to a large variety of ROS from both exogenous and endogenous sources. Exogenous sources of ROS can be identified in UV and γ radiations, microbes, allergens, car exhausts, certain foods, tobacco smoke, air pollutants, drugs and alcohol when assumed in a great amount. Nevertheless, despite the

extremely strong exposure of whole our organism to ROS coming from exogenous sources, endogenous ROS play the most important and extensive role, since, in the time course of our life, each body cell is continuously exposed to them. The major responsible of ROS production are mitochondria [5]; enzymes are another endogenous source of ROS. While most enzymes produce ROS as by-products of their activity (xanthine oxidase is a clear example) some of them are designed to produce ROS: nitric oxide synthase (NOS) yields NO radicals; Nicotinamide Adenine Dinucleotide Phosphate (NADPH) oxidase complex utilizes electrons to produce superoxide radicals from the oxygen molecule.

1.1.3 Balance/Unbalance of ROS

At appropriate concentration, ROS are known to act as important signaling molecules. Free radicals and reactive species are essential to wellbeing, having various regulatory roles in cells. For example, ROS are produced by immune cells (neutrophils and macrophages) during the process of respiratory burst in order to eliminate antigens [6]. They also serve as stimulating signals of several genes encoding transcription factors, differentiation, and development as well as stimulating cell-cell adhesion, cell signaling, vasoregulation, fibroblast proliferation and antioxidant enzymes increasing expression. The latter example is observed in subjects performing chronic exercise and will be further discussed (see below in the text). At the same time, antioxidant enzymes are essential functional cell regulators of metabolic pathways.
Moreover the effects of ROS are dose dependent. In plants, for an example, ROS are used to facilitate an array of essential biological processes, as growth and development, seed germination and stress acclimation [7].
By contrast, "**Oxidative Stress**" term indicates a range of deleterious states, resulting from an imbalance between antioxidant defense systems and ROS, towards these latter, produced in a great extent. This state is associated with damage to proteins, lipids and DNA together with functional impairment of metabolic processes as the mitochondrial respiratory chain [8, 9]. Indeed, a) the oxidative attack on proteins results in site-specific amino acid modification, fragmentation of the peptide chain, aggregation of cross linked reaction products, altered electrical charges and increased susceptibility to proteolysis [10]; b) the lipid peroxidation is a complex process involving the interaction of oxygen-derived free radicals with polyunsaturated fatty acids, resulting in a variety of highly reactive electrophilic aldehydes [11]; and finally c) DNA, causing deletions, mutations and other lethal genetic effects. Characterization DNA damage has indicated that both sugar and base moieties are susceptible to have been oxidized, causing base degradation, tandem lesions, single and double strand breakage and protein cross links [12].

1.1.4 Mitochondria: primary site for ROS production

As mentioned above, the mitochondria are a primary site for ROS production under physiologic condition [5]. The mitochondria are present in every eukaryotic cell.

The electron transport chain for generation of adenosine tri-phosphate (ATP) in the inner membrane of mitochondria permanently generate superoxide ion ($O_2^{\bullet -}$). It is estimated that 1-2% or even 4% of oxygen consumption undergoes transformation to $O_2^{\bullet -}$. [13]. The mitochondrial respiratory chain transfers electrons to molecular oxygen, permanently producing ROS as a by-product of oxidative phosphorylation (OXPHOS). Some oxygen consumed by mitochondria is only partially reduced to superoxide radical ($O_2^{\bullet -}$), which can then be converted to hydrogen peroxide (H_2O_2) by superoxide dismutase (SOD), and then further to water by catalase (CAT) or to the very reactive hydroxyl radical in the presence of transition metals (e.g. Fe^{2+}). Five enzyme complexes are localized on the inner mitochondrial membrane. Complexes I–IV (the electron transport chain) are involved in transporting electrons through a series of proteins via REDOX reactions, with the final destination being an oxygen molecule.
Under normal situation, this oxygen is then converted to water in complex IV, and the energy stored in the proton gradient is used to drive ATP production in complex V. However, during this process, it would occur an inadequate coupling of the electron transfer between the complexes I and III: complex I (namely, the iron-sulfur clusters) releases the reactive oxygen species (superoxide anion) only towards the mitochondrial matrix, whereas complex III (the ubiquinol oxidation site) releases superoxide into both matrix and outside the inner membrane. So a small percentage of the oxygen consumed by the mitochondria at complex IV is converted to ROS rather than water. Thus, paradoxically, the most fundamental of processes in enabling eukaryote life (OXPHOS) is also one of the chief culprits of ROS production. Summarizing, many reports have demonstrated that mitochondrial superoxide production is mostly a result of incomplete reduction of oxygen at sites of respiratory complexes I and III, which therefore can be considered as the main sources for mitochondrial ROS (see **Figure 1**) [14, 15].

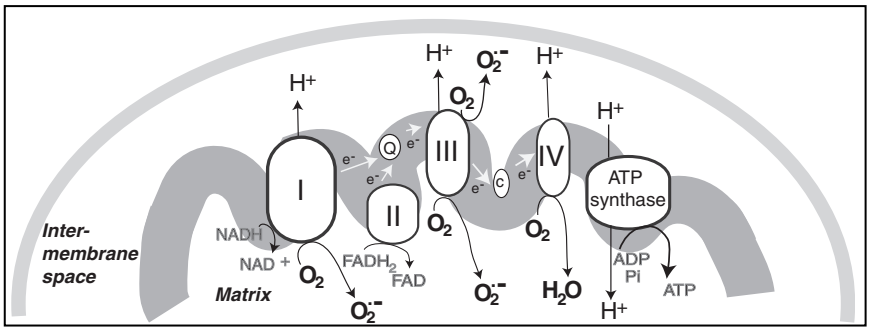

***Figure 1**: Mitochondrial sites of superoxide production. Electrons are transferred from complexes I, II, and III to IV. Inadequate coupling of electron transfer can cause leakage, generating superoxide anions at different complex levels. [by Handy DE, Loscalzo J.- 14].*

For the complex and fundamental role of mitochondria, it is very important to maintain the functional integrity of mitochondria. Because of pivotal role for cellular survival, mitochondrial dysfunction is associated at neurological diseases (e.g. Parkinson's disease (PD), Huntington's disease (HD), Alzheimer's disease (AD), Amyotrophic Lateral Sclerosis (ALS) and various peripheral neuropathies) as well as the normal aging process [17]. Also, several non-mitochondrial sources of ROS are present in the cell, such as membrane-bound NADPH oxidase [18]. NADPH oxidase plays an important role in pathological states of reperfusion, hypertension and atherosclerosis. However it is involved in defense against pathogens too.

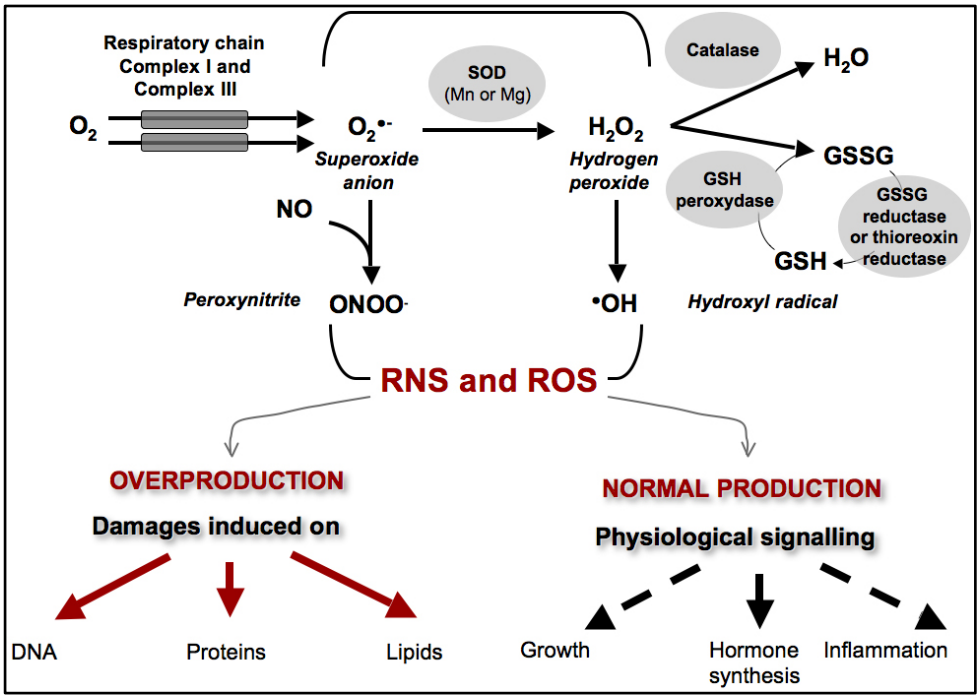

***Figure 2**: Mitochondrial signaling by ROS, adapted from Bellance et al, 2009 [16]. The mitochondrion is implicated in the generation of Reactive Oxygen Species (ROS) and Reactive Nitrogen Species (RNS). In most cells, the mitochondrial respiratory chain is recognized as the major site of ROS production in the form of superoxide, hydrogen peroxide and the hydroxyl free radical. These molecules can be considered as positive products that contribute to cell signaling. However, excessive amounts of ROS are deleterious for the cell, contributing to a variety of pathological processes. ROS generation can result in the set up of a vicious cycle of oxidative damage causing a progressive alteration of DNA and mitochondrial function that in turn leads to energy deprivation, redox imbalance and cell dysfunction.*

Due to the potential role that reactive species and free radicals have in lipid, protein, and DNA damage, it is not surprising that a network of antioxidant defense mechanism is present in the body. In general, antioxidants are often reducing agents, which exist both intracellularly and extracellularly and have the capacity to react with free radicals and reactive species, minimizing their actions and, thus, delaying or preventing oxidative stress.
Antioxidants can be both synthesized in vivo and absorbed through diet. They can be divided into two groups: enzymatic and non-enzymatic. The main enzymatic antioxidants include superoxide dismutase (SOD), glutathione peroxidase (GPX), and catalase (CAT). Each of these enzymes is responsible for the reduction of a different ROS, and they are located in different cellular compartments.
One of the primary enzymatic ROS scavenging mechanisms involves dismutating superoxide to hydrogen peroxide (H_2O_2), via the SOD. The H_2O_2 is subsequently detoxified via other enzymatic reactions (see **Figure 2**) [14].
The non-enzymatic antioxidant group includes glutathione, vitamin C, vitamin E, carotenoids, uric acid, and others. Similarly to the enzymatic antioxidants, these are present in different cellular compartments and elicit distinct antioxidant properties, which maximize their effectiveness. [19]. Reduced glutathione (GSH) is a water-soluble low-molecular-weight tripeptide that exerts various essential functions in the body, amongst these a major antioxidant role. Further, there is an evidence that bilirubin can act as antioxidant to help neutralize certain free radicals [20]. The delicate balance between advantageous and detrimental ROS effects plays a great physio-pathological importance. The redox state of a cell is kept within a narrow range under normal conditions, similar to the manner in which a biological system regulates its pH.

1.1.5 ROS and disease

When ROS overwhelm the cellular antioxidant defense system, whether through an increase in ROS levels or a decrease in the cellular antioxidant capacity the delicate balance oxidant/antioxidant is broken. In this case, as shown until now, not only mitochondrial dysfunction caused by the attack of ROS induces many neurological diseases, but the high levels of ROS result in number of other degenerative processes affecting a wide variety of physiological functions.
So ROS are involved in the pathogenesis of diseases states such as atherosclerosis, diabetes, ischemia/reperfusion injury, inflammatory diseases (rheumatoid arthritis, inflammatory bowel diseases and pancreatitis), cancer, neurodegenerative diseases (Parkinson, Amyotrophic Lateral Sclerosis, Alzheimer, [21], cardiovascular and/or respiratory insufficiency, etc. [22-24]. These diseases have as a common thread tissue hypoxia and/or structural alterations, dysfunction of mitochondria and consequently the increased ROS production.

1.1.6 ROS and physical exercise

The physical exercise is perhaps one of the most characteristic examples demonstrating that ROS are not necessarily harmful, considering that the well-

known benefits of regular exercise on muscle function and health accompanied by repeated episodes of oxidative stress [25]. But this is true? This is one of the questions that we tried to answer in these three years of work. We are aware that the exercise is associated with a dramatic increase in oxygen uptake by the whole body and particularly by skeletal muscle [26]. Sen [27] reported an increase of 10–15-fold in the rate of whole body oxygen consumption and an increase of more than 100-fold in the oxygen flux in active muscles during whole-body aerobic exercise, so resulting in increased ROS formation shifting the cellular environment from a reduced to an oxidized state independently of physical activity (aerobic, anaerobic or resistance types of activities) [28].
The most of the oxygen consumed by the body is utilized in the mitochondria for substrate metabolism and ATP production. An increased ATP demand accompanying exercise increases both aerobic and/or anaerobic metabolism [29]. So many factors might contribute to the oxidative stress induced by exercise and a variety of factors can influence the oxidative rate, such as the muscle groups recruited, the modes of contraction, the exercise intensity, the exercise duration, and the exercising population. Recent reports have indicated the potential role that blood may play at rest or during exercise on ROS production. Some important factors, that contribute to the oxidative stress during the exercise, are easily visible in the blood: increased in blood temperature, decrease in blood pH, decrease in blood oxygen partial pressure and increase in the concentration of blood lactate [25]. The whole blood or parts of it (plasma [30], erythrocytes [31], neutrophils [30,32], lymphocytes [33], platelets [34] have reported an increase production of various reactive species after exercise. However, the majority of the relevant human studies have measured the redox status of the plasma (plasma is about 55% of the blood volume; its composed mostly water, about 90% and contains dissolved protein, glucose, lipids, mineral ion), this is probably for two reasons: the assumption that plasma better reflects tissue redox status and the easiness of plasma collection.
Blood is able to produce ROS during exercise, yet it's equally evident that skeletal muscle is able to produce reactive species during increased contractile activity. Referring to the appropriate level of reactive species, ROS are important signaling molecules for muscle contractions. At the molecular level, the exercise active the p38γ MAPK (mitogen-activated protein kinase) which promotes PGC-1α activity and expression in control of mitochondrial biogenesis and angiogenesis in skeletal muscle [35]. The promoting effects of regular exercise on different cellular functions include the up-regulation of antioxidant, oxidative damage repairing systems, neurogenesis, and induction of trophic factors [35].

1.1.7 Exercise, pathological state and hypoxia.

The physical exercise and some pathological status can be seen as a typical example of an acute, intermittent or long-lasting/chronic hypoxic exposure or condition. One model of chronic intermittent hypoxia (common and life-threatening condition that occurs in many different diseases) is the hypertension and consequent cardio - and cerebrovascular diseases but also metabolic disorders such as diabetes [36] and atherosclerosis. Recent studies suggest that hypoxia can be one of the underlying mechanisms of the atherogenesis and carcinogenesis.

Despite this, most commonly, the term hypoxia brings to mind the mountain and the high altitude. Hypoxia exposure can lead to altitude mountain sickness and sometime to high-altitude pulmonary or cerebral or edemas when the exposure is severe. In fact, there are indirect evidence from cells and tissue experiments that acute hypoxia induces accumulation of ROS [37,38]. The increase in accumulation of ROS during exposure to hypoxia have important systemic implications [39] and more particularly at brain level with damage of vascular endothelium, neurons, glia, and down-regulation of Na^+-K^+-ATPase, Ca^{2+}-ATPase, Na^+/Ca^{2+} exchanger activities. [37]. Significantly effects of high altitude exposure have been shown on the cell-proliferative activity and expression of pro-inflammatory cytokines with evident impairment of leucocyte function [38].
The evidence of impact of the hypoxia on metabolism appears from muscle proteomic analysis in man and animals [40,41]. The transcription factor responding to changes of available oxygen in cellular environment of animal and human body is the Hypoxia Inducible Factor 1 (HIF-1). HIF-1 is a heterodimetric complex consisting of a constitutively expressed β subunit (also known as the aryl hydrocarbon receptor nuclear translocation, ARNT) and a hypoxia inducible subunit, α subunit. It controls a wide range of genes involved in adaptation to low oxygen pressure, indeed is a potent mediator of hypoxic responses by regulating both oxygen delivery (angiogenesis and red cells production) and oxygen consumption (glycolytic metabolism). HIF-1 activation is regulates through mitochondria and NADPH oxidase-mediated ROS production. The specific tissue partial O_2 pressure (pO_2) that induces a response depends on many variables including diffusion distances, blood flow velocity, metabolic rate, myoglobin concentrations and the dynamic influence of NO on mitochondrial electron transport [42].
Thus, hypoxia is involved in physiological, para-physiological, and pathological conditions.

1.1.8 Myoglobin (Mb), NO and Hypoxia

Myoglobin (Mb), otherwise named as “muscle Hemoglobin”, is a relatively small globular metalloprotein (153 [43] or 154 [44] residues). Historically, Mb was the first protein to be solved at atomic level, [45] (**Figure 3**) and, also because of its size, has been often employed as a model system for larger and more complex globular proteins (**Figure 4**) [46-49].
Indeed, it is widely considered as the ‘hydrogen atom of biology and a paradigm of complexity’ [47] to test new models and investigation techniques. For a very long time, it has been simply considered an O_2 storage/delivery system necessary to maintain its physiological concentration gradient across the cell [50]. The general consensus about restriction of Mb expression to the skeletal and cardiac muscle of mammals, together with the observation that the diving species exhibit a more than tenfold higher concentration of Mb, compared with the non-diving ones at sea level, strengthened the idea about its role as an O_2 repository [46,47,49,51].
However, more recent studies revealed its widespread expression in various non-muscle tissues, as well as in many other living organisms, including fishes, birds, reptiles, mollusks, and even bacteria and protozoa [52].

***Figure 3**: Max Perutz (left) with his model of hemoglobin and John Kendrew with his model of myoglobin in 1962 [Photo by Nobel Prize.org].*

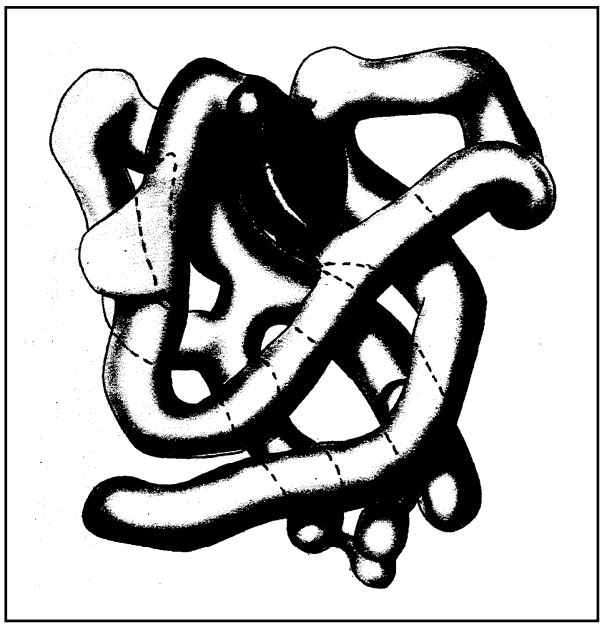

***Figure 4**: Model of the Myoglobin molecule, derived from the 6Å Fourier synyhesis. The Haem group is a dark grey disk (centre top) [by John Cowdery Kendrew. Myoglobin and the structure of proteins. Nobel Lecture, December 11, 1962].*

In particular, an over-expression in response to hypoxia has been reported, [53,54] with even possible implications in tumors' development [55]. Since 1962, U.S. Military studies, in human subjects (young native of Cerro de Pasco – 4400m s.l.) have suggested that higher concentration of myoglobin seen in the altitude native was probably real since the nitrogen content of the muscle, the lean body mass and the body water continent were the same in both high altitude and sea level subjects. [56]. Anyway, in the literature, a relationship between Mb expression and hypoxia started to emerge, leading to the idea that this supposedly well-known protein might have alternative/complementary roles, such as NO scavenging [57] and NO^{2-} reduction, [58] being regulated by O_2 concentration, NO is a highly diffusive and reactive molecule, produced, in the cells, by the NO synthases enzymes (NOS), using L-arginine and O_2 as substrates [59,60]. Among many different and fundamental roles as a signaling molecule, NO is a well-known inhibitor of the mitochondrial respiratory chain, having the cytochrome-c-oxidase as its primary target [61]. Under normoxic conditions, (see equation 1) if NO concentration becomes too high, oxy-Mb is able to scavenge and oxidize it to NO^{3-}, [62] maintaining mitochondrial O_2 consumption, thus cellular respiration, at the optimum.

Normoxia (scavenger): $MbO_2 + NO \rightarrow metMb + NO_3^-$ (1)

On the contrary, under hypoxia (see **equation 2**), the low O_2 availability leads to NOS inactivation (being substrate limited).

Hypoxia (producer): $DeoxyMb + NO_2^- + H^+ \rightarrow MetMb + NO + OH^+$ (2)

The few O_2 would be mostly consumed by the respiratory chain, resulting in a dramatic shortening of its concentration gradient through the tissue [61] However, in this condition, Mb was found to be able to act as a NO^{2-} reductase [58,62]. The NO produced by Mb down-regulates mitochondria O_2 consumption, contributing to elongate the intracellular oxygen gradient [61] and limiting the formation of deleterious reactive oxygen species [63]. In addition, Mb-produced NO might contribute to hypoxic vasodilatation [64]. The vasodilatory property of NO^{2-}, at physiological concentrations in vivo, has been previously described and associated to its conversion to NO by deoxy-hemoglobin [65]. Then, the nitrite reductase activity of Mb at very low pO_2 levels, as it occurs during exercise or ischemia, has been associated to a rapid conversion of tissue nitrite to NO as well [61]. Thus, Mb's nitrite reductase activity might participate both in the modulation of tissue mitochondrial respiration and in the limitation of ischemia-reperfusion injury, under hypoxic conditions.
In humans, up to five different Mb isoforms are reported in the literature, Mb-I (75-80%; pI 8.57), Mb-II (15-20%; pI 7.29), Mb-III, Mb-IV and Mb-V (all together 5%; pI 6.83) [66,67].
More recently, three alternatively spliced transcript variants (see **Figure 5)**, encoding for the same protein, have been reported.
[http://www.genecards.org/cgi-bin/carddisp.pl?gene=MB].

Taking Mb-II as a reference, these proteins differ only for one external amino acid and, namely, they can be seen as the E54K (Mb I) [68], K133N (Mb III) [69], R139Q (Mb IV) [70] and R139W (Mb V) [71] mutants, whose specific functions, if any, are completely unknown (see **Figure 6A**).
In the context of the aforementioned O_2 level dependent multiple roles, it is interesting to note that, when compared to low-lander populations, high altitude natives, like those from Tibet plateaus [54] or Andean slopes, [72] are characterized by a higher muscle Mb concentration. In particular, a recent proteomic investigation [54] pointed out that the greater concentration of Mb in Tibetans natives (+20%) is totally attributable to the increase of the isoform Mb-II. Thus, together with the observation that Tibetans are also characterized by higherefficiency of locomotion, a relationship between Mb-II over-expression and their evolutive adaptation to high altitude was put forward [54,73].

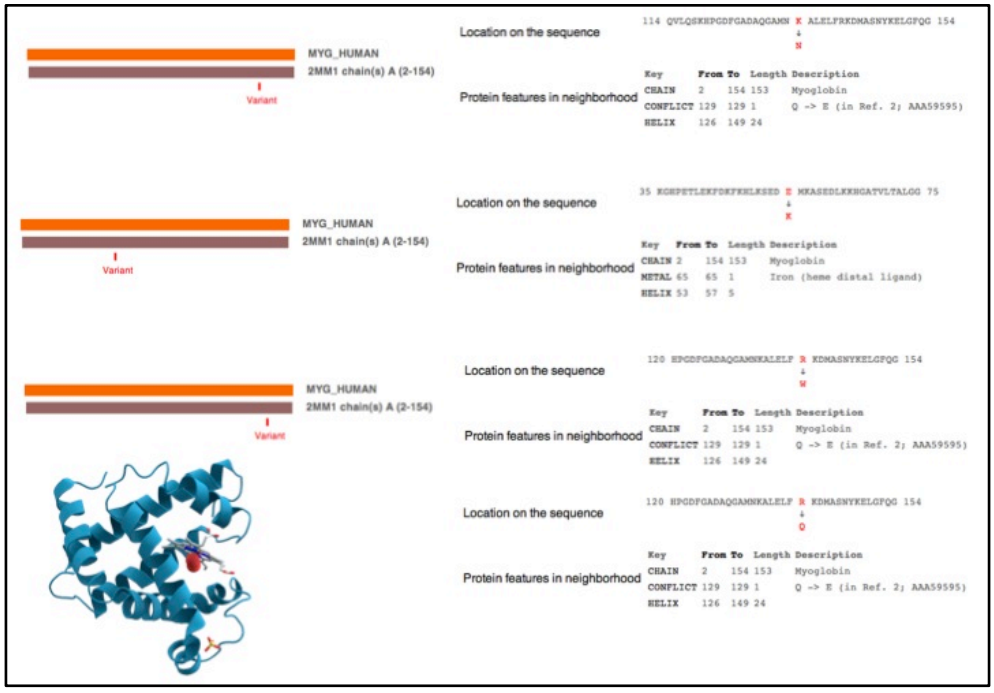

***Figure 5**: Three alternatively spliced transcript variants in Mb [by UniProtKB/Swiss-Prot variant pages].*

Looking only two more expressed isoforms, the single-point mutation occurs in the CD-region (i.e. from residue 35 to 58, comprising the C- and the D-helix, together with the long loop in-between), where the distal histidine (H64) is located (see **Figure 6B**) [75].

Thus, the difference between the human Mb and those from other mammals should stem from some other structural/dynamical diversities. It is important to cite here as well, that some (quite extensive) mutations of the CD-region were investigated on different sperm-whale Mb mutants [79], where, in particular, residues 51÷55 (i.e. the entire D-helix) have been deleted, or mutated with alanines. It was found that these mutations or the deletion of the D-helix had a little effect on both O_2 and CO binding, but a deep impact on hemin loss. However, in the light of the above cited ref. [62], human Mb reactivity seems to be somewhat different from that of other mammals and, moreover, that investigation was not performed at various pO_2 levels but simply at ambient pressure. On the contrary, this might be particularly important, as highlighted in a very recent paper [80], where many different mutants of sperm-whale Mb have been compared in terms of their O_2 storage and O_2 transport activity, separately. Important differences emerged only at a very low pO_2, and some organism-specific differences were also remarked, comparing the sperm-whale to the human Mb [80]. In addition, in a recent experimental work of some of the authors [81], the two more expressed human Mb isoforms have been investigated through NMR spectroscopy. Both resulted to be stable in solution and non hemin loss has been observed, together with no significant structural differences in the heme region [81].

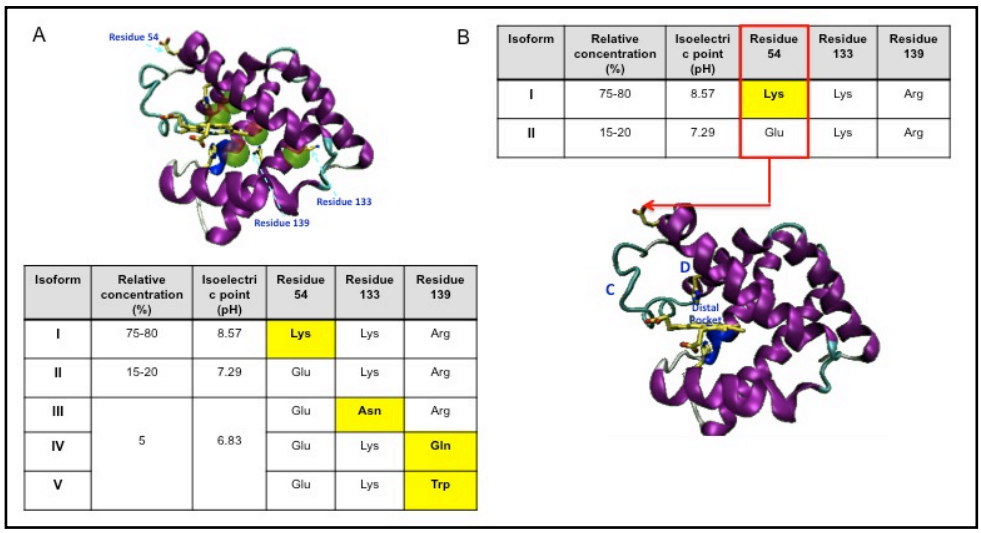

Isoform	Relative concentration (%)	Isoelectric point (pH)	Residue 54	Residue 133	Residue 139
I	75-80	8.57	**Lys**	Lys	Arg
II	15-20	7.29	Glu	Lys	Arg
III	5	6.83	Glu	**Asn**	Arg
IV			Glu	Lys	**Gln**
V			Glu	Lys	**Trp**

***Figure 6**: A) Five different Mb isoform are expressed in humans differing for only one external amino acid (in yellow the differences). Taking Mb-II as a reference: E54K (Mb-I), K133N (Mb-III), R139Q (Mb-IV) and R139W (Mb-V) mutants, whose specific functions, if any, are completely unknown. B) The E54K mutation site, the D helix and CD loop are shown. The two most expressed isoform differ only for the residue 54, playing a great effect on the surface charge. They are stable in solution showing no dramatic differences in their cavity structure.*

As a matter of fact, such a single external point-mutation causes a significant shift of the isoelectric point, but possible allosteric effects on the internal cavities have been excluded by NMR, [81] thus addressing further investigations focused on the protein surface and the mutation region, by adopting other suitable techniques. The computer simulations represented one method that provide an atomic-level description about proteins' thermal motions that may be difficult to obtain with experiments [82], together with fundamental information on protein-solvent interplay [83].
Besides, EPR technique has been widely used for both structural and functional studies on different metallo-proteins, mainly Hemoglobin and Myoglobin, and, in particular, to identify and characterize the symmetry of the electronic cloud around radical species. In addition to the determination of the heme orientation relative to the crystallographic axis in the two cases, detailed information about the symmetry of the electric field surrounding the heme-iron, as well as conformational changes upon ligand binding, were attained [84]. EPR technique was considered particularly suitable to investigate NO binding to Mb. Indeed, nitrosyl-heme is characterized by an unpaired electron, such that, from the very beginning, NO was used as a spin-labeled ligand for probing the electronic structure of the heme group and its environment, also in the light of the fact that the O_2 - Hb/Mb complex is diamagnetic, thus EPR invisible [85]. NO binding to the metallo-heme protein's center can be directly measured in vitro and in vivo. In fact, by virtue of differences in the line shape and position of the magnetic field (g values) of the EPR absorption, spectra are sensitive to conformational changes of the protein's moiety, which, in turn, produce geometrical changes at the metal site. The binding of NO to these proteins gives rise to a unique EPR spectrum, with characteristic symmetry and hyperfine coupling [86].

1.2 Free radicals: how can we measure them?

Since the discovery of oxygen in the early 18th century by Antoine Laurent Lavoisier, the necessity of controlling oxygen levels has been recognized. An elusive molecule, oxygen plays contradictory roles, one essential for life and the other as a toxic substance. Sure is that Oxygen is required by prokaryotic and eukaryotic cells for energy production, often via the electron transport chain in the mitochondria. In a pioneering paper in 1954, Rebeca Gerschman et al. (**Figure 7**) anticipated the toxic effects of elevated oxygen levels on aerobes to those of ionizing radiation, and proposed that oxygen toxicity is due to free radical formation [87].

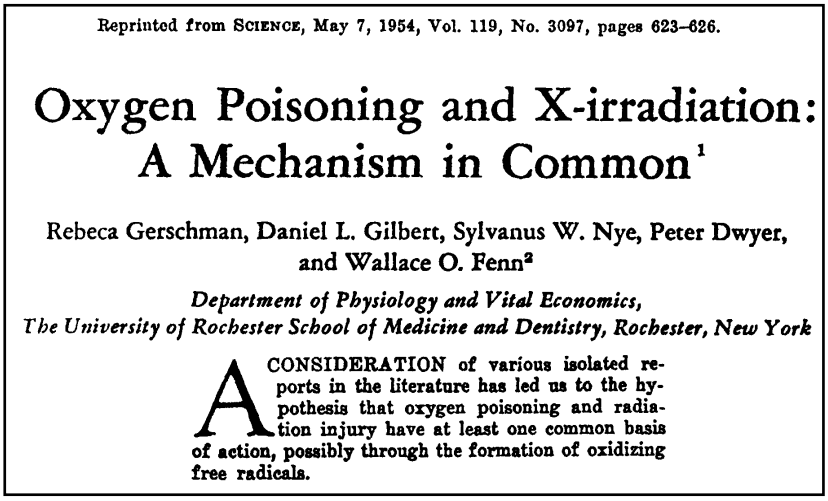

Reprinted from SCIENCE, May 7, 1954, Vol. 119, No. 3097, pages 623–626.

Oxygen Poisoning and X-irradiation: A Mechanism in Common[1]

Rebeca Gerschman, Daniel L. Gilbert, Sylvanus W. Nye, Peter Dwyer, and Wallace O. Fenn[2]

Department of Physiology and Vital Economics, The University of Rochester School of Medicine and Dentistry, Rochester, New York

A CONSIDERATION of various isolated reports in the literature has led us to the hypothesis that oxygen poisoning and radiation injury have at least one common basis of action, possibly through the formation of oxidizing free radicals.

***Figure** 7: The May 7, 1954 Science paper which postulated that oxidizing free radicals were involved in oxygen toxicity (@1954, American Association for The Advancement of Science).*

From this time, the scientists published a series of articles on the role of ROS in the pathogenesis of aging [88]. In subsequent years, numerous investigations were conducted in which it was shown that ROS play a key role in senescence and some of the underlying mechanisms were elucidated.

Because most radicals are short-lived species, they react quickly with other molecules. As already pointed out, the most vulnerable biological targets for oxidative damage are proteins, membrane lipids and DNA. Many approaches allow evaluation and demonstration of the participation of ROS in biochemical events. Indeed, the literature is replete with descriptions of different methodologies and approaches for these purposes. ROS are difficult to measure because they are produced in low quantities, have a very short half-life and are quite unstable due to their interaction with antioxidation enzymes and cellular components like thiol residues, molecular oxygen, and metalloproteins.

Alternative approaches for the direct determination of ROS are developed. Techniques for quantification of oxidative damage markers are often called fingerprinting methods by which specific end products resulting from the interaction of the ROS with biological macromolecules, such as DNA, proteins, lipid [24], and low molecular weight antioxidant are measured. The appearance of these end products serves as proof of the prior existence of ROS that left their footprints in the cell. Some techniques are available today to measure reactive species and oxidative damage in biological samples (blood, cellular culture, biological fluid). Depending on the type of samples, some methods are preferred over others. The currently available methods include assays based on oxidation of chromophores, chemiluminescence techniques, Mass Spectrometry (MALDI, MS/MS), fluorescence-based assays, immunological assay, enzymatic assays, High Performance Liquid Chromatography (HPLC), flow cytometry, and Electron

Paramagnetic Resonance spectroscopy (EPR) each with their own benefits and limits. Also, there are news questionable spectrophotometric methods, including: d-ROM (Reactive Oxygen Metabolites) test and its variant the FORT (Free Oxygen Radical Test) [89]. The manufacturer claims that these tests can quantify the oxidative status by measuring the hydroperoxides of organic compounds. However the clinical interest or the relevance biological of these methods remains to be investigated and unclear [90].
Lastly, a fascinating technique such as L-band EPR with probe and Magnetic Resonance Imaging (MRI) spin trapping are under development to measure reactive species directly in whole animals, but no probes are currently suitable for human use [91,92].
Attributable to the methods used in the thesis, are presented below only two types of techniques: enzymatic methods and the EPR.

1.2.1 Indirect Method

The enzymatic assay methods are the indirect methods have been developed just to measure the ROS-induced damage, basing on the determination of specific end products resulting from the interaction of ROS just with these biological macromolecules [93,94]. The enzymatic assay methods adopted were measurement of damage products of proteins and lipids [95]. Evaluation of protein oxidative damage can be accomplished using the carbonyl assay the most commonly used marker is protein carbonyl (PC). Carbonyls are produced from the attack of ROS on amino-acid residues in proteins [96]. Redox cycling cations such as Fe^{2+} or Cu^{2+} can bind to cation binding locations on proteins and with the aid of further attack by H_2O_2 or O_2 can transform side-chain amine groups on several amino acids (i.e., lysine, arginine, proline, or histidine) into carbonyls.
All cellular membranes are especially vulnerable to oxidation due to their high concentrations of unsaturated fatty acid. The damage to lipids, usually called lipid peroxidation, occurs in 3 stages. The first stage, initiation, involves the attack of a reactive oxygen metabolite capable of abstracting a hydrogen atom from a methylene group in the lipid to form a conjugated diene. When oxygen is in sufficient concentration in the surroundings, the fatty acid radical will react with it to form $ROO^{\cdot}$ during the propagation stage. These radicals themselves are capable of abstracting another hydrogen. The propagation stage allows the reaction to continue. A single initiation can lead to a chain reaction. The last stage, chain termination, occurs following interaction of one $ROO^{\cdot}$ with another radical or antioxidants. In the last stage of the peroxidation process, peroxides are decomposed to aldehydes like malondialdehyde (MDA), which can be detected by thiobarbituric acid that gives a pink color easily measurable. The Thiobarbituric Acid Reactive Substances (TBARS) are considered to be a general indicator of oxidative stress rather than a specific marker of lipid peroxidation [97].
Since the primary substrate for lipid peroxidation is polyunsaturated fatty acids, it has been suggested that the amount of substrate available in the sample (i.e., levels of triglycerides) may be a major determinant of the amount of TBARS produced [97].
Indeed, as recently reviewed [98], wide literature data can be found, obtained by these methods in human blood (plasma, serum and red cell samples). In particular,

in plasma, oxidative damage was related to an increase of protein (e.g. albumin) oxidation as well as lipid (e.g. phospholipids, triacylglycerol's, cholesterol) peroxidation.
Carbonylation of protein often leads to a loss of protein function, which is considered a widespread marker of severe oxidative stress, damage and disease derived protein dysfunction in various pathophysiologies. Accumulation of protein carbonyls has been observed in Alzheimer's disease, diabetes, inflammatory bowel disease, and arthritis [96].
Also, increased level of lipid peroxidation products were found in plasma of patients with gynecological malignancies, respiratory distress syndrome, breast cancer, squamous cell carcinoma, colon cancer and various types of leukemia [99].
The methodological description of the enzymatic assay is presented in *chapter 2: Materials and Methods paragraph 2.5.*

1.2.2 Direct Method

However enzymatic assays can be considered 'a posteriori' methods with respect to Electron Paramagnetic Resonance (EPR), the technique able to provide direct detection of the 'instantaneous' presence of free radical species in the sample [100]. Nevertheless ROS half life (superoxide [$O_2^{\cdot -}$] $t_{1/2}$ (s): 10^{-4}; Nitric oxide [$NO^{\cdot}$]: 0,4s at ambient temperature), is too short if compared to the EPR time scale so they are EPR-invisible: only when 'trapped' and transformed in a more stable radical species they become EPR detectable [101,102].
Moreover, in EPR spectra, signal areas are proportional to the number of the excited electron spins, leading to absolute concentration levels, when adopting a stable radical compound as reference.
Despite the great interest in measuring ROS in biology and medicine, EPR technique has not till now been widely used because of several technical and methodological problem.
However, some works report about ROS identification in healthy subjects and in patients affected by various diseases (iron-deficient anemia; chronic gastritis, duodenal and gastric ulcers, ischemic heart and hypertension) [101].
Recently, Spasojevic I. [103] has described the ten most important features of the ROS experiments with EPR. That including the detect nanomolar concentrations of paramagnetic species, use of spin-probe, trap or label, few minutes for the acquisition, small samples (~100 μL), different type of sample fluid (e.g. plasma, cerebrospinal fluid, extracellular fluid, saliva, etc.), tissue samples, biopsy specimens, cell cultures, and solid samples (bones, tooth enamel); measured can be performed at changed temperature, atmosphere, or light regime. Moreover, the exact concentration is obtained from intensity/concentration calibration curve, which may be prepared by using synthetic paramagnetic compounds; also, the author emphasizes the importance of comparing the EPR data with biochemical methods, such as enzymatic assay methods, but also NMR, fluorometry, HPLC, and others.
EPR technique is the prince of all the work done, and for this reason, it seems appropriate to devote a little 'space.

1.2.2.1 EPR History

EPR was first detected in 1944 by Yevgeny Zavoisky at Kazan state university in the Soviet Union. The instrumentation required for EPR was greatly benefited by the development of radar during World War II, which required the use of reliable and tunable microwave sources. After the war, the necessary components for an EPR spectrometer were cheap and available. Initially, the field was advanced with the production of home-built EPR spectrometers. In the 1980s, commercially built EPR spectrometers became available. The German company Bruker leads the field in the production of commercially available EPR spectrometers, as well as NMR spectrometers and MRI detectors. Today, EPR spectroscopy is done at a wide range of frequencies and fields. In many ways, the physical properties that are the basis of EPR theory and methods are analogous to Nuclear Magnetic Resonance (NMR). The most obvious difference is the direct probing of electron spin properties in EPR as opposed to nuclear spin NMR. EPR is a spectroscopic technique, which detects species that have unpaired electrons. These include free radicals (FR) many transition metal ions, molecular structures. EPR is a non-destructive technique and the samples are very sensitive to local environments. EPR spectroscopy theory is described in *chapter 2: section 2.2.*

AIM OF THE STUDY

Aim of the research developed in the time course of the three years of my Doctoral course in Molecular Medicine was to shed light into the mechanisms involved in oxidative stress responses in man at both integrative and molecular levels.
Present study was to gain insight into the dual role-played by ROS as A) signaling or otherwise B) scavenged specimens developing a quantitative EPR method for their absolute ROS concentration assessment.
A) Signaling molecules were studied in human's blood. A mini-invasive procedure was developed and its reliability tested.
The method was then applied to environments where:

i) an increase (exercise, hypoxia)
ii) a decrease (training, antioxidant supplementation)
iii) an unbalance (pathologies)

of ROS level was accepted
For this reason several groups of selected subjects were selected. Point by point will be described the subjects' characteristics.
B) Molecules to be scavenged, in particular nitric oxide (NO), were studied in vitro. The role played by Myoglobin and in particular by Human Mb isoforms as NO scavenger was investigated.

2 MATERIAL AND METHODS

2.1 Metabolic measurements

2.1.1 Anthropometric

On all occasions upon arrival at the laboratory, subject body (kg) and height (cm) were measured by mean of a balance and a stadiometer respectively.
The body surface area (BSA) was calculated without direct measurement. We have used a Du Bois formula:

$$BSA = ((0{,}007184 * ((H^{0{,}725} * W^{0{,}445})) \quad (3)$$

where BSA is in m^2, W is weight in kg, and H is height in cm. BSA is a better indicator of metabolic mass than body weight because it is less affected by abnormal adipose mass.

2.1.2 Oxygen Saturation (SaO_2)

Arterial hemoglobin oxygen saturation (SaO2) was measured using finger pulse Oximetry - Ohmeda TuffSat (GE Healthcare, Helsinki, Finland) or/and Biox 3740 Pulse Oximeter Ohmeda, (Denver, CO, USA). Care was taken positioning the sensor on the end of an index finger. The light emitter portion was placed on the fingernail side and the detector on the site opposite to the nail. The pulse oximeter shines red and infrared light through the tissue and detects the fluctuating signals caused by arterial blood pulses. The accuracy of this measurement has been estimated at ± 2%.

2.1.3 Gas exchange (VO_2 and VCO_2)

VO_2max measure the maximum capacity of an individual's body to transport and use oxygen during incremental exercise, which reflects the physical fitness of the individual. This is reached when oxygen consumption remains at steady state despite an increase in workload. VO_2 max is expressed either as an absolute rate in liters of oxygen per minute (l/min) or as a relative rate in milliliters of oxygen per kilogram of bodyweight per minute (ml/kg/min). The subjects performed a grated exercise test with increasing oxygen consumption (VO_2max) with variation uphill and of velocity.
O_2 uptake (VO_2) and CO_2 output (VCO_2), both expressed in STPD (Standard Temperature (= 0°C), Pressure (=760mmHg), Dry (=0%) were determined breath by breath using a computerized metabolic cart Vmax 29c (SensorMedics, Bilthoven, Netherlands). Expiratory flow measurements were performed using mass flow sensor, calibrated before each experiment with 3-liter syringe at three different flow rates. VO_2 and VCO_2 were determined by continuously monitoring PO_2 and PCO_2 at the mouth throughout the respiratory cycle and from established mass balance equations, after alignment of the expiratory volume and expiratory

gases tracing and analog-to-digital conversion.
Calibration di O_2 and CO_2 analyzer was performed before each experiment by using gas mixtures of known composition. Digital data were transmitted to a personal computer and stored on disk. Gas exchange ratio was calculated as VCO_2/VO_2. Gas Exchange Threshold (GET) was determined using Standard methods [105].

2.1.4 Near Infra-Red Spectroscopy (NIRS)

In some experiments, the oxygenation changes in the vastus lateralis muscle were evaluated by Near Infra-Red Spectroscopy (NIRS). A portable near infrared single-distance, continuous-wave photometer (HEO-100, Omron, Japan), which adopts an algorithm based on diffusion theory, was utilized. Briefly, the instrument provides separate measurements of changes in deoxygenated Hemoglobin (Hb) and Myoglobin (Mb) concentrations:

$$\{\Delta[\text{deoxy(Hb+Mb)}]\} \quad (4)$$

expressed in arbitrary units [105]. Δ[deoxy(Hb+Mb)], with respect to an initial value arbitrarily set equal to zero, were calculated and expressed in arbitrary units. Δ[deoxy(Hb+Mb)] is the result of the balance between VO_2 and O_2 delivery in the portion of tissue investigated by the NIRS probe and, therefore, is conceptually similar to fractional O_2 extraction [106,107]. A “physiological calibration” of the Δ[deoxy(Hb+Mb)] values was performed: data obtained during the exercise protocol were expressed as a ratio of the values determined by obtaining a maximal deoxygenation of muscle after the exercise period, by pressure cuff inflation (at 300–350 mmHg) at the root of the thigh (subjects in the sitting position on the cyclo-ergometer) for a few minutes until Δ[deoxy(Hb+Mb)] increase reached a plateau. NIRS measurements in muscle tissue [108] have been shown to be well correlated with local venous O_2 saturation. Average values of Δ[deoxy(Hb+Mb)] were calculated during the last 10s of each workload. The resulting Δ[deoxy(Hb+Mb)] data were expressed as a function of work rate and were fitted by a sigmoid function of the type:

$$f(x) = f0 + A/[1+e^{-(-c+dx)}] \quad (5)$$

When t0 represents the baseline, A the amplitude and c is a constant dependent on d, the slope of the sigmoid. In this function c/d gives x values corresponding to (f0+A)/2, which is the work rate corresponding to half-amplitude.

2.2 The theory of EPR spectroscopy

The basic concepts of EPR are analogous to those of NMR, but it's electron spins that are excited instead of the spin of atom nuclei. Because most stable molecules have all their electrons paired, the EPR technique is less widely used than NMR.
The phenomenon of EPR (see **Figure 8**) is based on an intrinsic magnetic moment of the electron that arises from its spin. In most system, electrons occur in pairs, such that the net magnetic moment is zero. However, if an unpaired electron is present, its magnetic moment can suitably interact with a magnetic field. This effect is called the Zeeman effect.
Because the electron has a magnetic moment, it acts a compass or a bar magnet when it's placed in a magnetic field. Since energies are quantized, a single unpaired electron has only two allowed energy states. It has a state of lower energy when the moment of electron, μ, is aligned with the magnetic field and a higher energy state when μ is aligned against the magnetic field.
The two states are designated by the projection of the electron spin, m_s, on the direction of the magnetic field. Because the electron is a spin 1/2 particle, the parallel state has m_s=-1/2 and the antiparallel state has m_s=+1/2. The difference between the energies of these two states, caused by the interaction between the electron spin and the magnetic field is shown in equation 6.

$$\Delta E = g\mu_B B_0 \Delta m_s = g\mu_B B_0 \quad (6)$$

When g is g-factor, μB is the Bohr magneton, which is the natural unit of the electron's magnetic moment, and the change in spin state is Δms = 1. The energy, ΔE=hν, that is required to cause a transition between the two spin states is given by

$$\Delta E = h\nu = g\mu_B B_0 \quad \text{and} \quad \mu_B = g_e \beta/2 \quad (7)$$

Absorption of energy occurs when the magnetic field "tunes" the two spin states such that the energy difference matches the energy of the applied radiation. This field is called the "field for resonance". Because of difficulties in scanning microwave frequencies and because of the use of a resonant cavity for signal detection, most EPR spectrometers operate at constant microwave frequency and scan the magnetic field. The field for resonance is not a unique "fingerprint" for identification of a compound because spectra can be acquired at different microwave frequencies. The g-factor

$$g = h\nu / \mu_B B_0 \quad (8)$$

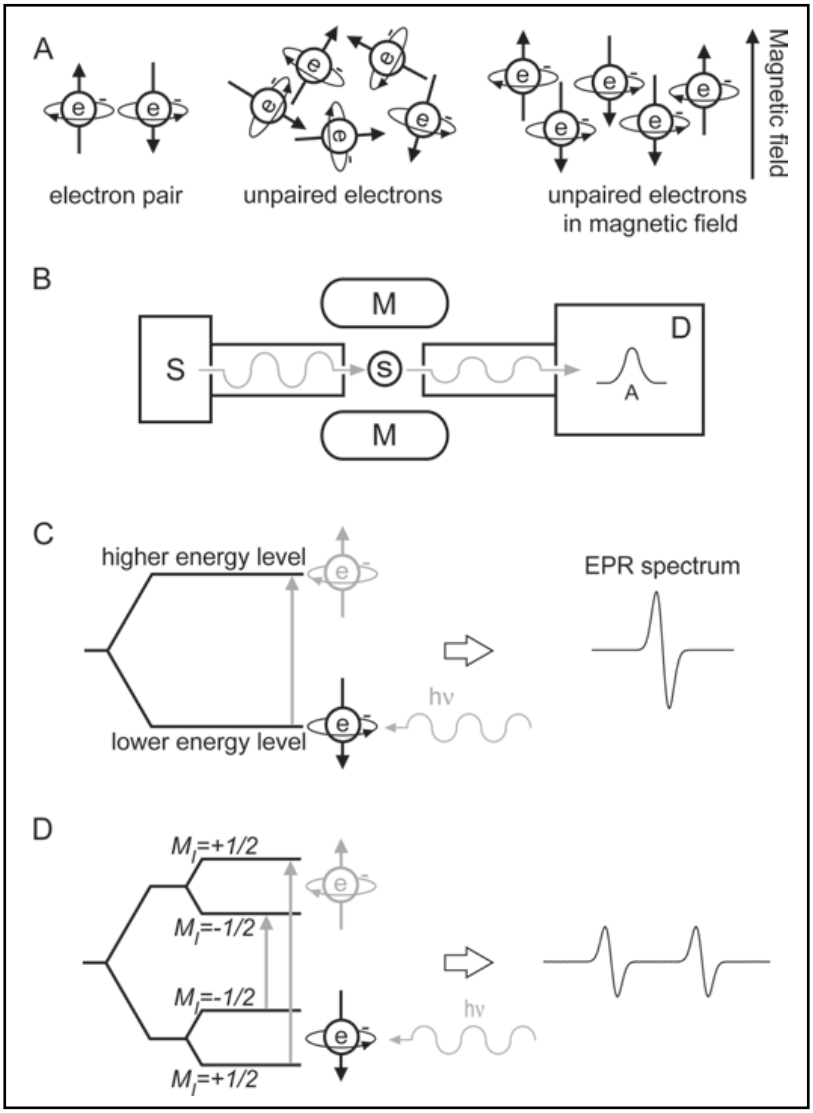

***Figure 8**: Schematic description of the basic principles of EPR spectroscopy. **A**) Electron out and in the magnetic field. **B**) The scheme of the EPR spectrometer (S: the source of the oscillating magnetic filed; M: magnets generating static magnetic field; s: sample; D: detector; A: absorption line). **C**) The energy-level scheme of unpaired electron showing EPR absorption and corresponding spectrum with one line. **D**) The energy-level scheme of unpaired electron coupled with a nucleus with I=1/2, showing two resonant transitions and corresponding spectrum with two lines.*

is independent of a microwave frequency, so the g-factor is a better way to characterize signals. Those high values of g occur at low magnetic fields and vice versa. The g-factor helps to distinguish and identify types of sample.
Additional information about the species that contains the unpaired electron can be obtained from nuclear hyperfine interactions. The nuclei of the atoms in a molecule or complex often have magnetic moments, which produce a local magnetic field at the electron. The interaction between the electron and the nuclei is called the hyperfine interaction. It gives a wealth of information about the sample such as the identity and number of atoms that make up a molecule or complex: as well as the electron spin density at nuclei that have magnetic moments.
The magnetic moments of the nucleus acts like a bar magnet and produces a magnetic field at the electron, b_i. In a general case of interaction with the nucleus spin i=1/2 the number of hyperfine components is defined by the following formula:

$$2nI + 1 \tag{9}$$

2.2.1 EPR Instrument

EPR spectroscopy can be carried out by either 1) varying the magnetic field and holding the frequency constant or 2) varying the frequency and holding the magnetic field constant (as is the case for NMR spectroscopy).
frequency constant, opposite of NMR spectrometers. The majority of EPR spectrometers are in the range of 8-10 GHz (X-band), though there are spectrometers which work at lower and higher fields: 1-2 GHz (L-band) and 2-4 GHz (S-band), 35 GHz (Q-band) and 95 GHz (W-band).
EPR spectrometers work by generating microwaves from a source (typically a klystron), sending them through an attenuator, and passing them on to the sample, which is located in a microwave cavity (**Figure 9**). Microwaves reflected back from the cavity are routed to the detector diode, and the signal comes out as a decrease in current at the detector analogous to absorption of microwaves by the sample. Now I will explain the proprieties of microwave (EPR) cavities and how changes in these proprieties due to absorption result in an EPR signal. Resonators are used to amplify weak signals from the sample. There is no loss of generality if descriptions are based on a microwave cavity, which is simply a metal box with a rectangular or cylindrical shape that resonates with microwaves much as an organ pipe resonates with sound waves. Resonance means that the cavity stores the microwave energy. Cavities are characterized by their Q or quality factor, which indicates how efficiently the cavities stores microwave energy. As Q increases, the sensitivity of the spectrometer increases.
The Q factor is defined as:

$$\boldsymbol{Q} = \frac{\boldsymbol{2\pi\ (energy\ stored)}}{\boldsymbol{energy\ dissipated\ per\ cycle}} \tag{10}$$

where the energy dissipated per cycle is the amount of energy lost during one microwave period. Energy can be lost to the side walls of the cavity because the microwave generate electrical currents in the side walls of the cavity which in turn generates heat. Q factor can be measured easily because there is another way of expressing Q:

$$\boldsymbol{Q} = \frac{\boldsymbol{\nu_{res}}}{\boldsymbol{\Delta\nu}} \tag{11}$$

where ν_{res} is the resonant frequency of the cavity and $\Delta\nu$ is the width at half height of the resonance.

Microwaves are coupled into the cavity via a hole called an iris. The size of the iris controls how much of the microwave power is reflected back from the cavity and how much enters the cavity. The iris accomplishes this by carefully matching or transforming the impedance (the resistance to the waves) of the cavity and the waveguide. An iris screw in front of the iris lets the user adjust the "matching". When the impedances are matched, the resonator is said to be "critically coupled".

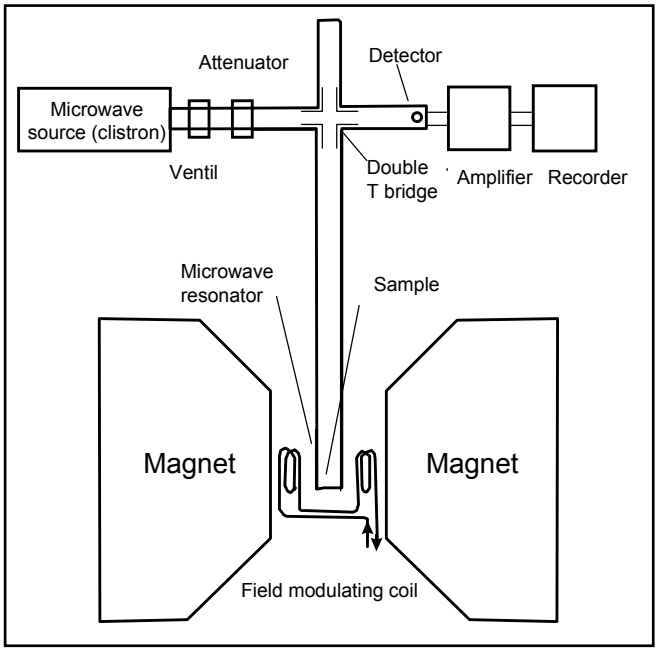

***Figure 9**: Microwave cavities.*

2.2.2 The Signal Channel

All individual components of the EPR spectrometer work together to produce a spectrum (see below **Figure 10**).

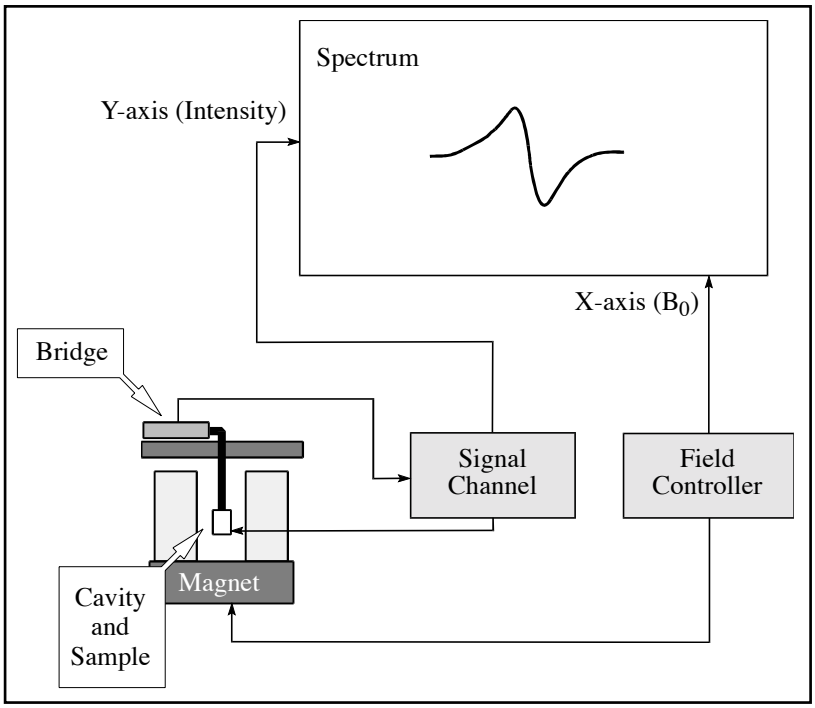

***Figure 10**: Block diagram for an EPR spectrometer.*

EPR spectroscopy uses a technique known as phase sensitive detection to enhance the sensitivity of the spectrometer. The signal channel contains the required electronics for the phase sensitive detection. The magnetic field strength, which the sample sees, is modulated sinusoidally at the modulation frequency. The modulation frequency should be less than the line width, since it causes side bands at a distance of the modulation frequency.

With that we get the complete time dependency of the magnetic field:

$$\boldsymbol{B = B_{initial} + const\,.\,t + B_{modulation}\,.\,sin(2\pi\nu_{modulation}.\,t)} \quad (12)$$

If there is an EPR signal, the field modulation quickly sweeps through part of the signal and the microwaves reflected from the cavity are amplitude modulated at the same frequency.
For an EPR signal that is approximately linear over an interval as wide as the modulation amplitude, the EPR signal is transformed into a sine wave with amplitude proportional to the slope of the signal (**Figure 11-12**). The signal channel produces a DC signal proportional to the amplitude of the modulated EPR signal. Any signals (such as noise and electrical interference) that do not fulfill these requirements are suppressed. To further improve the sensitivity, a time constant is used to filter out more of the noise.

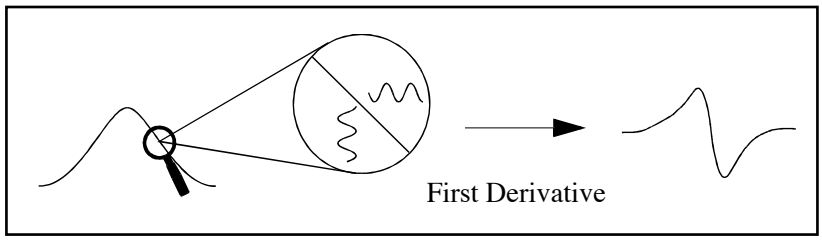

***Figure 11**: Field modulation and phase sensitive detection.*

Phase sensitive detection with magnetic field modulation can increase the sensitivity by several orders of magnitude; however, the user must be careful in choosing the appropriate modulation amplitude, frequency and time constant. At low modulation amplitudes, as the amplitude of the magnetic field modulation is increased, the height of the detected EPR signals increased. If the modulation amplitude is too large, the detected EPR signal broadens and becomes distorted (**Figure 13A**). To get the most accurate information about signal line-shape, the modulation amplitude should be less than 10% of the distance (in Gauss) between the positive and negative peaks in the derivate spectrum. Higher modulation amplitudes cause broadening of the signal, the integrated intensity of the signal continues to increase linearly with modulation amplitude so if the goal of the experiment is primarily spin quantitation, higher modulation amplitude may be used to further improve signal-to-noise. Time constants selected by the operator will affect the noise in the spectrum. Increased time constant filter out noise by slowing down the response time of the detection circuit. As the time constant is increased, the noise level decreased. If a time constant is selected that is too long for the rate at which the magnetic field is scanned, the signal may be distorted or even missed. **Figure 13B** shows the distortion and disappearance of a signal as the time constant is increased. **Figure 13C** shows an example with very narrow or closely spaced EPR signals (~50 mG), the signal is broadened if the modulation frequency is too high. The 100 KHz modulation frequency corresponds to 35 mG sidebands on the EPR signal.

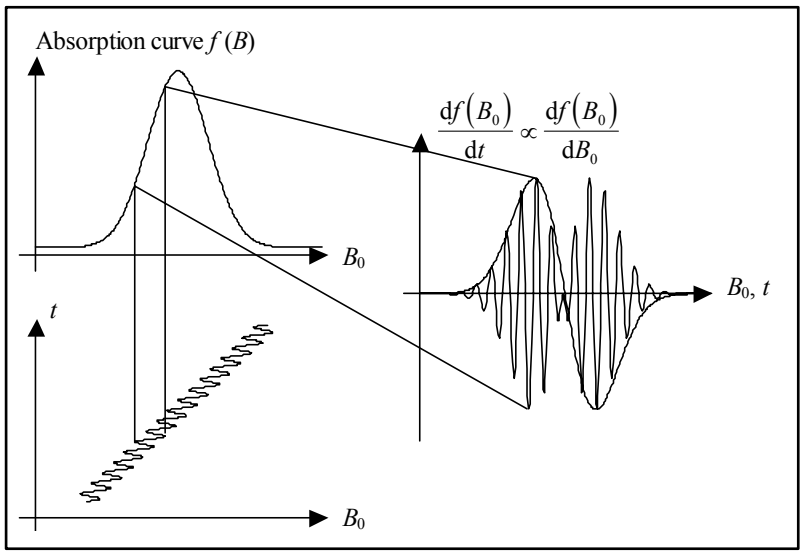

***Figure 12**: Differential scanning and phase sensitive detection. Show how the Gaussian line defined as $\int(\boldsymbol{B}) = \boldsymbol{exp}\{-\boldsymbol{B} - \boldsymbol{\alpha})/\boldsymbol{\beta}\}$ is differentially scanned. The lower left of figure shows the time dependency of the magnetic field from equation 12. The field B_0 scans the absorption signal like a characteristic curve. The dotted lines indicate the passage of half a modulation period in the time domain. The steeper the slope (first derivative) of the absorption signal, the larger is the energy difference between two peeks of the modulation field. At the maximum of the absorption curve, this difference is zero. During passage through the maximum, the phase of the oscillating signal drawn lightly in the right part of figure with the frequency $v_{modulation}$ jumps by 180°C. The oscillating signal is applied to the input of the phase sensitive detector (look in amplifier), and the phase sensitive detected signal is shown as a thick stretched-out line on the right side of figure.*

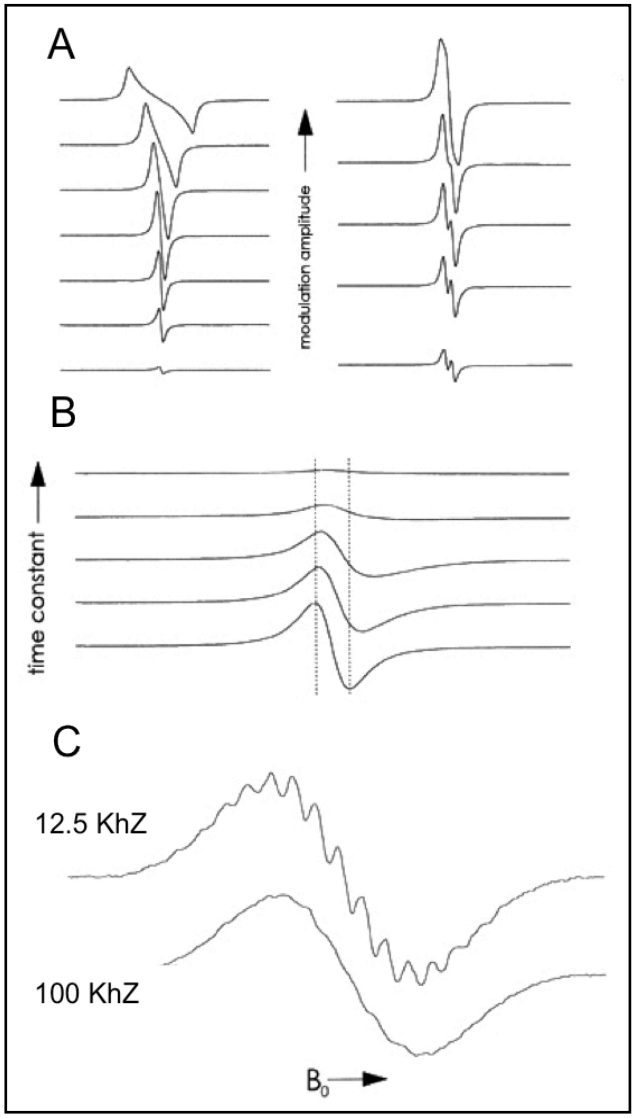

***Figure 13**: **A**) Signal distortions due to excessive field modulation; **B**) Signal distortion and shift due to excessive time constant; **C**) Loss of resolution due to high modulation frequency.*

2.3 Subjects

ROS production rate (at rest and after exercise/training) was assessed in different healthy subjects' categories:

- Healthy sedentaries (one hundred; age 45 ± 7; 50 male and 50 females)
- Healthy sedentary woman (10 females; mean age 48.80 ± 5.32; height 164 ± 3 cm; body mass 56.81 ± 10.35 Kg)
- Healthy sedentaries (12 females and 10 males, age 66 ± 5.4)
- Hockey players (18 males, age 19.70 ± 1.16; height 178 ± 4 cm; body mass 77.65 ± 6.97 Kg)
- Swimmers (10 males, age 30 ± 5; height 1.82 ± 4,7; body mass 78.6 ± 5Kg)
- Triathletes (28 males, age 42 ± 7.8; height 174.6 ± 5 cm; body mass 70.7 ± 7.2 Kg, years of training 5 ± 1.5). The mean time race was 6.14'.43" in short (ShC) and 12.48'.21" in long (Ironman)

Hypoxia effects were tested in thirty-six subjects at different heights on sea level:

- 4100 m: n=4, (2 males and 2 females, age 23 ± 1.25; height 175 ± 5 cm; body mass 75.55 ± 4.95 kg)
- 3480 m: n= 14, (5 males and 9 females, age 33.30 ± 7.6, height 168 ± 7 cm; body mass 58.5 ± 12.6 Kg)
- 1860 m: n= 18 males (age 19.70 ± 1.16, height 178 ± 4 cm; body mass 77.65 ± 6.97 Kg)

Unbalance ROS production were assessed in patients affected by degenerative diseases:

- type II Diabetic Neuropathies (4 males and 4 females, age 64.5 ± 2.6)
- Mild Cognitive Impairment (MCI) (17 males and 19 females, age 73 ± 4.2)
- Sporadic Amyotrophic Lateral Sclerosis (ALS) (16 males and 6 females, age 60.7 ± 12)

A written informed consent was signed by all participants after being informed of all risks, discomforts and benefits involved in the study. Procedures were in accordance with the Declaration of Helsinki, and institutional review board approval was received for this study.

2.3.1 Increase ROS production

2.3.1.1 Physical Exercise

In laboratory (IBFM – CNR Laboratory of Milan), the exercise effects on ROS production were tested in: I) hockey players and II) swimmers. During the physical effort electrocardiogram (ECG) was registered to detect possible cardiac pathologies. In *section 2.1.3* description of gas exchange.

I) Varese **hockey team** were recruited to participate in the study. The subjects visited the laboratory two times. On the first day, blood collection and anthropometric measures were collected and an incremental test on treadmill (1% of grade) up to voluntary exhaustion to assess gas exchange threshold (GET) and peak O_2 uptake (VO_2 peak) was also performed. After six minutes of warm up exercise (according to the subject's estimated level of physical fitness), the speed was increased 1 km $\cdot$ h^{-1} every minute. On the second visit, at least seven days after, the subjects performed a 10 minutes constant-load submaximal exercise (CLE) at heavy-intensity and speed corresponding to a VO_2 equal to ~50% of the difference between GET and VO_2 peak. The experimental protocol is shown in **Figure 14**. Voluntary exhaustion was defined as the inability to maintain the running frequency, despite vigorous encouragement by the operators, as well as by maximal levels of self-perceived exertion using the validated Borg scale (**Table 2**) [109]. EPR data were compared with complementary enzymatic assays of PC, TBARS.

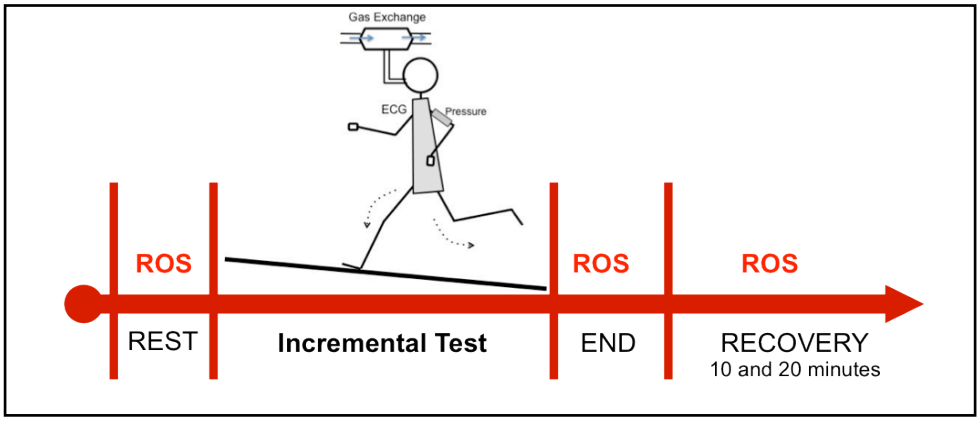

***Figure 14**: EPR protocol adopted to measure ROS production rate in Hockey players.*

Level	Borg Rating of Perceived Exertion Scale
0	Nothing
1	Really easy
2	Easy
3	Moderate
4	Sort of Hard
5	Hard
6	
7	Really Hard
8	
9	Really, Really Hard
10	Maximal

***Table 2**: The Borg Scale: takes into account the fitness level and is a simple method of rating perceived exertion*

II) Saronno master **swimmers** were recruited and the subjects visited the laboratory two times (pre and post eight weeks training protocol – **Figure 15**). A mechanical arm-ergometer (Monark 891E, Stockholm, Sweden) was utilized. The ergometer had an adjustable seat and handlebars, which were set to suit each individual subject. All subjects were instructed to remain seated during the test. Blood collection and anthropometric measures were collected in every time. In these subjects were tested the immediate effects of incremental test (IT) up to voluntary exhaustion and the long-term training effects were tested.
Voluntary exhaustion was defined as the inability to maintain the armful frequency, despite vigorous encouragement by the operators, as well as by maximal levels of self-perceived exertion using the validated Borg scale (**Table 2**) [109]. Arm-ergometer workload was adjusted by manually placing weights on the attached basket. **Table 3** below shows the characteristics of the swimmers.

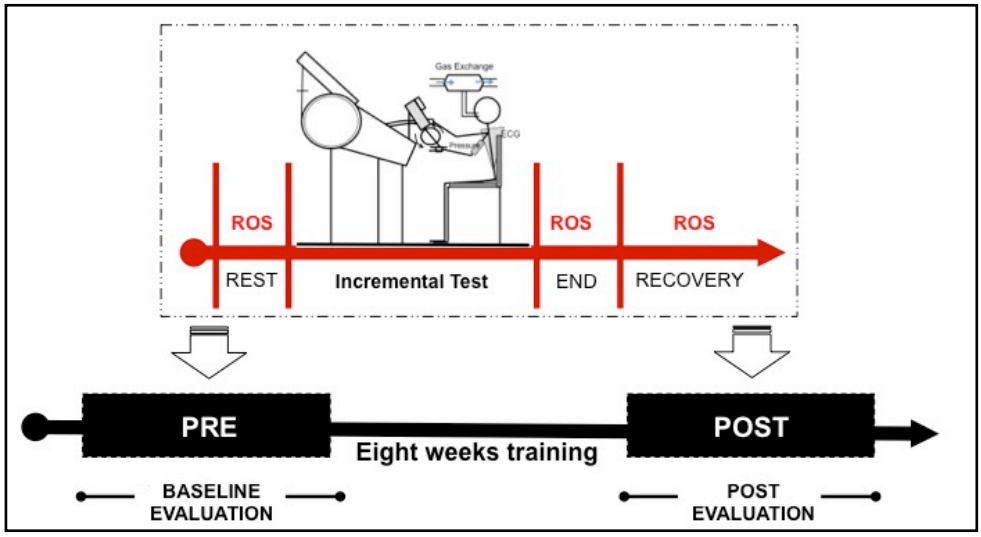

***Figure 15**: EPR protocol adopted to measure ROS production rate in swimmers.*

Features of Swimmers (mean ± DS) N° = 10, all males		
	PRE	**POST**
Age (years)	32.4 ± 5.08	32.4 ± 5.08
Weight (kg)	78.6 ± 5	78.8 ± 5.1
Height (cm)	182.2 ± 4.7	182.2 ± 4.7
BMI	23.7 ± 16.8	23 ± 3.2
Fat Mass	16.8 ± 3.6	13 ± 2.9
Free Fat Mass	65.3 ± 2.3	65.7 ± 2.9
BSA	2.18 ± 0.07	2.18 ± 0.08
BORG	16.8 ± 1.6	17.2 ± 1.3
VO_2max ($mL \cdot Kg^{-1} \cdot min^{-1}$)	36.1 ± 4.2	40.6 ± 5.7

***Table 3:** Features of the swimmers. The "PRE" indicates the value at baseline (before training) and "POST" indicates the value after training. (BMI: Body Mass index; BSA: Body Surface Area; BORG: Rating of Perceived Exertion Scale)*

2.3.1.2 Long-Duration Exercise

Long-Duration exercise effects were tested in triathletes during **Triathlon competition** (Elbamen 2012, 8th edition, 30 September 2012).

Anthropometric measures, SaO_2 and blood sample for chemical laboratory analysis were collected in two time: at rest (pre competition) and immediately after endurance competition; 13 athletes who performed a short-competition (ShC 7.3): swim 1.9Km, bike 94Km and run 21,1Km; 15 performed a long-competition (Ironman): swim 3.8Km, bike 180Km, run 42.2Km. The protocol adopted to measure the ROS production s shown in **Figure 16**. The characteristics of the triathletes are shown in **Table 4**.

EPR data were compared with complementary enzymatic assays of TBARS, PC, values by blood chemical laboratory test and anthropometrics measures.

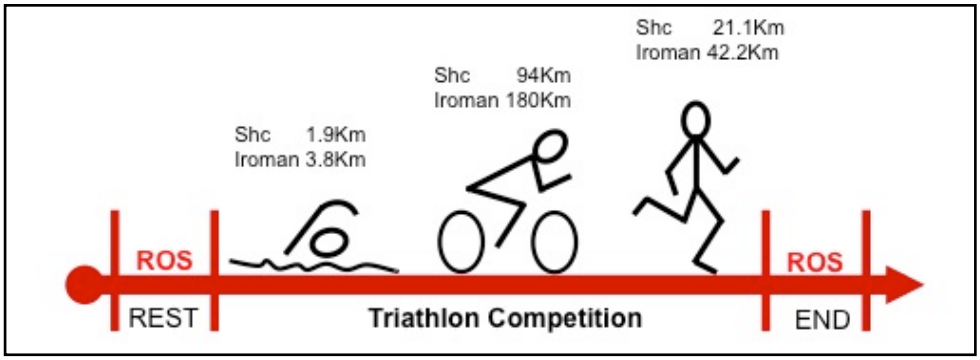

***Figure 16**: EPR protocol adopted to measure ROS production rate in Triathletes.*

Features of Triathletes (mean ± DS) N° = 28, all males					
	ShC 7.3			IRONMAN	
	PRE	POST		PRE	POST
Age (years)	42.9 ± 8.8	42.9 ± 8.8		41.3 ± 7.1	41.3 ± 7.1
Weight (kg)	71.2 ± 7.4	69.5 ± 7.7		70.3 ± 5.2	68.4 ± 5
Height (cm)	174.3 ± 5.6	174.3 ± 5.6		174.9 ± 4.5	174.9 ± 4.5
PAS (mmHg)	125.5 ± 3.4	122.8 ± 17.7		122.5 ± 17	121.4 ± 12.7
PAD (mmHg)	72.5 ± 13.5	68.5 ± 8.5		72.5 ± 10.4	71.6 ± 8.5
BSA	2.02 ± 0.12	1.99 ± 0.13		2.01 ± 0.09	1.99 ± 0.09
HR	60.5 ± 8.7	85.2 ± 17.2		59.1 ± 16.7	80.8 ± 14.2
SO_2	97.8 ± 0.6	96.6 ± 1.3		97.6 ± 0.9	97.4 ± 1.5

Table 4: *Features of the Triathletes: PAS: Sistolic Pressure; PAD: Diastolic Pressure; BSA: Body Surface Area; HR: Heart Rate; SO_2:Oxygen Saturation.*

2.3.1.3 Acute Normobaric Hypoxia

Sedentary subjects (n=4, aged 23 ± 1.25 years; height 1.75 ± 0.05 m; body mass 75.55 ± 4.95 kg) reported to the laboratory early in the morning after a light breakfast, and sat comfortably on a chair where remained over the 6 h. The room temperature was kept constant at 21°C. Venous and capillary blood samples were withdrawn for oxidative markers and ROS determination (0 h). Subsequently, subjects started breathing a normobaric hypoxic mixture (12.5% O_2 in air, simulating about 4100m altitude) obtained by removing a controlled amount of oxygen from air (MAG-10, Higher Peak LLC, Winchester, MA, USA). The mixture was delivered through a facemask at 30 l min^{-1}. Excess airflow was diverted outside the mask to prevent inspired oxygen pressure from increasing above 90 Torr. Arterialized blood oxygen saturation was monitored by finger pulse oximetry (Biox 3740 Pulse Oximeter, Ohmeda, Denver, CO, USA); venous and capillary blood samples were withdrawn at different times during the test. At the end of the fourth hour subjects were switched to normoxic breathing conditions and blood samples withdrawn for up to 2 h.

2.3.1.4 Acute Hypobaric Hypoxia

ROS production was determined in sedentary subjects (aged 33.30 ± 7.6 years; height 1.68 ± 0.07 m; body mass 58.5 ± 12.6 kg). Capillary blood samples were withdrawn before (at Turin) and during 24 hours sojourn at Plateau Rosà (3480m s.l.) (see **Figure 17A**).

2.3.1.5 Prolonged Hypobaric Hypoxia

ROS production at rest was determined in male elite athletes (aged 19.70 ± 1.16 years; height 1.78 ± 0.04 m; body mass 77.65 ± 6.97 kg) before and 1 week after the return at sea level after 2 weeks exposure to moderate altitude (Livigno, 1860m s.l.) and 1 week after the return at sl. Data were compared with complementary enzymatic assays of TABARS and PC (see **Figure 17B**).

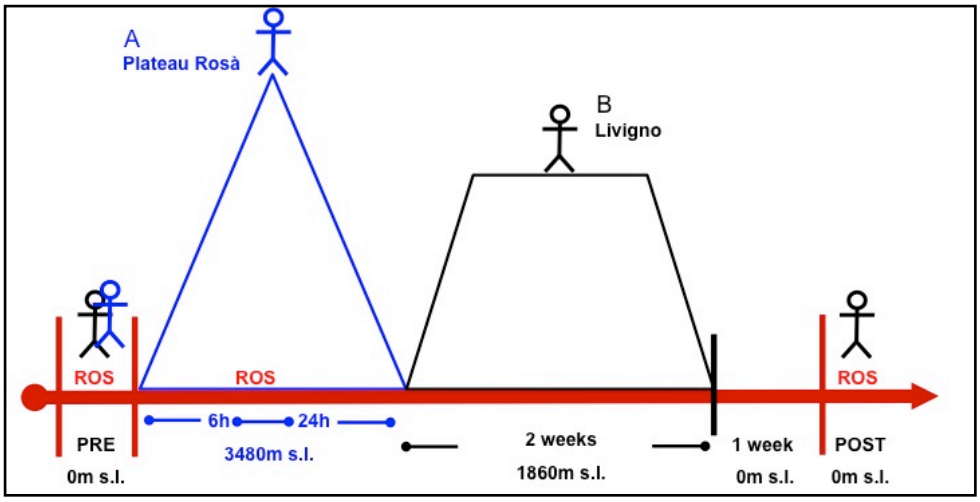

***Figure 17**: EPR protocol adopted to measure ROS production rate in **A**) Acute Hypobaric Hypoxia; **B**) Prolonged Hypobaric Hypoxia.*

2.3.2 Decrease ROS production

2.3.2.1 Training

Training effect was tested in master **swimmers**. Features of athletes are reported in **Table 3** (*see section 2.2.1.1*). Training was performed for 8 weeks with a high-volume/low intensity program.

Before (PRE) and after (POST) training they were tested by an arm-ergometer incremental test (IT). ROS production was analyzed at REST, at the END and after 10 minutes of passive recovery (RECOVERY). **Figure 15** (*see section 2.3.1.1*) show the protocol adopted to measure the ROS production by EPR.

2.3.2.2 Antioxidant Supply

The effect in acute antioxidant treatment (R-Thioctic acid: 1cp * 1.6g) was studied in ten healthy sedentary woman (mean age 48.80 ± 5.32 years; height 1.64 ± 0.03 m; body mass 56.81 ± 10.35 kg). Time course of ROS production rate was calculated at pre (0 minutes) and at 20, 40, 60, 90, 120 and 180 minutes after antioxidant supplementation. Control experiments were performed in the same subjects without supplementation.

2.3.3 Unbalance ROS production

Unbalanced ROS production in neurodegenerative pathologies (patients affected by type II Diabetic Neuropathy (type II DN), Mild Cognitive Impairment (MCI) and sporadic Amyotrophic Lateral Sclerosis (sALS)) was checked at baseline. The effect of exercise/training and/or the antioxidant supply was investigated.

Two projects are currently in progress.

2.3.3.1 type II Diabetic Neuropathy

i) CNR-IBFM and Istituto Auxologico of Milan collaborations: project to test the antioxidant effects on type II diabetic patients (n° = 8) with peripheral neuropathy after supplementation R-Thioctic acid: (1cp * 1.6g)*30 days.

In healthy subjects, preliminary test were conducted to get an idea of the kinetics of absorption and effect of the integrator. Results have been encouraging (Data not shown in this thesis).

[Diabetic neuropathy is the most common cause of neuropathy and clinically manifests as diffuse or focal forms. Furthermore, oxidative stress plays a central role in the pathogenesis of peripheral neuropathies since it determines a reduced supply of metabolites in nerve cells, resulting in cellular necrosis. It therefore aggravates the impairment of nerve conduction, worsening symptoms and the quality of life of patients. An improvement on the signs of neuropathy is reported in the literature, in patients who have been administered the α lipoic-acid (600mg/die), which interacts with many enzymes to convert glucose, fatty acids and other energy sources in (ATP).
EPR determination may be useful for the analysis of the effects of antioxidant substances (see section 3.1.7.2)].

The drafting of a project followed these on patients with the approval of the hospital Ethics Committee. The protocol study (show in **Figure 18**) included collected venous and capillary blood sample started a couple of months ago.

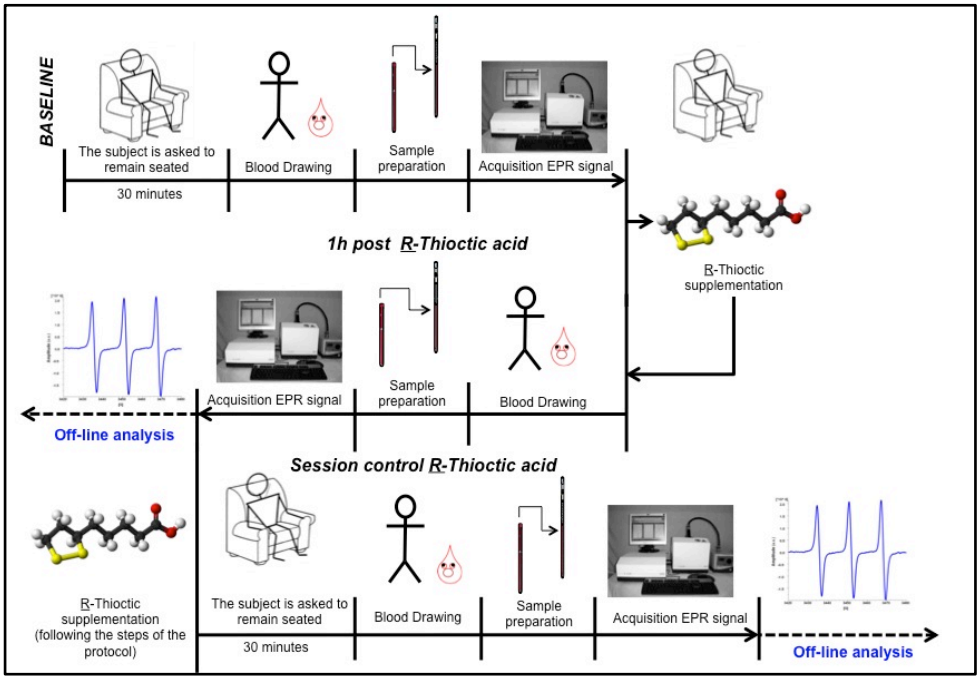

***Figure 18**: Protocol adopted to measure ROS production rate in type II Diabetic Neuropathic patients after R-Thioctic acid supplementation.*

2.3.3.2 sporadic Amyotrophic Lateral Sclerosis

ii) CNR-IBFM and Fondazione Maugeri (Veruno – Novara) collaboration: project to test the exercise and training effects in sporadic Amyotrophic Lateral Sclerosis (sALS) patients (n°=24).

[ALS is a progressive neurodegenerative disease characterized by loss of motor neurons in the anterior horns of spinal cord, brainstem motor nuclei, cerebral cortex and ultimately to death due to respiratory failure, usually within 3 to 5 years after disease onset. ALS pathogenesis included oxidative stress, endoplasmic reticulum stress, excitotoxicity, mitochondrial dysfunction, neural inflammation, protein misfolding and accumulation, dysfunctional intracellular trafficking, abnormal RNA processing, and noncell-autonomous damage].

Each subject participated in two visits over a twenty weeks time period. (t0 pre and t1 post training). The experiments were conducted in the morning. **Figure 19** shows the experimental protocol.
The protocol evaluation included: collected venous (at rest and 15 minutes after the end of the exercise) (*see section 2.5.1*) and capillary blood sample (at rest, immediately after and 15 minutes after the end of the exercise); Incremental Test (IT) with Gas exchange (VO_2 and VCO_2) (*see section 2.1.3*) and NIRS analysis of oxygenation changes in the vastus lateralis muscle (*see section 2.1.4*); at the end

of exercise, pressure cuff inflation (at 300–350 mmHg) at the root of the thigh for a few minutes until Δ[deoxy(Hb+Mb)] increase reached a plateau (*see section 2.1.4*). After a 1-minute unloaded-cycling period, a ramp protocol at a pedaling rate of approximately 60 rpm was started. Pedaling frequency was digitally displayed to the subjects. Incremental exercise testing was conducted while the subject was seated on the electronically braked cycle ergometer (Ergo-Metrics 800S; SensorMedics; Yorba Linda, CA, USA) and breathing ambient air through a mouthpiece.

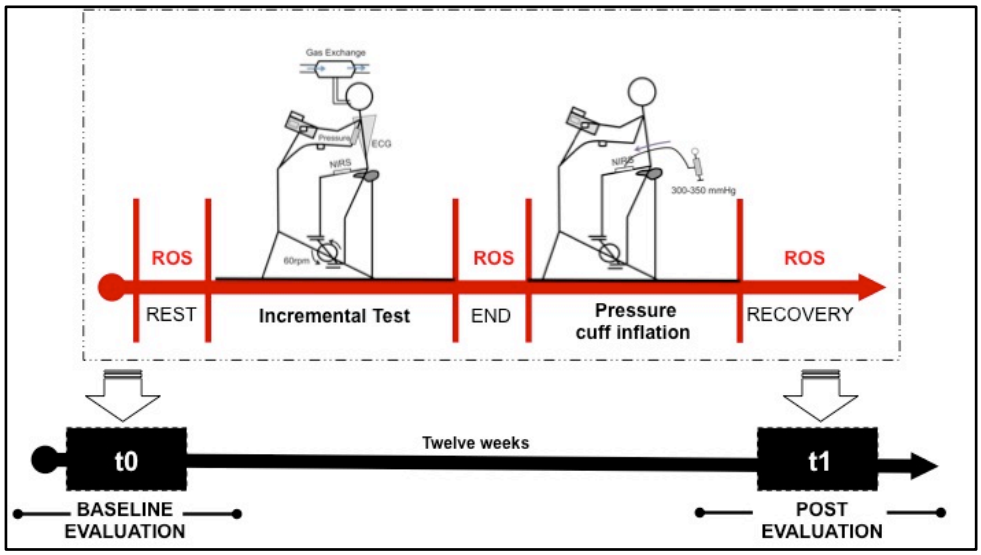

***Figure 19**: EPR protocol adopted to measure ROS production rate in sALS patients.*

2.4 EPR measurements "in Vivo"

All experiments were carried out by the e-scan EPR instrument (Bruker, Germany) operating at the common X-Band microwave frequency (~ 9.8 GHz). The instrument is interfaced to a temperature and gas controller Bio III unit (Noxigen Science Transfer & Diagnostics GmbH, Germany) allowing to maintain temperature at a constant chosen level and to regulate O_2, CO_2 and or other gas partial pressure.

2.4.1 Detection of ROS in Human Blood

2.4.1.1 Fresh Blood

The experimental protocol adopted for ROS detection is shown in **Figure 20**. All EPR spectra were recorded and processed by using a standardly supplied by Bruker software (Win EPR 2.11 version). For EPR experimental procedures, 50 µl of capillary blood, collected in heparinized capillary tubes (Cholestech LDX, Germany), were analyzed (see **Figure 20A**). Among spin trapping (otherwise labelled probe) molecules, suitable for biological utilization, 1-hydroxy-3-methoxycarbonyl-2,2,5,5-tetramethylpyrrolidine (CMH, Noxygen Science Transfer & Diagnostics, Germany) was adopted (see **Figure 21**). A 1 mM CMH solution was prepared in buffer (Krebs-Hepes buffer (KHB) containing 25 mM deferroxamine methane-sulfonate salt (DF) chelating agent and 5 mM sodium diethyldithio-carbamate trihydrate (DETC)) at pH 7.4. Blood was immediately treated with CMH (1:1). 50 µl of the obtained solution was put in the glass EPR capillary tube (Noxygen Science Transfer & Diagnostics, Germany), that was placed inside the cavity of the e-scan spectrometer (Bruker, Germany) for data acquisition (see **Figure 20B**). Acquisition EPR parameters were: microwave frequency = 9.652 GHz; modulation frequency: 86 kHz; modulation amplitude: 2.28 G; center field: 3456.8G, sweep width: 60 G, microwave power: 21.90 mW, number of scans: 10; receiver gain: $3.17*10^{1}$. Sample temperature was firstly stabilized and then kept at 37°C by the Temperature & Gas Controller "Bio III" unit, interfaced to the spectrometer. The actual amount of solution analysed was chosen to fill the entire sensitive area of the resonator cavity. An example of the recorded EPR signal showing the triplet coming from the interaction of the ^{14}N-OH group of CMH with the ROS oxygen unpaired electron ($NOH + O_2^{\bullet} \rightarrow NO^{\bullet} + H_2O_2$) is displayed in **Figure 20C**. The radicals generated by the reaction of the probe with the blood radicals were acquired and the spectra sequentially recorded for about 5 min (**Figure 20D**) in order to calculate the ROS production rate. The EPR signal is proportional to the unpaired electron numbers and could, in turn, be transformed in absolute produced micromoles ($\mu mol \cdot min^{-1}$): the stable $CP^{\bullet}$ (3-Carboxy-2,2,5,5-tetramethyl-1-pyrrolidinyloxy) radical signal was recorded in a separate session and used as reference.

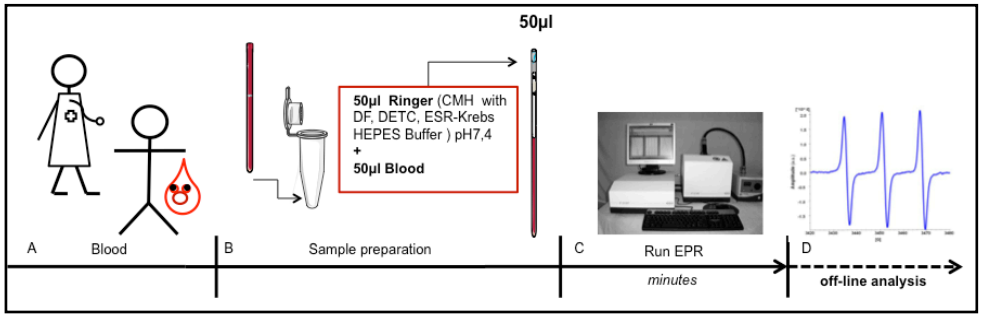

***Figure 20**: Step by step sketch of the EPR experimental protocol adopted to measure the ROS production rate in fresh blood.*

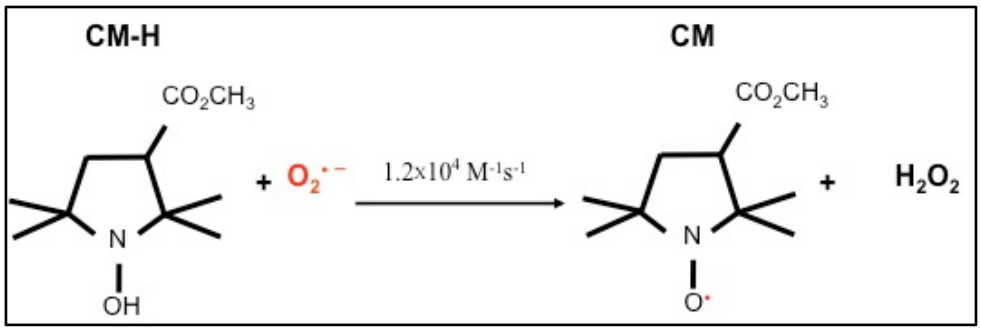

***Figure 21**: Detection O_2 with EPR spectroscopy spin-probe using 1-hydroxy-3-methoxycarbonyl-2,2,5,5-tetramethylpyrrolidine (CMH) molecule.*

2.4.1.2 Frozen Blood

Figure 22 shows the EPR protocol adopted for samples of frozen human blood. Approximately 2 ml of venous blood was drawn from an antecubital vein, with subjects lying on a bed (see **Figure 22A**). The samples were collected in heparinized vacutainer tubes (Vacutainer, Becton Dickinson, USA). 100µl of venous blood was immediately treated with CMH (1:1), as described in the previous *section 2.4.1.1*, and incubated for 15 minutes at 310K (see **Figure 22B**). During sample incubation, two previously filled of buffer containing DF and DETC (200µl each) and then in liquid nitrogen (N_2) frozen caps were put inside a 1ml insulin syringe. After incubation, 200ul of blood sample were inserted into the syringe and in turn frozen in liquid N_2 (see **Figure 22C**). EPR measurements were

carried out on the so frozen blood samples transferred in an EPR tube held by a finger-tip liquid nitrogen dewar (NOX-G.5-LND Noxygen Science Transfer & Diagnostics, Germany). Spectra were recorded at 77 K by using an e-Scan spectrometer. The EPR signal, generated by the reaction of the spin probe (CMH) with whole blood ROS, was then recorded: acquisition parameters: modulation amplitude: 5 G; centered field: 2.0023 g, sweep time 10 s, field sweep 60 G, microwave power: 1 mW, number of scans: 10; receiver gain: $1*10^3$ (see **Figure 22D**). The timing of the procedure is shown in sketches.

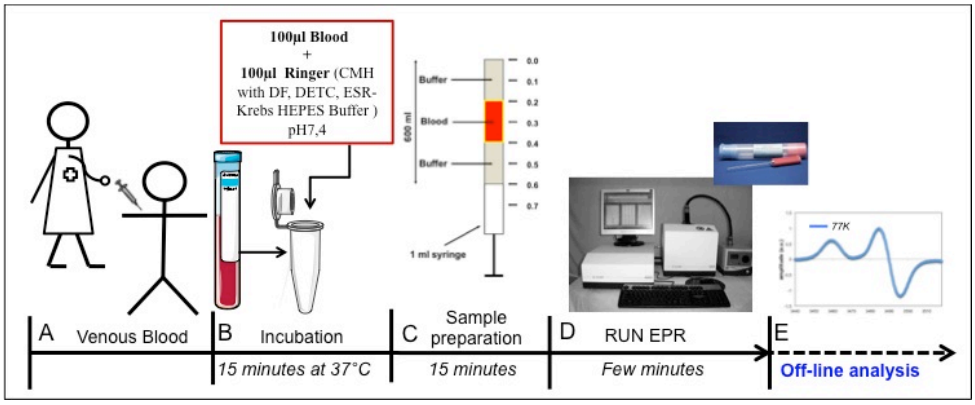

***Figure 22**: EPR protocol adopted to measure ROS production in frozen samples.*

2.4.1.3 pO2 / NOX calibration

In order to calculate the real ROS production, a calibrate curve is necessary taking in account partial pressure of oxygen (pO_2) values.

Assuming a linear behavior of the EPR signal when changing pO_2, the paramagnetic oxygen-sensitive probe Oxyethidium was used (NOX-Oxyethidium. Noxygen Science Transfer & Diagnostics, Germany). In capillary blood samples, prepared by using the protocol described in *section 2.4.1.1*, a 1µl of NOX (2µM) was added and the EPR signal, proportional to the oxygen amount bound to the probe, was recorded. Acquisition parameters were: microwave frequency = 9.734 GHz; modulation frequency: 86 kHz; modulation amplitude: 1.02 G; center field: 3481.5G, sweep width: 60 G, microwave power: 21.90 mW, number of scans: 10; receiver gain: $3.17*10^1$, T= 310K.

The experiments were carried out by using O_2 permeable capillaries (PT Noxygen Science Transfer & Diagnostics, Germany) and starting from ambient PO2 (200 mmHg, maximum signal) and then following N_2 until the EPR signal reached its minimum due to the radical signal alone, that is without O_2 bound (pO_2=0). The experimental data and the regression line is shown in **Figure 23**. From the obtained data a calibration factor of 0.0917 µmol·min^{-1} was calculated. In this way

we were able to compare data collected under different pO_2 conditions, by eliminating the effect of changing pO_2 on ROS production. Without this correction, raw data collected at high altitude result in a lower level with respect to those obtained at sea level, even if, on the contrary, at altitude the ROS production generally increases, due to an in coming relative hypoxic state.

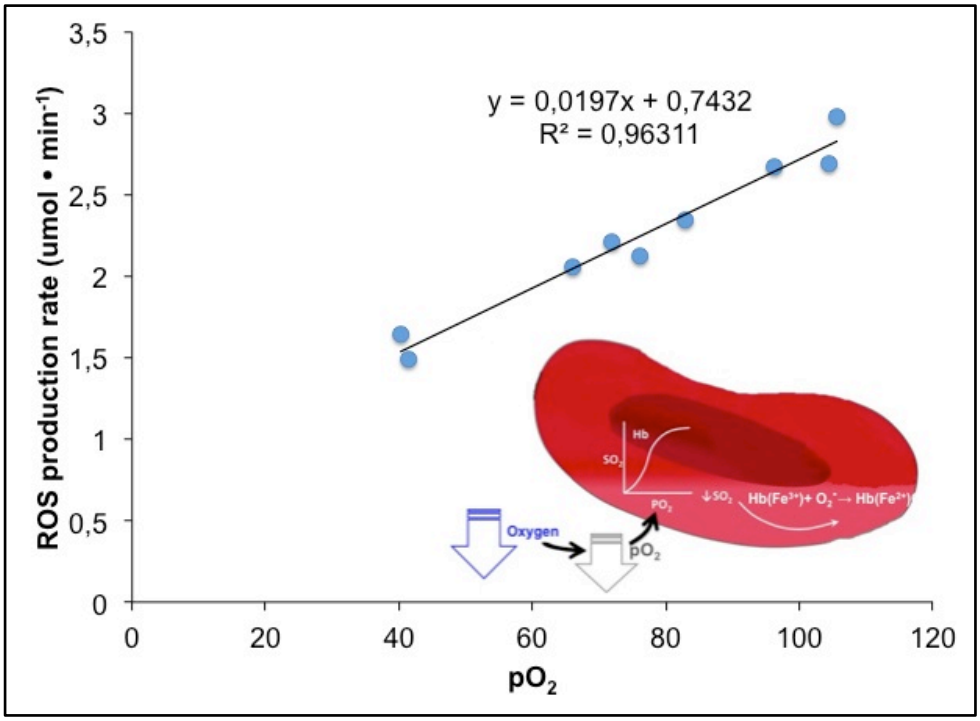

***Figure 23**: Calibration curve pO_2/ROS.*

2.5 Enzymatic assays

ThioBarbituric Acid Reactive Substances (TBARS) and Protein Carbonyls (PC) were used to lipidic peroxidation indices and protein damage respectively.

2.5.1 Blood sample

Approximately 3 ml of venous human blood was drawn from an antecubital vein, with subjects lying on a bed. The samples were collected in heparinized vacutainer tubes (Vacutainer, Becton Dickinson, USA); plasma was separated by centrifuge (5702R, Eppendorf, Germany) at 1000 g for 10 min at 4 °C. All samples were then stored in multiple aliquots at -80 °C until assayed. Samples were thawed only once before analysis, performed within two weeks from collection.

2.5.2 ThioBarbituric

The measurement of Thiobarbituric acid-reactive substances (TBARS) is a well-established method to detect lipid peroxidation. We used TBARS assay kit (Cayman Chemical, USA) which allows a rapid photometric detection of the thiobarbituric acid malondialdehyde (TBAMDA) adduct at 532 nm. Samples were read by a microplate reader spectrophotometer (Infinite M200, Tecan, Austria). A linear calibration curve was computed from pure MDA-containing reactions. All samples were determined in duplicate and the inter-assay coefficient of variation was in the range indicated by the manufacturer (about 10%).

2.5.3 Protein Carbonyls

Reactive species produced directly or indirectly through lipid peroxidation intermediates also may oxidatively modify proteins. The accumulation of oxidized proteins was measured by content of reactive carbonyls. A Protein Carbonyl assay kit (Cayman Chemical, USA) was used to evaluate colorimetrically-oxidized proteins. The samples were read at 370 nm, by a microplate reader spectrophotometer (Infinite M200, Tecan, Austria), as described in detail by the manufacturer. Oxidized proteins values obtained were normalized to the total protein concentration in the final pellet (absorbance reading at 280 nm), in order to consider protein loss during the washing steps, as suggested in the kit's user manual. All samples were determined in duplicate and the inter-assay coefficient of variation was in the range indicated by the manufacturer.

2.6 "In Vitro" Myoglobin

2.6.1 Proteins preparation

Both 54K and 54E human Myoglobin (Mbs) were purchased from Asla (Riga, Latvia) and provided in the aquomet-form. They have been obtained by site-directed mutagenesis PCR approach and expressed in Escherichia coli BL21 (DE3) cells (Novagen).

2.6.2 EPR Sample preparation

The EPR experiments were carried out on the two proteins in the nitrosyl-Mb form. First, in order to avoid side-reactions between either free NO or NO-Mb and the oxygen, the starting ferric proteins (0.05 mM, MAHMA-NONOate, Alexis Biochemicals corporation) were reduced by addition of freshly prepared 100 mM sodium dithionite (SDT, Sigma) under free-O_2 condition. The ferrous deoxy-proteins were then incubated with the NO donor (0.05 mM) for 30 min.
Second, in order to investigate the NO binding affinity in a condition as physiologic as possible, we avoid the addition of any reducing reagents in excess. The two human Mb isoforms were incubated in the presence of the NO donor at three different O_2 concentrations, i.e. pO_2 equal to 0, 40 and 160 mmHg. To this aim, samples were prepared by dissolving the 54K and 54E isoforms (0.05 mM) in the aquomet-form in Krebs-Hepes buffer (20 mM); the pH was then adjusted to 7.4 by addition of NaOH.. Proteins were incubated in a temperature and gas treatment chamber (BIOV, Noxygen) in the presence of the NO donor (0.05 mM) at the chosen pO_2 level at 310 K. After 30 min. of incubation, each sample (400 µL) was put under liquid nitrogen overnight.

2.6.3 pO_2 Calibration

EPR experiments, as said, were carried out at three different values of pO_2 = 0, 40, 160 mmHg. While zero and ambient levels were easily obtained by incubating the Mb samples (in the presence of the NO donor) under 100% N_2 gas flow or exposed to air, respectively, a pO_2 calibration had to be performed, in order to establish the incubation time necessary to reach the desired oxygen level in the sample. To this aim, the oxyethidium (3,8-diamino-5-oxy-6-hydro-5-ethyl-6-phenylphenanthridine, Noxygen) radical (4 mM) was dissolved in buffer and put in apposite O_2 permeable capillaries (40 µL final volume). N_2 (100%) was previously flowed into the capillaries to completely remove O_2 from the solution. At regular time intervals, one of the aliquots was taken out of the chamber and put in a glass capillary for EPR analysis at 310 K. Experimental data were finally fitted with a straight line, going from the maximum EPR signal obtained from the air-exposed sample (pO_2 = 160 mmHg), until a low intensity residual resonance due to the radical's signal alone (incubation time 0 min.; pO_2 = 0). From this calibration curve (not shown), the deoxy-Mb samples were, thus, incubated for 30 min at 310 K to attain a pO_2 level of 40 mmHg.

2.6.4 EPR Mb Measurement

EPR experiments were carried out on frozen samples put in EPR tube, held by a finger-tip liquid nitrogen dewar (NOX-G.5-LND Noxygen Science Transfer & Diagnostics, Germany). Spectra were recorded at 77 K in E-Scan spectrometer.
All the spectra were recorded using the same acquisition parameters: 10 scans on average, 5.24 s sweep time, 8.16 G modulation amplitude, 86 kHz modulation frequency, 42 mW microwave power at a frequency of 9.786 GHz. EPR spectra were baseline corrected and the normalized spectral area (a.u.) calculated by double integration, using the standard EPR software supplied by Bruker (WinEPR, Version 3.1). Five repetitions were performed for each experiment

2.7 Statistical Analysis

All EPR spectra were obtained by using software standardly supplied by Bruker (version 2.11, Win EPR System). For ROS detection "*in vivo*", all spectra were collected by adopting the same protocol, as shown in **Figure 20** and above reported.
Descriptive statistics such as mean ± SD were used to summarize continuous variables. Data were analyzed using parametric statistics following mathematical confirmation of a normal distribution using repeated Shapiro-Wilks W test.
Experimental data were compared by ANOVA variance analysis followed by Bonferroni's multiple comparison test to further check the among groups significance (GraphPad Prism 6, Software Inc. San Diego, CA). The relationship between selected dependent variables was assessed using Pearson Correlation coefficents. $P < 0.05$ statistical significance level was accepted.

***Note to the reader**: in addition to the data reported in the tables, a ∆% estimation [((post value-pre value)/pre value)*100] is reported in the text, which gives often a more impressive result.*

3 RESULTS

3.1 *IN VIVO*

3.1.1 EPR Measurements: Fresh Blood versus Frozen Blood

In the first point was investigated the EPR signal by fresh blood versus frozen blood. As shown in **Figure 24A**, the two EPR signals of ROS: in green line the signal obtained by fresh blood (at 310 K) and in red line by frozen blood in N_2 (at 77 K). Different were the time for preparation of the samples and their acquisition, but otherwise is what we measure (**Figure 24B**). Quantitative detection of ROS rate production (μmol · min^{-1}) by fresh blood sample is possible because with the acquisition time (until the signal reaches plateau, in about 30 minutes), every measured value is available for calculating the kinetics of production. Conversely, frozen blood acquisitions provide only a value that reflects the amount of ROS at that precise instant.

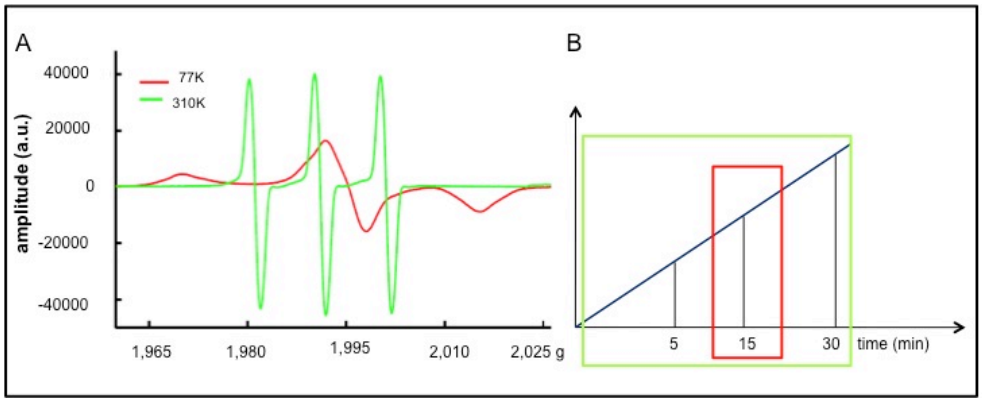

***Figure 24**: **A**) Two typical EPR signals obtained by fresh blood (green) and frozen blood (red); **B**) the plot represents the linear trend of ROS production as a function of elapsed time.*

Just one of the aims of our research was to obtain a quantitative measure of ROS production in blood. To this end, we have set aside the frozen protocol and have continued our experiments on fresh blood samples only.

3.1.2 Limits of detection and quantification with the selected EPR method

The limits of detection (LOD) and quantification (LOQ) can be estimated using the ICH Guidelines [110] that defines these parameters as the analytic concentrations at which the signal-noise ratios (SNR) are at least 3:1 and 10:1, respectively, and in EPR they depend upon the acquisition parameters, especially on the number of scans (NS), that influence linearly the SNR and the experimental time. In the EPR spectrum of a solution of ROS at known concentration (6μM) recorded under the same acquisition parameters adopted in the present study, the SNR of the line belonging to the ROS signal with NS = 10 was found to be 600. Therefore LOD and LOQ are immediately calculated as, respectively, 6μM × 3/600 = $30 \cdot 10^{-3}$μM and 6μM × 10/600 = $100 \cdot 10^{-3}$μM.

3.1.3 Reproducibility measurements

The high reproducibility of the EPR measurements shows up by the plots reported in **Figure 25**. The data are referred to a couple of EPR measurement data (test I (open squares), test II (closed squares)) performed on blood capillary samples taken from the same healthy subject six hours apart. The data are expressed as arbitrary units (a.u.) and refer to EPR signal double integrals. The regression lines obtained from the collected data show an excellent correlation coefficient (r^2 = 0.99) resulting almost super-imposable: test I (slope: 7.98, intercept: 15.49); test II (slope: 7.95, intercept: 15.95). The best fitting straight lines (r^2 = 0.99) were found almost superimposable: about the 0.5% discrepancy in the ROS absolute production rate (μmol · min^{-1}) was calculated between the measurements.
The stacked plot of the recorded EPR spectra during a single experiment is displayed at the upper left corner. The spectra are centered at g = 1.997. For each spectrum, the greatest signal amplitude difference in the triplet (a.u.) is returned by the acquisition routine, resulting in a point of the displayed graph. The ROS production rate (a.u.) is estimated by the best fitting line. It can be, in turn, converted in the absolute ROS production rate level (μmol · min^{-1}) throughout the acquisition of a stable radical compound like CP• (3-Carboxy-2,2,5,5- tetramethyl-1-pyrrolidinyloxy).

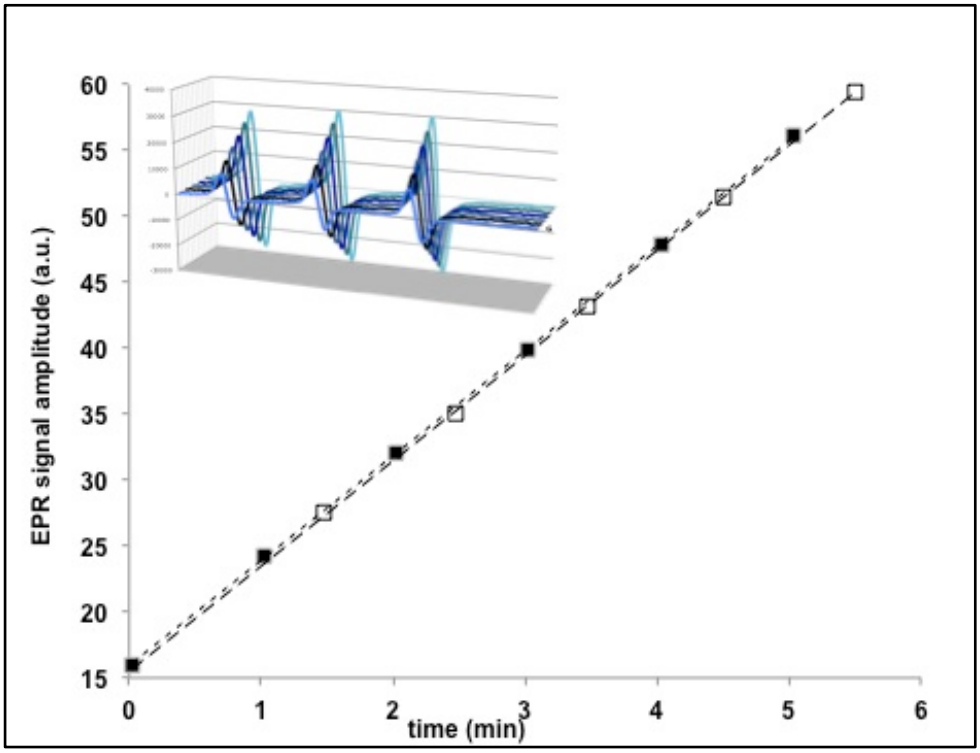

***Figure 25**: The high reproducibility of the EPR measurements is well demonstrated by the plots displayed in the figure showing the calculated EPR signal levels versus the elapsed time.*

3.1.4 Protocol design

The experimental protocol was developed to measure ROS production in human blood and then adopted in all experiments carried out in vivo (see **Figure 20** in *section 2.4.1.1*). As mentioned above, our experimental investigations have been focused to the study of ROS production in various conditions of hypoxic state: exercise, altitude effects and diseases. Now, point by point, will be reported the results.

3.1.5 Starting measurements

After checking the reproducibility of the EPR measurement from the collected data of different repeated tests in healthy subjects; we assessed the ROS production rate in human blood in about one hundred healthy subjects. As shown in the **Figure 26**, different ROS concentrations were obtained when collecting data, on the same resting subject, from different blood fractions.

In peripheral blood ROS production levels were found about 18 ± 4% greater (1.79 ± 0.12 µmol · min^{-1} vs 1.48 ± 0.29 µmol · min^{-1}) than in venous, owing to the different pO_2 (100 mmHg vs 75 mmHg respectively). Indeed a greater level was found in a sample containing only erythrocytes (2.97 ± 0.3 µmol · min^{-1}). On the contrary, significantly lower results (0.15 ± 0.05 µmol · min^{-1}) were found in plasma due to red cells absence, the main ROS producing elements in blood (see **Figure 26**). The data well demonstrate the crucial role played by some parameters (see **Figure 27**) (e.g. temperature, pO_2) on the results, suggesting that great care must be taken to keep all parameters at a constant level during the whole experimental procedure.

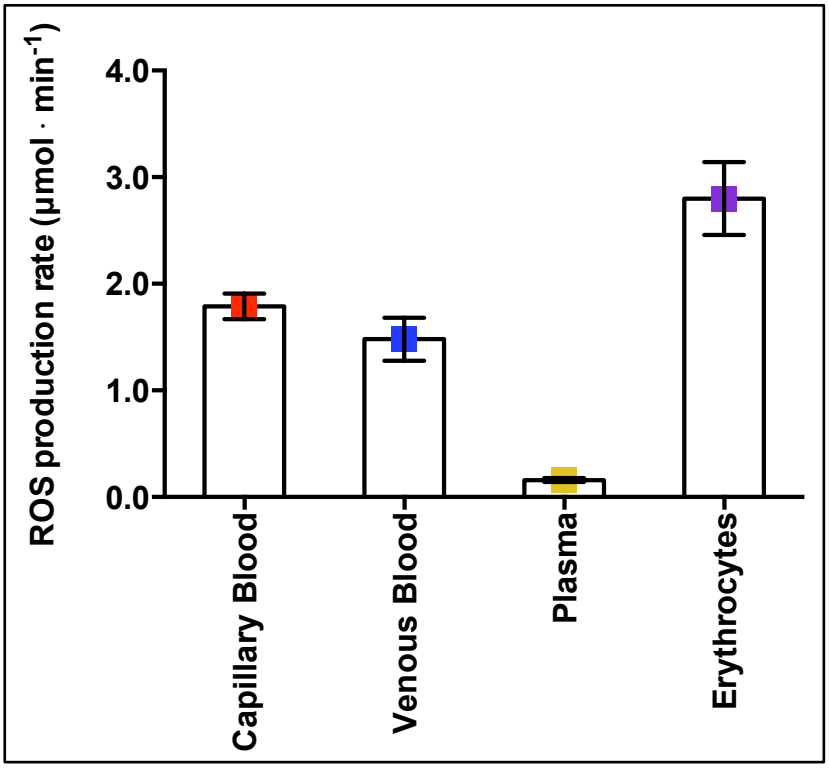

***Figure 26**: Histogram plot (mean ± SD) of the absolute ROS production rate blood concentration (µmol · min^{-1}) obtained from blood samples collected from more than 100 healthy subjects.*
The dependence of the values from the used sample is clearly shown in the figure (µmol · min^{-1}): capillary blood (red): 1.79 ± 0.12; venous blood (blue): 1.48 ± 0.29; plasma (yellow): 0.16 ± 0.02; erythrocytes (purple): 2.87 ± 0.3.

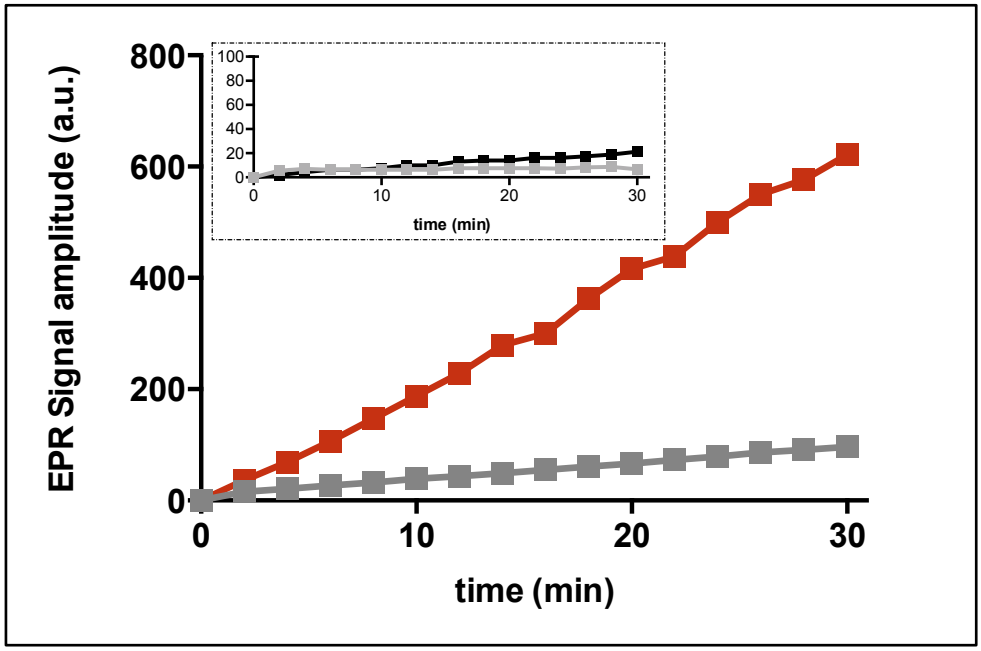

***Figure 27**:Temperature dependence of ROS production in blood: ROS amplitude (a.u.) at 310 K are indicated in red symbols and at 295 K are indicated in grey symbols. Temperature dependence of the Krebs-Hepes buffer is displayed in the upper left corner: buffer amplitude (a.u) at 310 K are indicated in black symbols and at 295 K are indicated in grey symbols.*

3.1.6 Increase ROS Production

3.1.6.1 Short duration exercise in laboratory

The exercise effects were studied in young athletes belonging to different categories: I) hockey players, II) swimmers.

I) In **Hockey player** exercise induced EPR detectable enhancement in-vivo ROS formation in capillary blood. The results are summarized in **Figure 28**. The kinetics of ROS production estimated by the EPR signal intensity levels variation at REST, immediately after Constant-Load submaximal Exercise (CLE) and during the 20 min of recovery after is shown. Compared with resting data, a statistically significant ($p<0.05$) increase of ROS production immediately at the END of CLE was observed (+7%), thereafter the ROS production returned to the pre exercise condition.

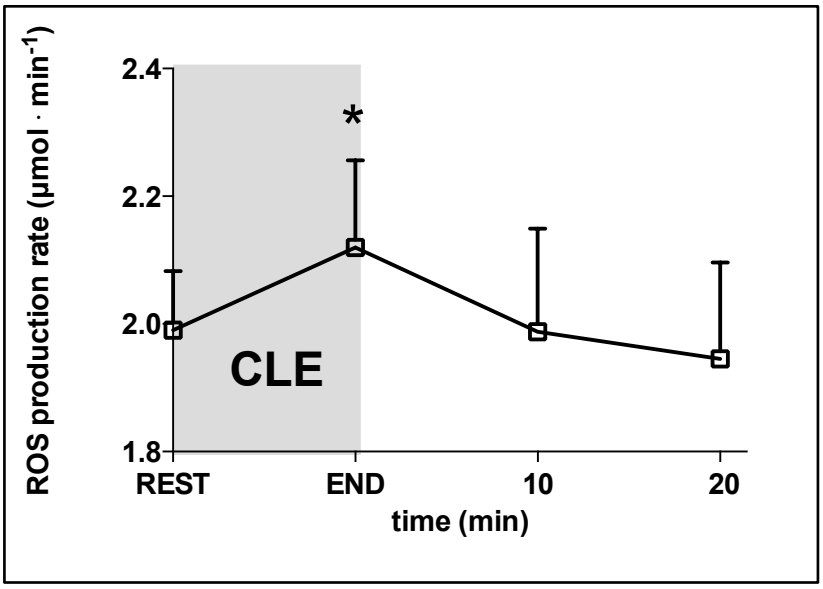

***Figure 28**: Time course of the ROS production rate (umol·min^{-1}) detected by EPR technique before (REST), immediately after the CLE (END) and at 10 and 20 minutes of recovery. Results are expressed as mean ± SD. Changes over time were significant at p<0.05 immediately post CLE compared to rest (* symbol).*

At the same time, as can be observed in **Figure 29A**, TBARS concentration increased immediately after exercise, significantly ($p<0.05$) peaked 20 minutes after exercise and returned toward baseline levels thereafter. Also PC concentration increased immediately after the end of CLE, even if showing a

slower rate. Its level became statistically significant ($p<0.05$) at 20 minutes after exercise; nevertheless the highest values were reached at 1 hour after the END of the exercise and declined thereafter (see **Figure 29B**).

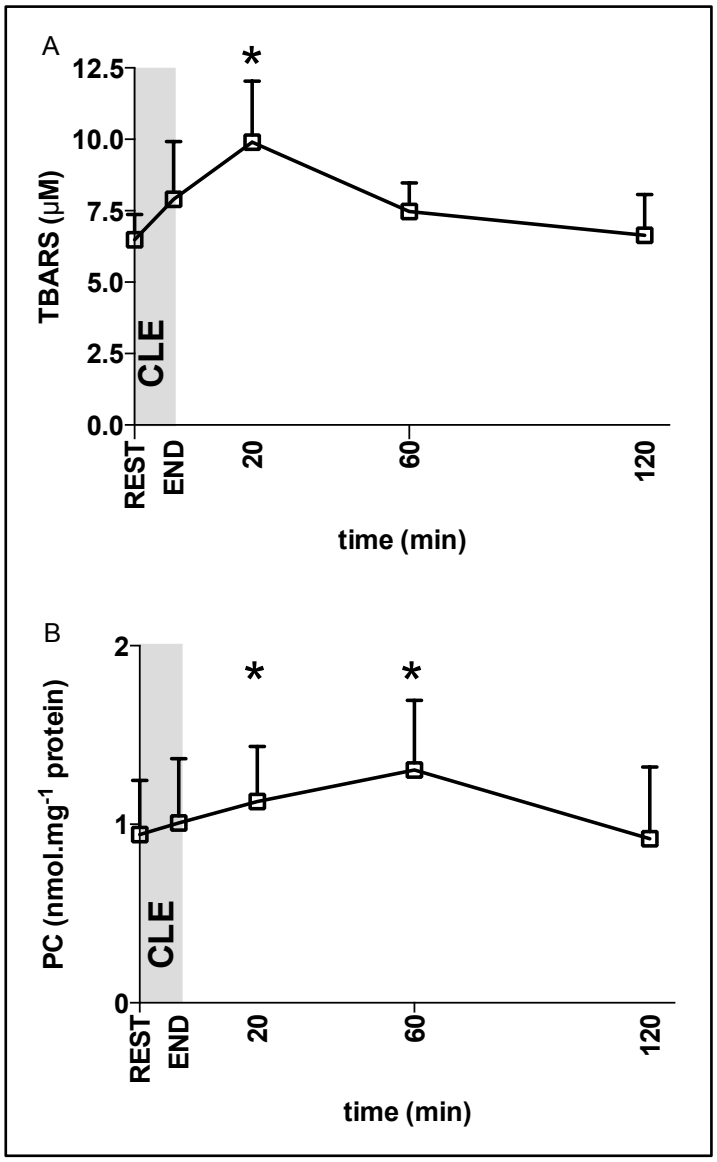

***Figure 29**: Time course of TBARS (**A**) and PC (**B**) concentration before (REST), immediately after the CLE (END) and at 20 min, 1 and 2 hours of recovery. Results are expressed as means ± SD. Changes over time were significant at $p<0.05$ compared to rest (* symbol).*

EPR data were compared to enzymatic measurements carried out on thawed plasma samples from the same subjects at rest. A good Correlation was found between ROS production and biomarkers of oxidative damage. **Table 5** reports the mean values of plasma TBARS and PC and the ROS production values of capillary blood. A positive relationship was found at rest between ROS production and plasma TBARS concentrations (r^2 = 0.74, $p<0.05$) (see **Figure 30A**) and with plasma PC concentrations (r^2 = 0.60, $p<0.05$) (see **Figure 30B**). At high resting ROS production rate levels corresponded greater plasma TBARS and PC concentrations.

TBARS (µM)	6.49 ± 1.01
Protein **C**arbonyls **(nmol • mg^{-1} protein)**	0.94 ± 0.40
ROS production rate **(µmol • min^{-1})**	1.99 ± 0.09

***Table 5**: Plasma TBARS and PC levels and ROS production rate in capillary blood of hockey athletes at rest. Results are presented as mean ± SD*

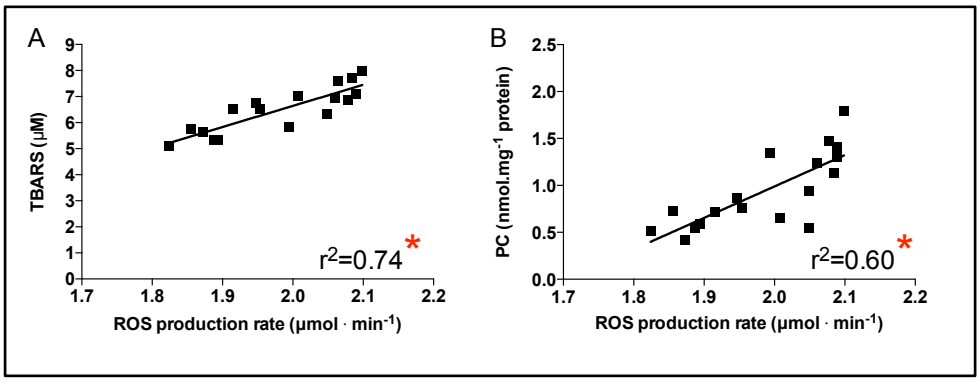

***Figure 30**: TBARS (A) and PC (B) content as determined by enzymatic assays methods versus the ROS production rate (µmol · min $^{-1}$) calculated by EPR data (solid symbols). The linear regression lines (solid lines) are reported. The variance analysis (Pearson product-moment correlation) indicated a positive association for both TBARS and PC (r^2 values 0.74 and 0.60, * $p<0.05$).*

II) In Master **Swimmers** a significant increase of the ROS production rate was found at the END of exercise: + 16% (see **Figure 31)** progressively returning to the basal level in the time course of recovery. The kinetics of ROS production estimated by the EPR signal intensity levels variation at rest, immediately after (END) Incremental Test (IT) and during the 10 min of recovery after is shown. Compared with resting data, a statistically significant ($p<0.05$) increase of ROS production immediately at the END of IT was observed.

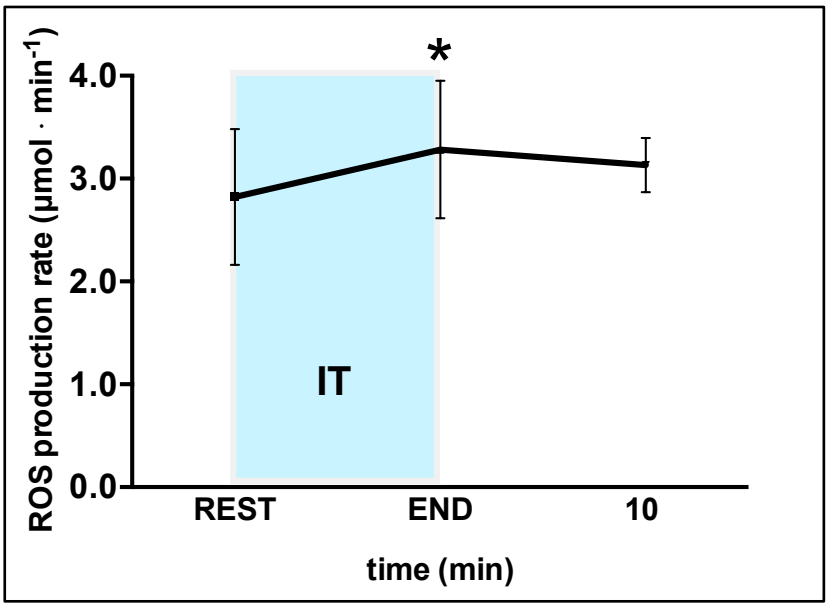

Figure 31*: Time course of the ROS production rate (µmol · min $^{-1}$) detected by EPR technique before (REST), immediately after the IT (END) and at 10 minutes of recovery. Results are expressed as mean ± SD. Changes over time were significant at $p<0.05$ immediately post IT compared to rest (* symbol).*

3.1.6.2 Long-duration Exercise: Triathlon competition

Short (**ShC 7.3**) and long (**Ironman**) **Triathlon competition** increased ROS production rate in capillary blood. Indeed in both athletic groups (ShC 7.3 and Ironman) a significant increase of the ROS production at the end of competition: +12.5% ($p < 0.001$) and +14% ($p < 0.0001$) respectively is shown (see **Figure 32)**.
According to **Figures 33**, **34** and in the **Table 6** the results show a significant ($p<0.0001$) increase in TBARS levels and PC after competition in both groups (ShC 7.3 and Ironman).

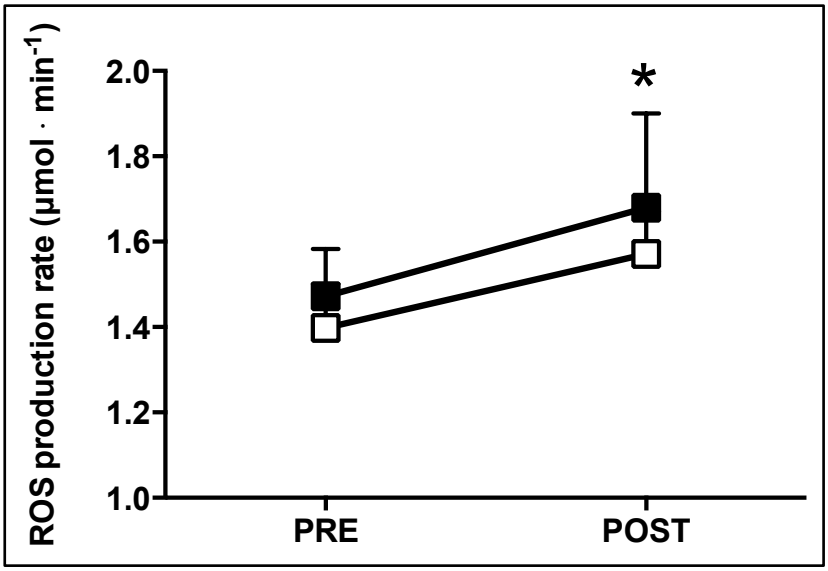

***Figure 32**: ROS production (µmol · min $^{-1}$) rate in Ironman Triathletes (long-competition) are indicated in closed symbols; ShC 7.3 Triathletes (short-competition) are indicated in open symbols. Results are expressed as mean ± SD. Changes over time were significant at $p<0.05$ (* symbol) compared to pre competition value.*

EPR data were compared to enzymatic measurements carried out on thawed plasma samples from the same subjects at rest. No relationship was found between EPR and enzymatic TBARS and PC determinations.

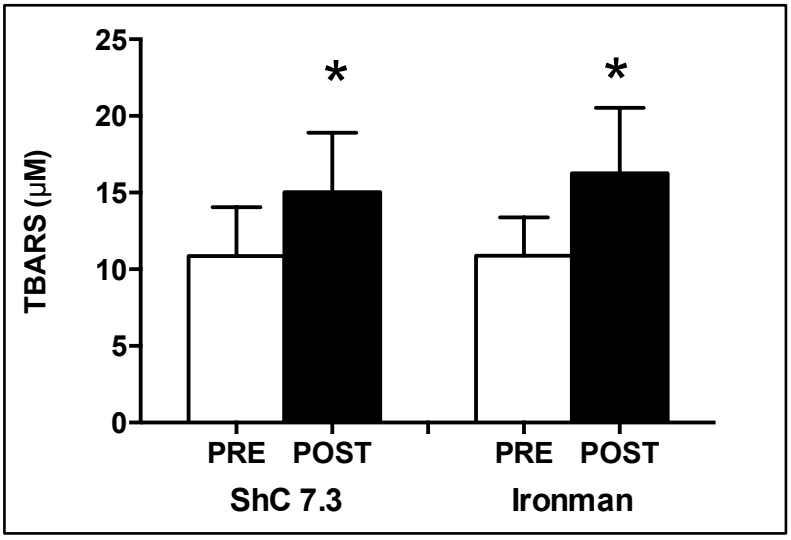

***Figure 33**: TBARS levels in plasma of triathletes (ShC 7.3 and Ironman) before (PRE) and after (POST) competition. The values are presented as mean ± SD. *p<0.05, significant difference in relation to pre competition.*

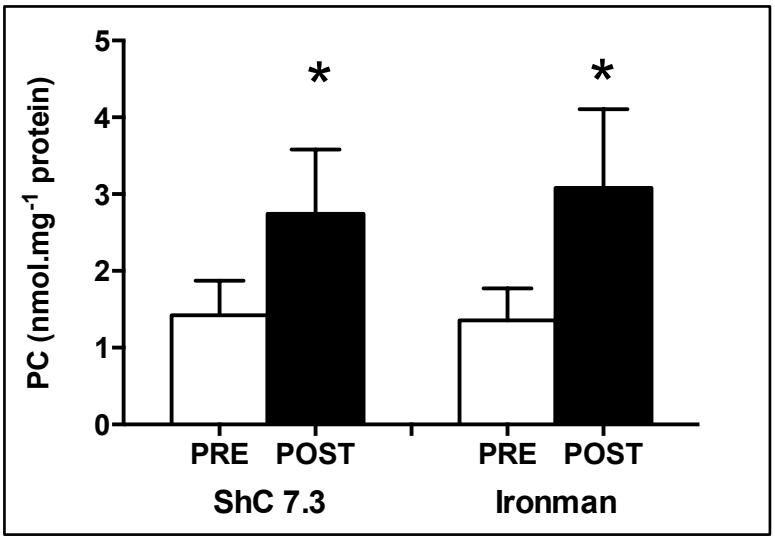

***Figure 34**: PC concentration in plasma of triathletes (ShC 7.3 and Ironman) before (PRE) and after (POST) competition. The values are presented as mean ± SD. *p<0.05, significant difference in relation to pre competition.*

	ShC 7.3		IRONMAN	
	PRE	***POST***	***PRE***	***POST***
TBARS (µM)	10.8 ± 3.2	15.02 ± 3.8*	10.9 ± 2.48	16.25 ± 4.2*
Protein **C**arbonyls **(nmol • mg^{-1} protein)**	1.42 ± 0.45	2.74 ± 0.83*	1.35 ± 0.41	3.08 ± 1.02*
ROS production rate (µmol • min^{-1})	1.39 ± 0.10	1.57 ± 0.09*	1.47 ± 0.1	1.68 ± 0.2*

Table 6*: Plasma TBARS, PC levels and ROS production rate in capillary blood of Triathletes pre and post competition. Results are presented as mean ± SD and the significant difference was from p<0.05 (* symbol)*

Changes in heart rate, saturation and body mass were found at the end of the race:

- **Shc 7.3** significant increase heart rate (p=0.0002; +41%) and significant decrease body mass index (p=0.0001; -2.73%), BSA (p=0.0001; -1%), SO_2 (p=0.008; -1.3%).
- **Ironman** significant increase heart frequency (p=0.0039; +37%) and significant decrease body mass index (p=0.0002; -2.7%) and BSA (p=0.0002; -1.2%). (Data not shown)

In ironman significant linear correlation was found between resting ROS and heart frequency pre-competition (r^2= 0.46) (Data not shown).

Also, chemical laboratory tests showed significant changes before and after competition and are summarized in **Table 7**:

- **Shc 7.3** post competition showed a significant increase: total cholesterol (+5%), HDL (+12.5%), sodium (+4%), glucose (+21%), leukocytes (+124%), erythrocytes (+4%), hemoglobin (+3.5%) hematocrit (+3%), platelets (+12%), neutrophils (+187%), monocytes (+112%), transferrin (+11%) and significant decrease: eosinophils (-83%) and corpuscular volume (-1%).
- **Ironman** post competition showed a significant increase: HDL (+17%), leukocytes (+218%), platelets (+19%), neutrophils (+347%), monocytes (+229%), Mean Corpuscular Hemoglobin Concentration - MCHC (+2.8), ferritin (+21%), transferrin (+6.5%) and significant decrease: LDL (-12.5%), iron (-56%), eosinophils (-97%), potassium (-16%), chloride (-4%), corpuscular volume (-2.5%).

	ShC 7.3		IRONMAN	
	PRE	***POST***	***PRE***	***POST***
Tot cholesterol (mg/dL)	192.08±19.64	202.08±25.19*	212.79±34.45	207.64±26.35
LDL (mg/dL)	106.67±19.72	108.69±22.69	117.43±26.7	102.71±20.5*
HDL(mg/dL)	62.85±12.21	70.77±14.39*	71.50±14.73	83.86±11.49*
Iron (µg/dL)	105.62±30.34	96.77±33.31	111.93±35.10	48.57±14.09*
Ferritin (ng/mL)	100±48	106.92±51.86	116.93±76.86	141.79±86.86*
Transferrin (mg/dL)	283.31±27.4	313.77±51*	275.7±37.4	293.5±37.9*
K (mEq/L)	6.12±0.6	6.04±0.5	6.15±0.89	5.15±0.48*
Na (mEq/L)	139.69±2.06	145.08±3.20*	139.71±2.20	140.21±2.72
Cl (mEq/L)	102.85±2.73	104.92±3.15	101.79±2.72	97.64±3.08*
Glucose (mg/dL)	81.15±5.52	98.54±20.10*	74.79±13.46	74.50±13.77
Leukocytes ($10^{\wedge 9}$/L)	6.37±3.17	14.31±3.12*	5.41±0.91	17.25±2.69*
Erythrocytes ($10^{\wedge 12}$/L)	4.86±0.24	5.04±0.34*	4.69±0.24	4.77±0.30
Hemoglobin (g/dL)	14.83±0.69	15.36±1.04*	14.20±0.67	14.52±0.87
Hematocrit (%)	48.32±1.74	45.02±2.56*	42.62±2.13	42.36±2.49
Platelets ($10^{\wedge 9}$/L)	204.50±30.95	229.91±19.21*	229.77±42.91	273.29±37.14*
Neutrophils ($10^{\wedge 9}$/L)	3.97±3.05	11.44±3.20*	3.09±0.72	13.85±2.71*
Lymphocytes ($10^{\wedge 9}$/L)	1.61±0.27	1.75±0.52	1.71±0.41	1.86±0.34
Monocytes ($10^{\wedge 9}$/L)	0.49±0.26	1.05±0.33*	0.44±0.13	1.46±0.38*
Eosinophil's ($10^{\wedge 9}$/L)	0.18±0.12	0.03±0.04*	0.14±0.08	0.00±0.00*
Basophils ($10^{\wedge 9}$/L)	0.04±0.03	0.04±0.02	0.03±0.01	0.03±0.01
MCHC (g/dL)	33.83±0.73	34.11±0.63*	33.33±0.66	34.29±0.63
Corpuscular Vol (Φ)	90.29±3.54	89.39±3.77*	91.15±3.01	88.94±2.81*

***Table 7**: Blood chemical laboratory test results in ShC 7.3 and Ironman pre and post competition. Results are presented as mean ± SD. Changes over time were significant at p<0.05 immediately after compared to pre (* symbol) competition*

EPR data were compared to chemical laboratory measurements from the same subjects in the time course of the same experimental session.
Pre and post competition, possible relationship between EPR data and laboratory measurement was searched: 1) grouping all the athletes (ShC + Ironman) because no statistical difference were observed in two groups before completion and 2) then maintaining distinct the two groups, inasmuch, workload in two races are different.

1) A direct correlation between ROS production rate (as determined by EPR measurements) and platelets (r^2= 0.53), iron (r^2= 0.43), HDL (r^2= 0.42), corpuscular volume (r^2= 0.40), Mean Corpuscular Hemoglobin - MCH (r^2= 0.44) was observed at rest (see **Figure 35A-E**). A minimal and almost significant correlation was found for lymphocytes (r^2= 0.23; p=0,05) (see **Figure 35F**) too.

2) In **ShC 7.3**: ROS production at rest versus pre-competition: significantly correlation were found between ROS production rate and MCH (r^2= 0.67) and corpuscular volume (r^2= 0.68). Moreover, notable but no significantly correlations were found between ROS production rate and hemoglobin (r^2= 0.34), hematocrit (r^2= 0.38), platelets (r^2= 0.48), eosynophils (r^2= 0.38), basophils (r^2= 0.38) and HDL (r^2= 0.37) (Data not shown).
A direct correlation between ROS production rate (as determined by EPR measurements) and hemoglobin (r^2= 0.63), MCH (r^2= 0.67), and MCHC (r^2= 0.61) was observed at the end of competition (see **Figure 36A-C**). Also, good but not significantly correlation in hematocrit (r^2= 0.54), sodium (r^2= 0.45) were found. (Data not shown).

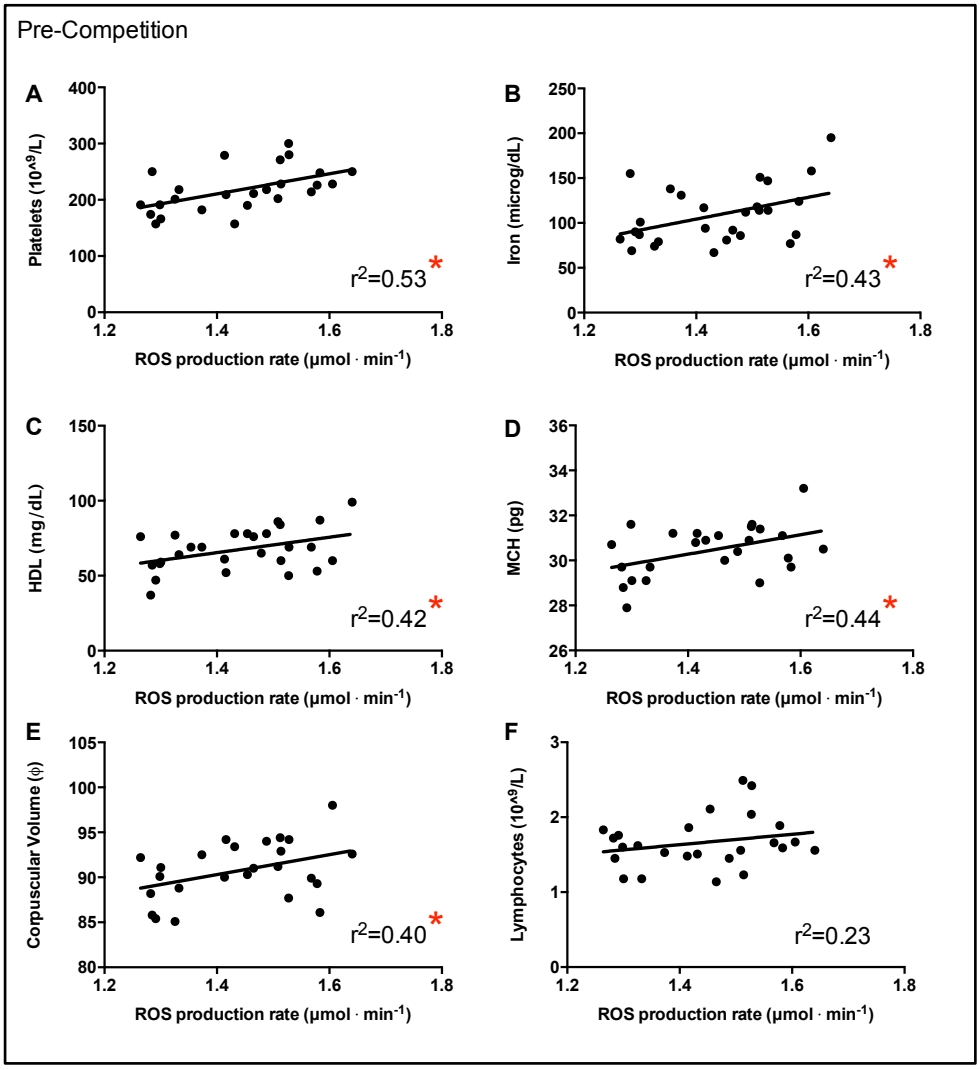

***Figure 35**: Correlation between ROS rate production and blood chemical laboratory test in triathletes pre-competition. Platelets (**A**), Iron (**B**), HDL (**C**), MCH (**D**), Corpuscular Volume (**E**) and Lymphocytes (**E**) content as determined by blood chemical laboratory test versus the ROS production rate (µmol · min $^{-1}$) calculated by EPR data (solid symbols). The linear regression lines (solid lines) are reported. The variance analysis (Pearson product-moment correlation) indicated a significant (* p<0.05) positive association for A,B,C,D,E. A minimal and almost significant correlation was found for lymphocytes (**F**).*

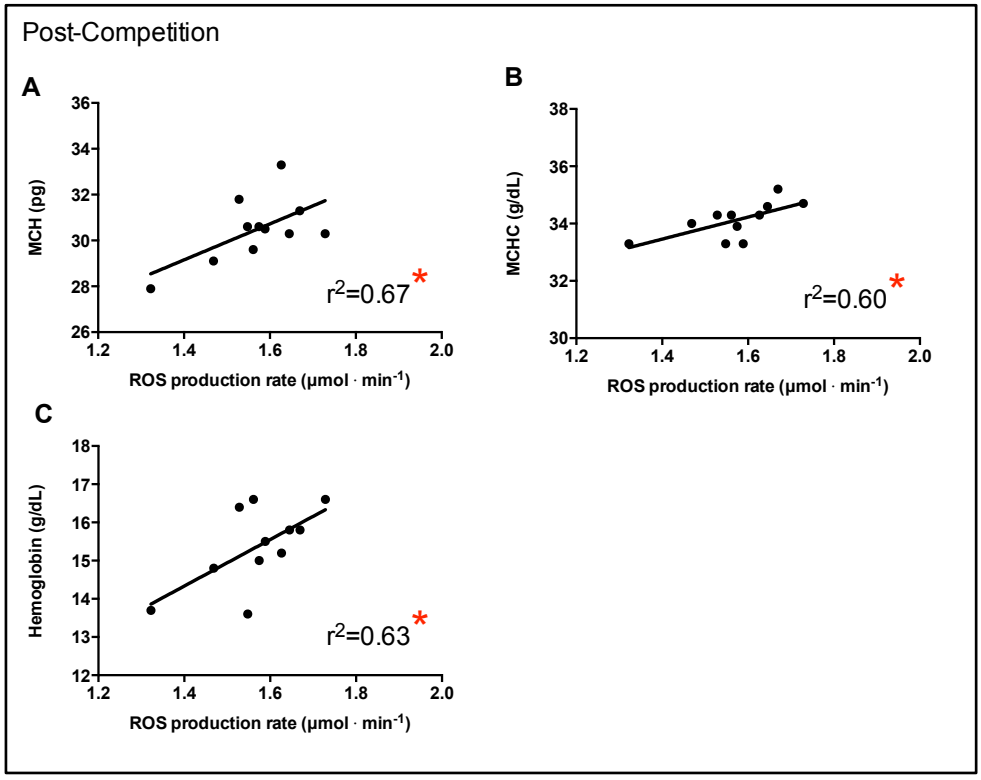

***Figure 36**: Correlation between ROS rate production and blood chemical laboratory test in triathletes ShC 7.3 post-competition. MCH (**A**), MCHC (**B**), Haemoglobin (**C**) content as determined by blood chemical laboratory test versus the ROS production rate (µmol · min $^{-1}$) calculated by EPR data (solid symbols). The linear regression lines (solid lines) are reported. The variance analysis (Pearson product-moment correlation) indicated a significant (* p<0.05) positive association.*

In **Ironman**, ROS production at rest versus pre-competition: a significant linear correlation ($p<0.01$), especially for Iron ($r^2= 0.66$) was found; increasing the ROS production rate, as determined by EPR measurements, hemoglobin ($r^2= 0.50$), hematocrit ($r^2= 0.33$) and platelets ($r^2= 0.50$) were found increased too. Data are not shown.

Lastly the ROS production at rest, were compared to years of training: only in **ShC 7.3** a significant linear correlation was found (r^2= 0.60) (see **Figure 37**).

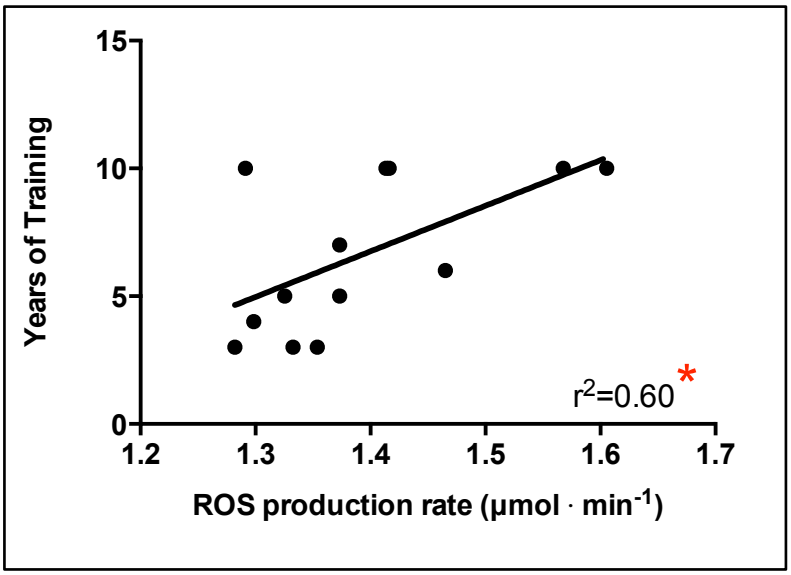

***Figure 37**: Correlation between ROS rate production pre competition and years of training in triathletes ShC 7.3. The linear regression lines (solid lines) is reported. The variance analysis (Pearson product-moment correlation) indicated a significant (* p<0.05) positive association.*

No correlation was found in ShC 7.3 and Ironman between ROS production and body weight.

3.1.6.3 Hypoxia

The **I)** Acute Normobaric, **II)** Acute Hypobaric and **III)** Prolonged Hypobaric Hypoxia effects were preliminarily studied at different heights on sea level.
The experiments in Acute Normobaric Hypoxia are still in progress. You will still be presented the results so far achieved.

I) Acute Normobaric Hypoxia was simulated at 12.5% O_2 in air, which corresponds to 4500m s.l. **Figure 38** show, a fast, initial elevation of ROS production, whose size appears to be related to the subjects' capillary SO_2, (**Figure 39**) followed, by a return to pre-hypoxia levels at the end of hypoxia exposure (4 hours). A burst of ROS (+ 38%) is formed in the transition to low intracellular O_2 tension. The Arterialized blood oxygen saturation was relatively constant at 85–90% (see **Figure 39**) during simulated hypoxia state.

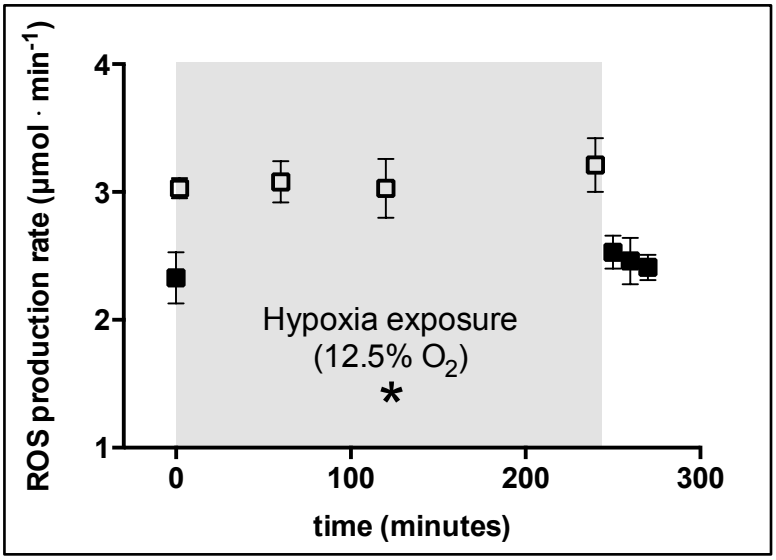

***Figure 38**:Time course of ROS production rate (umol·min^{-1}) detected by EPR technique. Black symbols are values before (0 minutes) and after hypoxia exposure (recovery); white symbols are values during hypoxia. Results are expressed as mean ± SD. Changes over time were significant at p<0.05 compared to pre exposure (* symbol).*

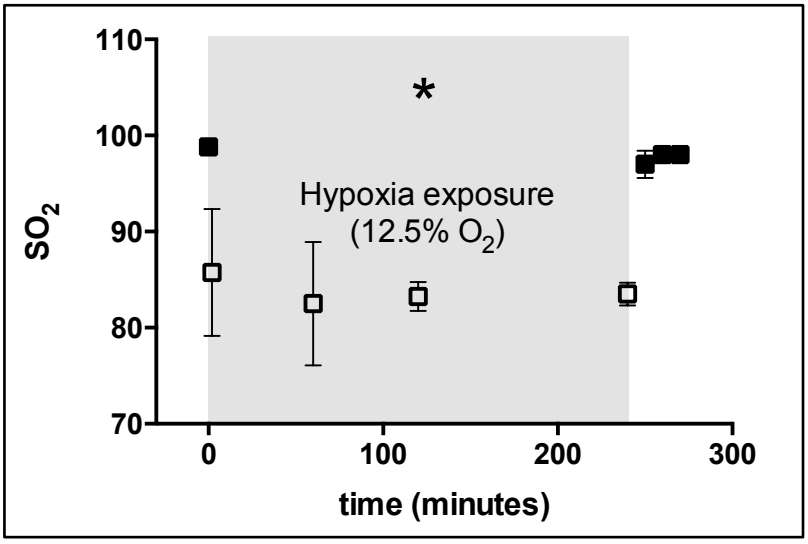

***Figure 39**: SO_2 during Acute Normobaric Hypoxia and recovery. Black symbols are values before hypoxia exposure (0 minutes) and during the recovery; white symbols are values during hypoxia. Results are expressed as mean ± SD. Changes over time were significant at p<0.05 compared to pre exposure (* symbol).*

Plasmatic concentrations of TBARS and PC were significantly increased after four hours of hypoxia exposure. During Acute Normobaric Hypoxia TBARS underwent only a 10% increase at four hours. By contrast, one hour after hypoxia offset the plasma concentration of TBARS was significantly (P<0.05) increased returning back to pre-hypoxia control value in the subsequent two hours (**Figure 40A**). PC concentration significantly increased, attaining the highest value (P<0.05) at four hours of hypoxia exposure. At hypoxia offset, PC decreased slowly, being still higher after two hours than at pre hypoxia exposure (**Figure 40B**).

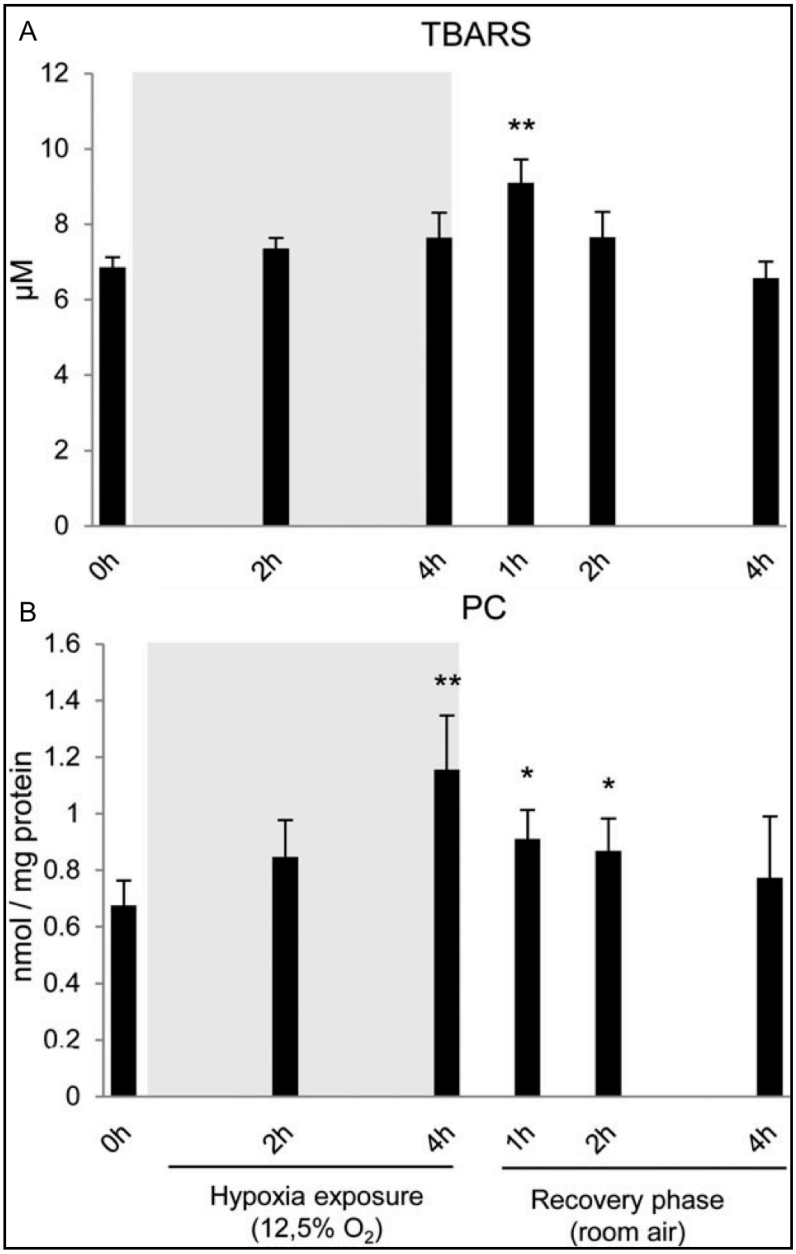

***Figure 40**: Histogram plot (mean ± SD) of (**A**) TBARS (µM) and (**B**) PC (nmol·mg^{-1} protein) obtained from plasma samples collected at 0, 2,4 hours of hypoxia exposure and 1,2,4 hours of recovery phase in room air. Changes were significant at p<0.05 (* symbol) or p<0.01 (** symbol) compared to pre hypoxia exposure.*

.

II) In **Acute Hypobaric Hypoxia** ROS production significantly increases at six hours after arrival at 3480m sl (+42%), and continues to increase at 24 h exposure (+47%) as shown in **Figure 41A**. These data are in agreement with a reduction of SO_2: -11 and -10% respectively (see **Figure 41B**).

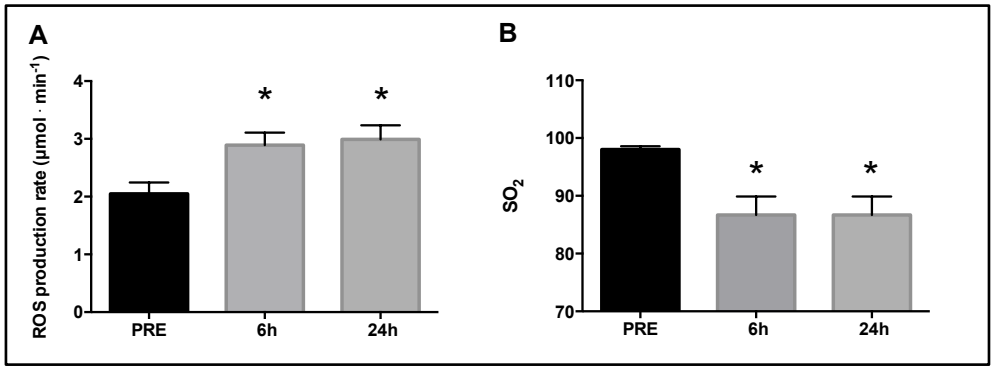

***Figure 41**: Histogram plot (mean ± SD) of (**A**) ROS production rate (µmol · min^{-1}) obtained from capillary blood samples collected at 0m s.l. (PRE) to 6 and 24h after 3480m s.l. exposure in sedentary subjects. (**B**) the SO_2 measured at the same time of blood sampling. Changes over time were significant (p<0.05) at 6 and 24h compared to PRE (* symbol).*

Frequency of Ventilation (FV) (**A**) and Heart Rate (HR) (**B**) were significantly increased in Acute Hypobaric Hypoxia (see **Figure 42**). At 6 and 24 h an elevation of FV and HR was observed: FV +43 and +36; HR +30% and +25% respectively.

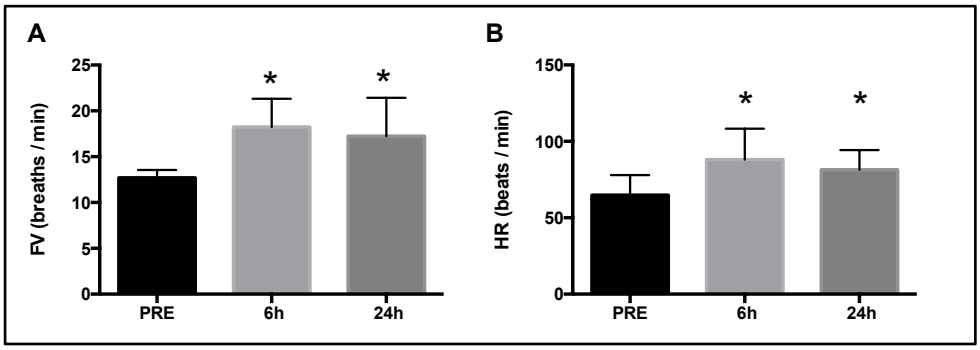

***Figure 42**: Histogram plot (mean ± SD) of FV (**A**) and HR (**B**) at PRE and 6 and 24h after 3480m s.l. exposure. Changes over time were significant (p<0.001) at 6 and 24h compared to PRE (* symbol).*

No correlation was found between the ROS production and the values FC and HR. Data are not shown.

III) In **Prolonged Hypobaric Hypoxia**, after two weeks at 1860m s.l, it was found a significant increase of ROS production (~ +33%); followed by a return to pre-hypoxia levels (-3%) after one week to s.l. recovery (POST) (see **Figure 43**).

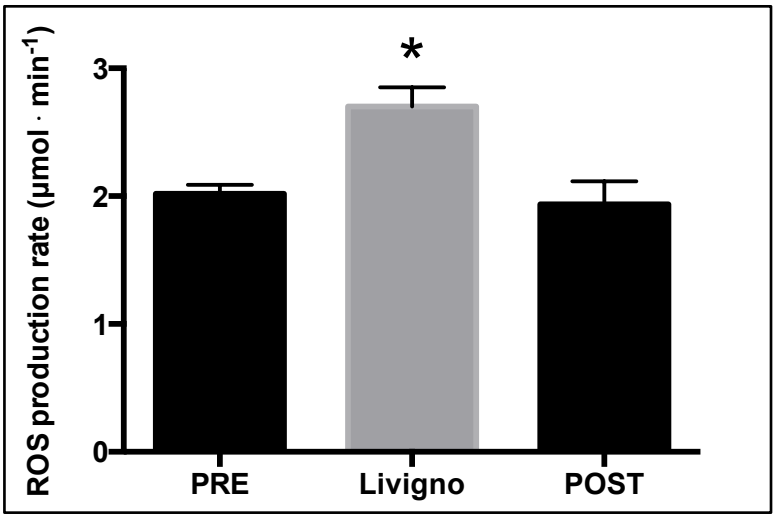

***Figure 43**: Histogram plot (mean ± SD) of ROS production rate (µmol · min^{-1}) obtained from capillary blood samples collected at 0m s.l. (PRE), after two weeks exposure to moderate altitude 1860 m s.l. (Livigno) and return at 0m s.l. (POST) by male elite athletes. Changes were significant (p<0.0001) by exposure compared to PRE and POST condition (* symbol).*

At the same time, two weeks exposure to moderate hypoxia induced significant changes in oxidative markers concentration: TBARS concentration significantly increased (+9%) after two weeks of exposure (**Figure 44A**) and PC concentration significantly decreased (-40%) at return at s.l. (POST) (**Figure 44B**).

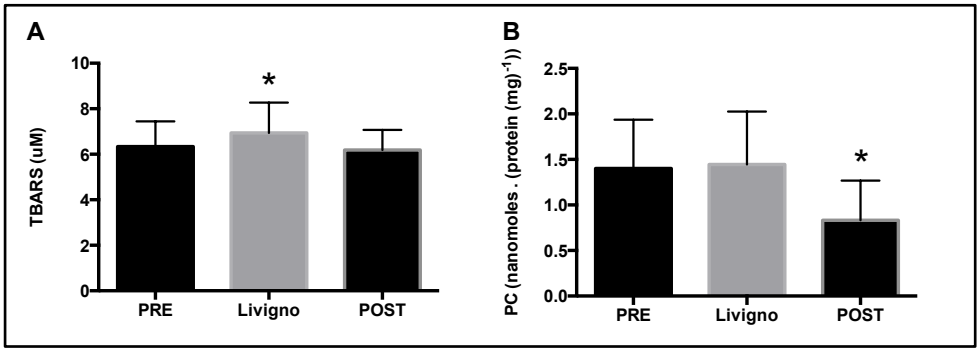

***Figure 44**: Histogram plot (mean ± SD) of (**A**) TBARS (μM) and (**B**) PC (nmol·mg^{-1} protein) obtained from plasma samples collected at 0m s.l. (PRE), after two weeks exposure to moderate altitude 1860 m s.l. (Livigno) and at one week after the return at s.l. (POST) by male elite athletes. Changes were significant at p<0.0001 compared to PRE (* symbol).*

3.1.7 Decrease ROS production

3.1.7.1 Training effect

In *section 3.1.6.1* were shown the effects of incremental test to master swimmers. These subjects were scheduled over a period of high-volume/low intensity program, and then required to undergo another incremental test. Our aim was to investigate the **training effects**.

Two session were defined: PRE (explained in *section 2.3.1.1 and Figure 15*) and POST the session after training.

In POST training session, compared with resting data, a statistically significant ($p < 0.001$) increase of ROS production immediately at the END of IT was observed, thereafter the ROS production returned to the pre exercise condition.

In swimmers, the training effects (twelve weeks) of moderate daily exercise showed a significant ($p<0.001$) decrease in ROS production (-20%) (see **Figure 45**).

Moreover the variance analysis (Pearson product-moment correlation) indicated an inverse correlation (r^2 values = 0.58, $p<0.05$) between ROS rate production and VO_2 max (see **Figure 46**).

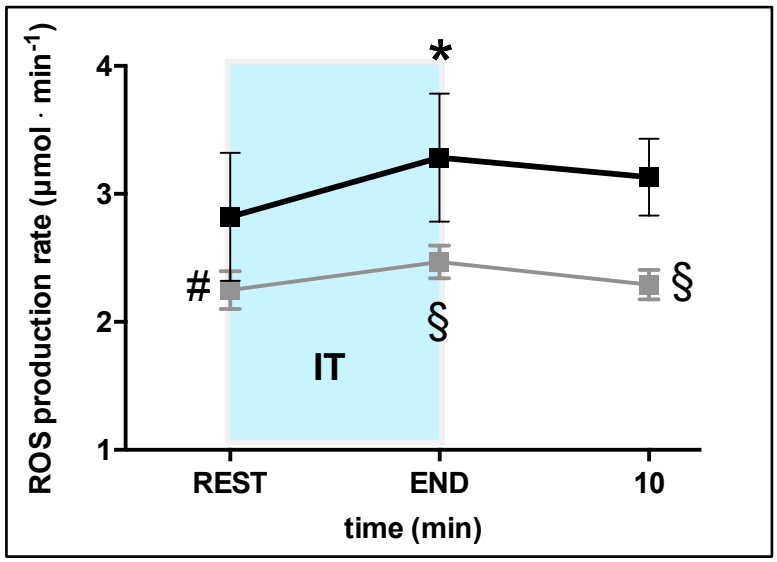

***Figure 45**: Time course of ROS production rate (umol·min^{-1}) detected by EPR technique before (REST), immediately after the IT (END) and at 10 minutes of recovery. Two session of IT are shown. In black line the first session: defined PRE (explained in Figure 8) and in grey line the session after POST training. Changes were significant at p<0.0001 compared to PRE (*, §symbol). Also, we founds significant at p<0,001 differences between rest PRE and rest POST training ($^{\#}$symbol).*

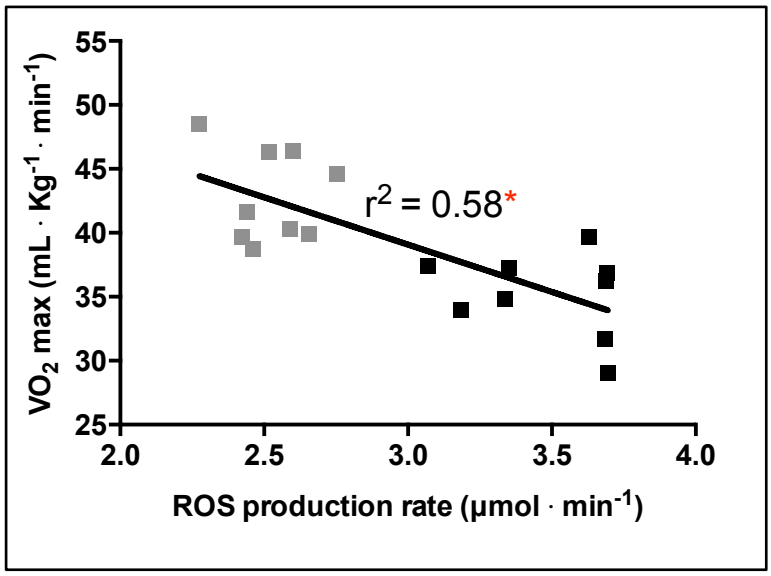

***Figure 46**: After exercise, correlation between ROS rate production and VO_2max.The linear regression (solid line) shows an inverse correlation between ROS production (umol·min^{-1}), at the end of exercise, and VO_2 max (mL·Kg^{-1}·min^{-1}) (r^2 values = 0.58, P<0.05). The black squares indicate PRE and grey squares indicate POST training value. The variance analysis (Pearson product-moment correlation) indicated a significant (* p<0.05) positive association.*

A good training, that is a moderate training, can have a positive effect on ROS production, leading to decrease ROS and increase the antioxidant capacity in whole body.

3.1.7.2 Antioxidant Supply

Antioxidant supplementation (R(+) Thyoctic acid) induced EPR detectable changes in formation of in-vivo ROS in capillary blood (**Figure 47**). The kinetics of ROS production estimated by the EPR signal intensity at rest, immediately and during the time period (up to 3 hours) following the R-Thioctic acid administration is shown in the **Figure 47** together with the data recorded without supplementation at the corresponding interval time. The ROS production rate level, subsequent to the supply, increased after 20 minutes, then decreased (40 minutes) and kept at a lower level with respect to the resting value, reaching its lowest significant ($p<0.01$) level at 90 min, then returning to the baseline. No significant difference was observed between experimental baseline and control data recorded without supplementation.

Contrary to the effects of the training, the exogenous administration (R(+) Thyoctic acid) has a limited effect in time.

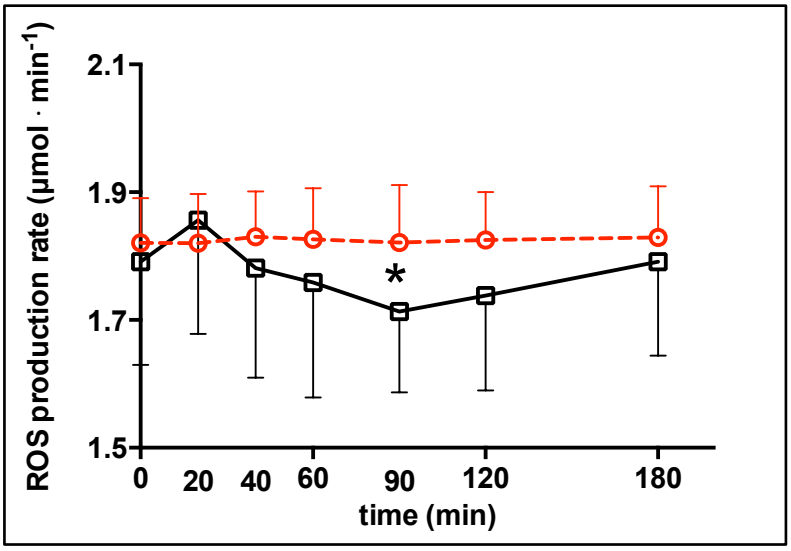

***Figure 47**: Time course of ROS production rate (µmol · min^{-1}) calculated by the EPR acquisition data without supplementation (red circle) and following antioxidant (R-thioctic acid) supply (black square). Results are expressed as mean ± SD. Changes over time resulted significant (P<0.01) at 90 min post, compared to pre-supplementation (*symbol).*

3.1.8 Under diseases: Unbalance of ROS production rate

ROS production in pathological subjects was tested. The data obtained on patients (at baseline) affected by Type II Diabetic Neuropathic (Type II DN), Mild Cognitive Impairment (MCI) and sporadic Amyotrophic Lateral Sclerosis (sALS) were compared to the baseline data collected on healthy subjects (**Table 8**), a significant increase ($p<0.05$) of the ROS production level was found as an effect of both neurodegenerative diseases (MCI +2% and sALS +20%) (see **Figure 48**).

	ROS production rate (µmol · min $^{-1}$) Baseline value
Healthy	1.84 ± 0.09
Type II DN	1.71 ± 0.2
MCI	1.87 ± 0.3
sALS	2.2 ± 0.4

***Table 8**: ROS production rate at baseline in healthy subjects and patients*

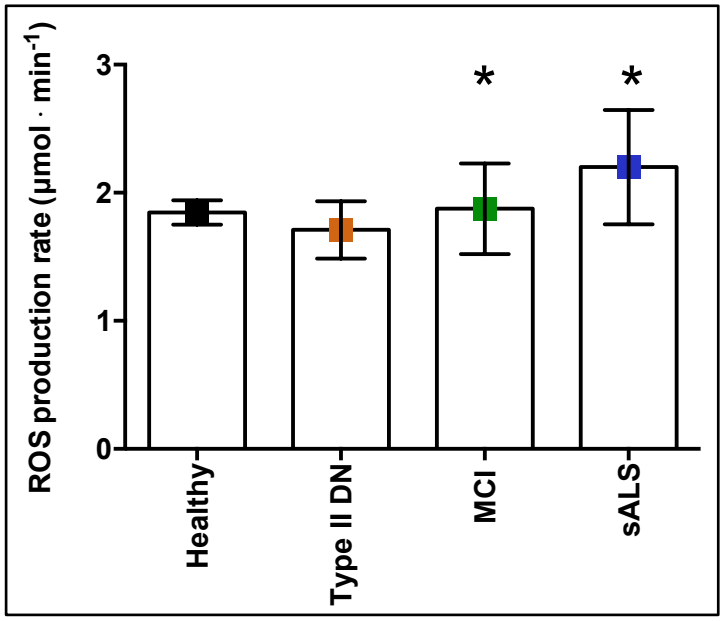

***Figure 48**: At baseline: histogram plot (mean ± SD) of the absolute ROS production rate (µmol · min^{-1}) obtained by capillary blood collected from healthy subjects (black) and patients: type II DN (orange), MCI (green), sALS (blue) sALS and MCI patients shown a significant ($p<0.05$) increase of ROS production rate (*symbols).*

The two studies presented below are in fieri and arised from collaborations:
i) Study on diabetic neuropathy in patients with Type II diabetes mellitus and antioxidant supplementation: IBFM-CNR and Istituto Auxologico of Milan
ii) Study on sALS patient: IBFM-CNR and Fondazione Maugeri of Veruno (Novara).

3.1.8.1 Type 2 Diabetes mellitus Neuropathic patients

Antioxidant supplementation (R(+) Thyoctic acid) induced EPR detectable changes in formation of in-vivo ROS in capillary blood (**Figure 49**) in **type II Diabetic Neuropathic patients (Type II DN)**.

The ROS production rate, subsequent to the supply of 1,6 g R(+) Thyoctic acid, significantly ($p<0.01$; -7%) decreased after 1 hour (1.71 ± 0.4 vs 1.59 ± 0.3 $\mu mol \cdot min^{-1}$). This acute decremental effect of the supply persisted after 15 days (1.56 ± 0.1 $\mu mol \cdot min^{-1}$) and 30 days (1.5 ± 0.1 $\mu mol \cdot min^{-1}$) of daily supplementation.

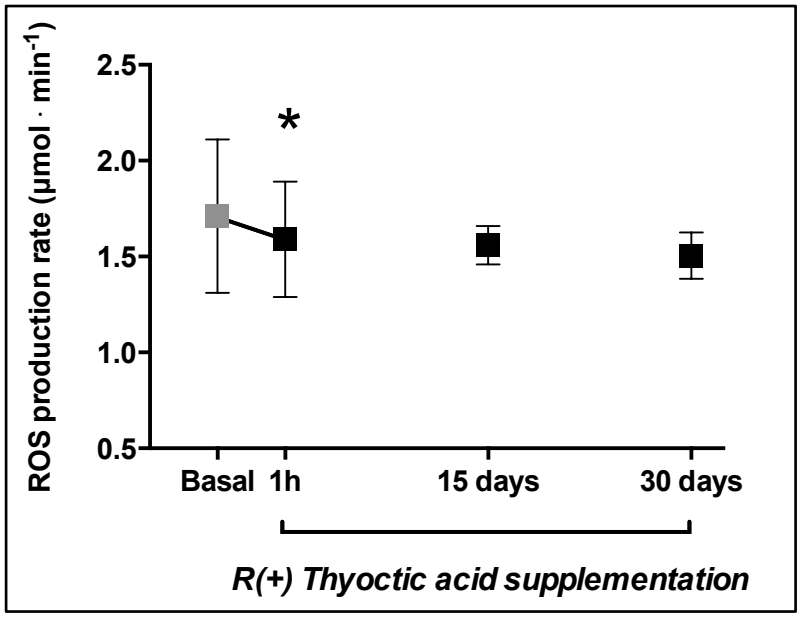

***Figure 49**: Time course of ROS production rate ($\mu mol \cdot min^{-1}$) calculated by the EPR acquisition data without supplementation (basal – grey square) and following antioxidant (R-thioctic acid) supply (black square). Results are expressed as mean ± SD. Changes over time resulted significant ($P<0.01$) at 1h post, compared to pre-supplementation (*symbol).*

At the same time, 15 days and 30 days antioxidant supplementation induced changes in oxidative markers concentration: TBARS concentration decreased (-15%) 30 days after (**Figure 50A**) and particularly PC concentration significantly ($p<0.01$) decreased (-18%) 30 days after (**Figure 50B**).

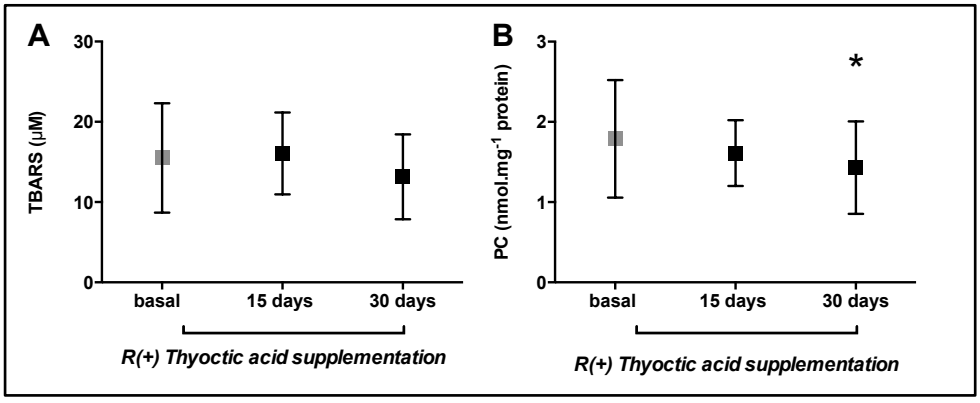

***Figure 50**: Time course of TBARS (**A**) and PC (**B**) concentration before and after (15 and 30 days) antioxidant supplementation. Results are expressed as means ± SD. Changes over time were significant at $p<0.05$ compared to basal value (* symbol).*

Moreover the variance analysis (Pearson product-moment correlation) indicated a good correlation (r^2 values = 0.85, $p<0.01$) between ROS rate production and TBARS concentration (Data no shown).

3.1.8.2 sporadic Amyotrophic Lateral Sclerosis

The exercise and training effects have also been tested in bulbar and spinal sALS patients. For exercise effects evaluation ROS production rate ($\mu mol \cdot min^{-1}$) was tested in capillary blood samples taken at REST, immediately END exercise and 15 minutes after the end of an incremental test (IT). Venus blood samples were taken at rest before and 15 minutes after the end of the IT for the assessment of oxidative damage markers too.

Two session were defined: t0 (pre training) and t1 (after 20 weeks of training).

Bulbar sALS:

In patients with bulbar sALS: at t0 a significant decrease ($p<0.05$) of the ROS production rate was found both immediately at the END of IT (-17%) and 15 minutes after exercise (recovery) (-17%) (see **Figure 51A**)

After 20 weeks training protocol (30 min/day cycling exercise) the test was repeated.

At t1 no significantly modification of the ROS production rate was found immediately after IT (-4%) and 15 minutes in the recovery (-6.5%).

At t1 compared with t0, similar ROS production rate at rest was observed (2.36 ± 0.4 $\mu mol \cdot min^{-1}$and 2.31 ±0.3 $\mu mol \cdot min^{-1}$).

At t0 TBARS and PC concentration decreased (-3.5% vs -2.5%) at the “END” of the exercise (**Figure 52A-B**).

At t1 TBARS and PC concentration increased (+8% vs 22%) at the END of the exercise (**Figure 52A-B**).

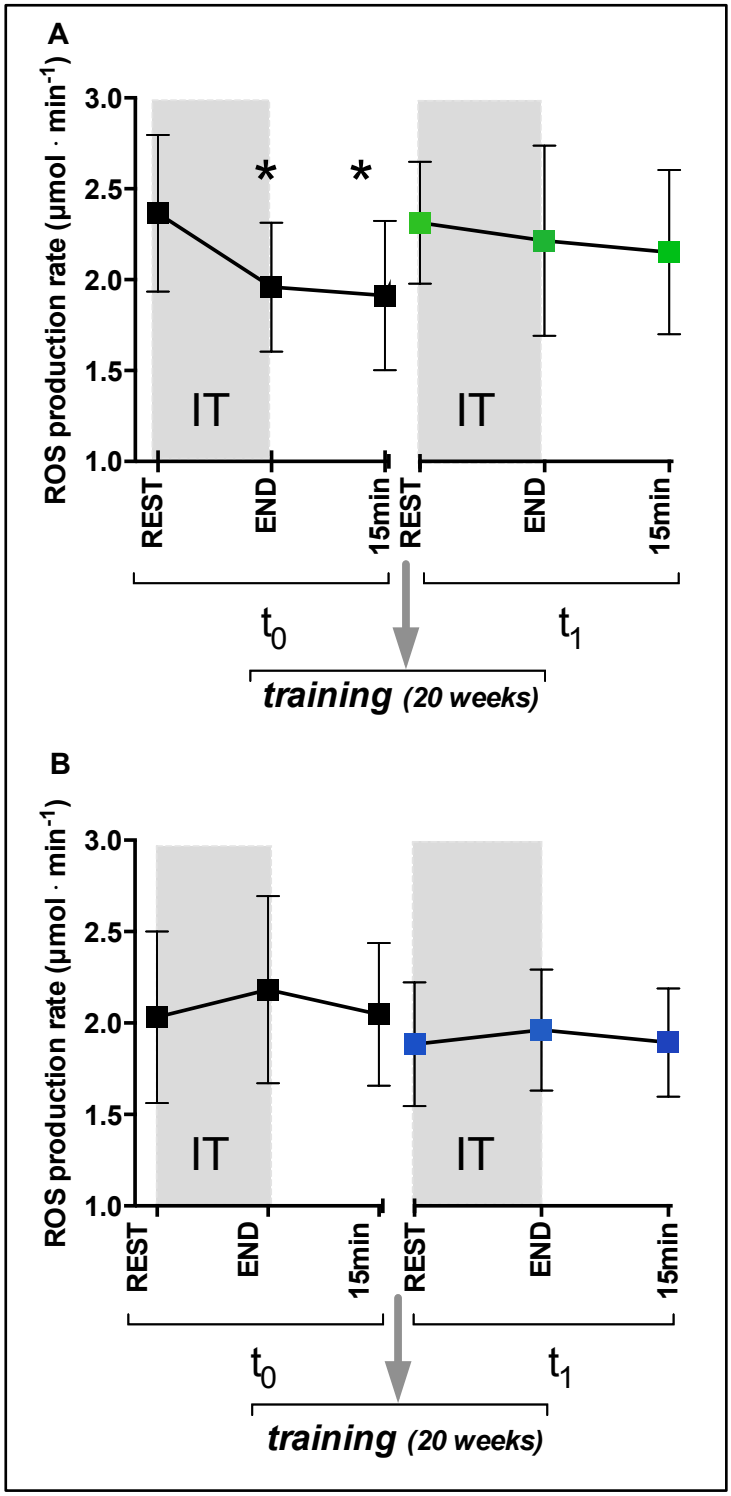
A
ROS production rate (µmol · min-1)
3.0
2.5
2.0
1.5
1.0
*
*
IT
IT
REST
END
15min
REST
END
15min
t0
t1
training (20 weeks)
B
ROS production rate (µmol · min-1)
3.0
2.5
2.0
1.5
1.0
IT
IT
REST
END
15min
REST
END
15min
t0
t1
training (20 weeks)

***Figure 51**: Exercise and training effects in sALS patients. Time course of ROS production rate (umol·min^{-1}) calculated by EPR technique before (REST), immediately after the IT (END) and at 15 minutes of recovery in (**A**) bulbar sASL and (**B**) spinal sALS patients. Two exercise session: t0 before training (black square) and t1 after 20 weeks of training (green square in bulbar and blue square in spinal sALS patients). Results are expressed as mean ± SD. Changes over time were significant at p<0.05 immediately post CLE compared to rest (* symbol).*

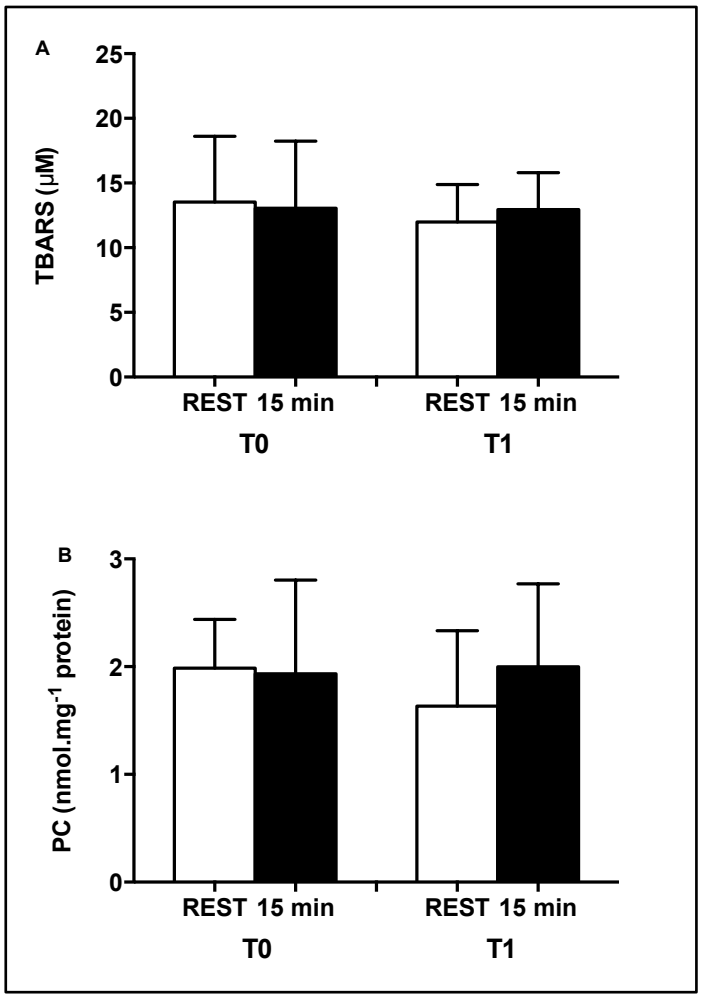

***Figure 52**: Histogram plot (mean ± SD) of (**A**) TBARS (μM) and (**B**) PC (nmol·mg^{-1} protein) obtained from plasma samples in bulbar sALS patients. Plasma was collected before (REST) and after the end IT (15 minutes) in two session: t0 (pre training) and t1 (after 20 weeks of training).*

Spinal sALS

In patients with **spinal sALS**: at t0 a non significant increase (+7%) of the ROS production rate was found immediately after exercise followed by a progressive returning to the basal level after 15 minutes (+0.5%) (see **Figure 51B**).

After 20 weeks of training protocol (30 min/day cycling exercise), the test was repeated.

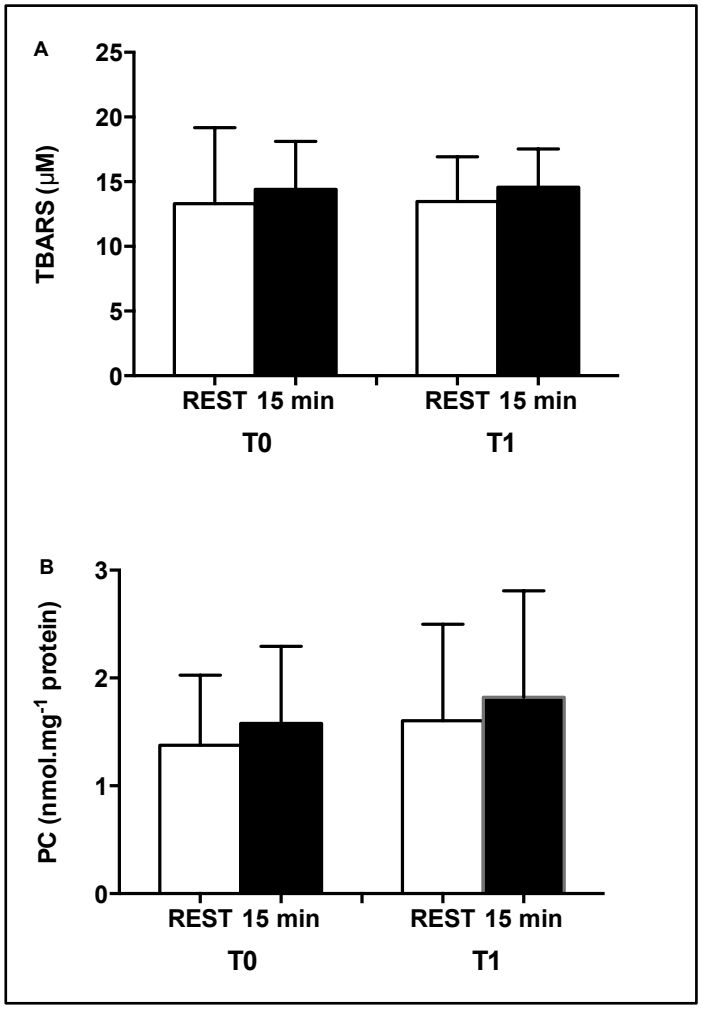

***Figure 53**: Histogram plot (mean ± SD) of (**A**) TBARS (μM) and (**B**) PC (nmol·mg^{-1} protein) obtained from plasma samples in spinal sALS patients. Plasma was collected before (REST) and after the end IT (15 minutes) in two session: t0 (pre training) and t1 (after 20 weeks of training).*

At t1 a non-significant increase (+4%) of the ROS production rate was observed; progressively returning to the basal level after 15 minutes (+0.5%).
Between two REST values (t0: 2.03 ± 0.4 μmol·min^{-1} and t1: 1.88 ± 0.3 μmol·min^{-1}) a decrease of about 7% was found.
At t0 and t1: TBARS concentration increased (+8%) at the END of the exercise (see **Figure 53A**); PC concentration increased (+14% in t0 and +13% in t1) (see **Figure 53B**).

In order to evaluate the training effect on the basal level progression a Control group (Ctrl) of patients (sALS), matched for age, sex and degree of pathology, was recruited.
At t0 an increase of ROS production was observed immediately at the end of IT and the subsequent returned to the pre exercise condition were analogue to those reported above.
20 weeks after the test was repeated and no significant modification of the ROS production rate trend was found (Data not shown).
The positive training effects are highlighted in **Figure 54** and **55**. Indeed, at REST, after training spinal sALS had shown a decreased of ROS production not evidenced in the Ctrl group and in bulbar sALS. This data are also supported by the mean values of fractional O_2 muscle extraction [Δ[deoxy (Hb+Mb)]$_{peak}$/[Δ(deoxy (Hb+Mb)]$_{isch}$] determined by NIRS. After training, the ability of O_2 muscle extraction was improved (+85%) in sALS patients versus Ctrl group.

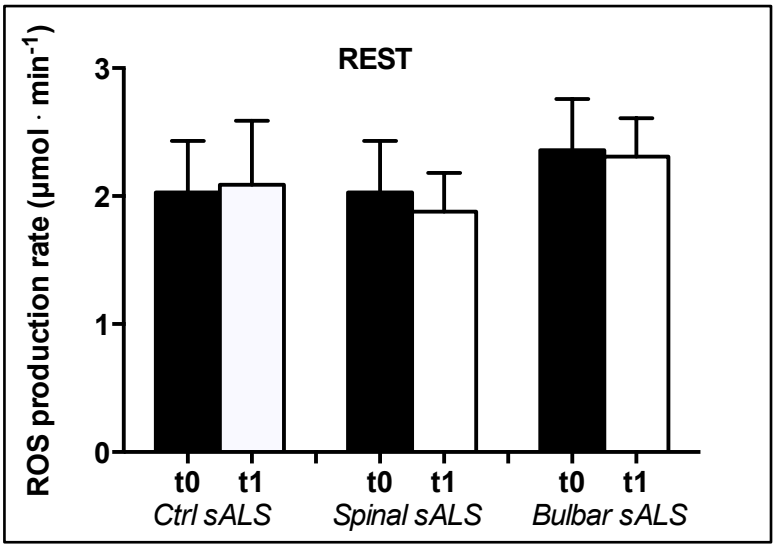

***Figure 54**: Histogram plot (mean ± SD) of the absolute ROS production rate (μmol · min^{-1}) obtained at REST by capillary blood collected from sALS patients (three group: control, spinal and bulbar sALS) in two session (t0 pre and t1 after 20 weeks).*

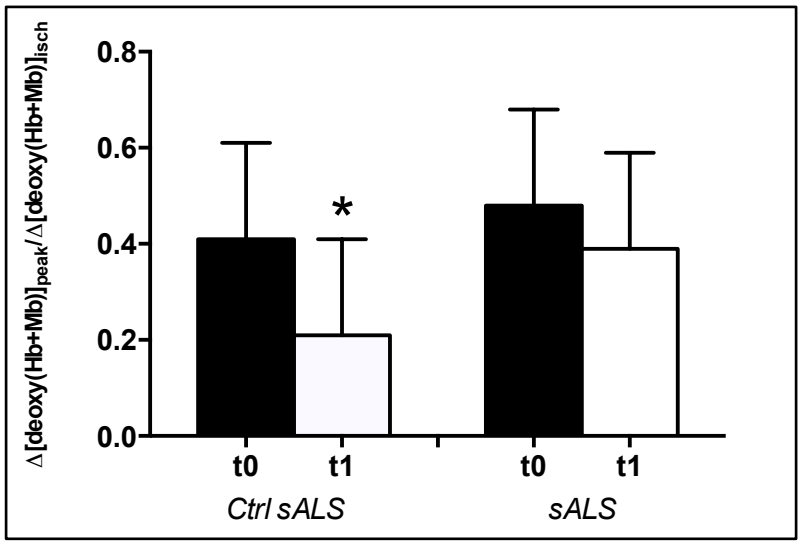

***Figure 55**: Histogram plot (mean ± SD) of fractional O_2 muscle extraction determined by NIRS obtained at REST in control and spinal sALS group. In t1 (after 20 weeks) the untrained group (Ctrl) has a significantly ($p<0.05$) worsening O_2 muscle extraction (* symbol).*

3.2 IN VITRO

3.2.1 Myglobin-NO

Firstly, since in some of our experiments, incubation with the NO-donor was performed starting from the aquomet-Mb, an extremely important preliminary investigation had to be carried out, in order to ascertain whether the EPR spectrum of the latter might interfere with that of the nitrosyl-form we were interested in.
The EPR spectra recorded from the two proteins in the aquomet-form, showed the characteristic axial symmetry (data not shown). The sample was placed in a microwave resonant cavity and irradiated with microwaves of fixed frequency v in the MHz range. The magnetic field H was varied and the absorption spectrum was recorded. Resonances are defined by the following relationship:

$$g = \frac{h}{\beta} \cdot \frac{v\,[MHz]}{H[G]} \qquad (13)$$

where h/β is a constant with a value of 0.714484. The position of the absorption bands is therefore given by the spectroscopic splitting factor, i.e. the g factor, which is independent of the microwave frequency applied and is suitable to identify any given free radical. For one electron in a isotropic environment the absorption function is Lorentzian, with a unique g value. The convention in EPR spectroscopy is to show the first derivative of the absorption function. On the other hand, in an anisotropic environment, unpaired electrons become sensitive to two types of symmetry elements, axial and rhombic. In particular, in heme compounds, where iron is covalently bound to the four nitrogen atoms of the porphyrin ring, such a semi-rigid square and planar arrangement of the nitrogens imposes a tetragonal symmetry upon the iron-ligand system (the symmetry around the high spin iron is determined by the chemical nature of the ligands surrounding it and by their geometrical arrangement).
As a consequence, constraints on the heme can perturb this tetragonal symmetry. If the free radical is in an anisotropic environment with axial symmetry, the EPR spectrum is defined by two distinct g values: $g_{\parallel}$ and $g_{\perp}$.

In the present study, the very low intensity observed for the latter in the case of human Mbs, assured us that, even if the aquomet-form was present, the corresponding signal did not perturb the peak due to the nitrosyl-Mb. As said, this was an important preliminary check since, after the incubation with the NO donor, conversion from aquomet-to nitrosyl-Mb might be lower than 100%, and a residual amount of the former might be still present in solution.
Figure 56 shows the spectra of both the 54K and 54E human Mb isoforms (0.05 mM), recorded after reduction to the deoxy-form, and subsequent incubation in the presence of the NO donor, in the absence of oxygen.

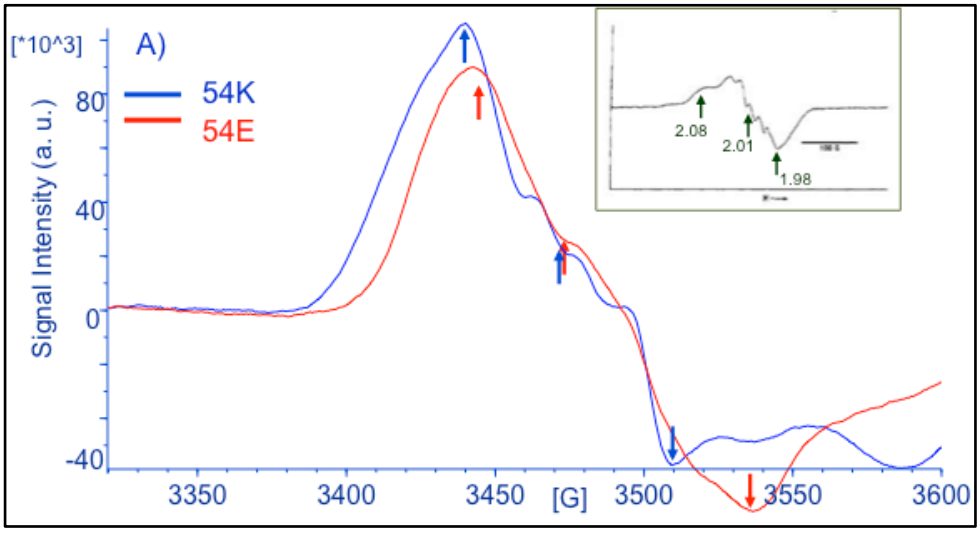

***Figure 56**: EPR spectra of nitrosyl-54K and 54E isoforms. Spectra were recorded after reducion to the deoxy-form (0.05 mM) by sodium dithionite addition and successive incubation with the NO donor (0.05 mM). Spectra were not normalized to allow for a better comparison. Three distinct g values are shown, indicated by the arrows. 54K: g_x=2.03, g_z=2.00, g_y=1.99; 54E: g_x=2.02, g_z=1.99, g_y=1.97. The g values were calculated by equation (13) from the absorption frequencies displayed in the spectra (G) and the microwave irradiation frequency of 9786 MHz. An EPR spectrum reported in the literature for the "native" human nitrosyl-Mb is shown in the inset and the g factors indicated.*

The peculiar spectral shape, similar in both the proteins, suggested the formation of the nitrosyl-Mb form. Three effective g values could be detected in the spectra: one peak on each side of the horizontal line were identified as the x and y in-plane absorption (g_x and g_y), whose directions are mutually perpendicular and approximately parallel to the heme plane. Their g values were 2.027 and 1.986, and 2.025 and 1.971, for the 54K and 54E isoforms respectively. In between, an 'inverted S shape' is displayed, located at g ≈ 2.004 for both the proteins.
The axial absorption, i.e. the g_z factor, showed the hyperfine splitting due to the NO nitrogen, and was found at 1.999 and 2.004 for 54K and 54E respectively.
From the EPR spectrum of the "native" human nitrosyl-Mb, g factors approximately equal to 2.08 (g_x), 2.01 (g_z) and 1.98 (g_y) have been previously reported in the literature (see the inset in **Figure 56**).
As expected, the g factors of the two proteins were found to significantly deviate from the free electron spin value (2.0023), indicating that the 3d orbitals of the iron ion are strongly involved, as a result of the spin-orbit interaction.

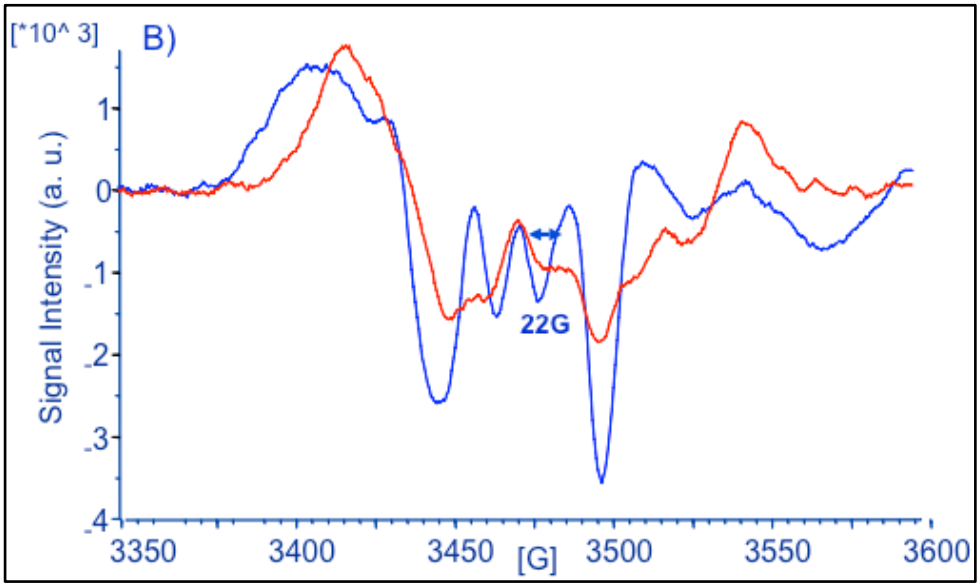

***Figure 57**: EPR spectra of nitrosyl-54K and 54E isoforms. The second derivative of the spectra reported in Figure 56 is shown. The difference between the spectra is emphasized and, in particular, the z-hyperfine coupling constant of 7G is marked.*

Super-hyperfine interaction with another axially bound ^{14}N nucleus should be expected: the sixth ligand of the heme-iron was identified as the unprotonated nitrogen belonging to the residue H93 (i.e. the proximal histidine), and the coupling constant of the super-hyperfine splitting of resonance lines, due to the covalent bond between heme-iron and this residue, estimated to be ~7G (see **Figure 57**). Indeed, in a hexacoordinate nitrosyl-form, a nine-line hyperfine splitting is theoretically expected, originated from the interaction of the unpaired electron both with the ^{14}NO nitrogen and the ^{14}N nucleus of the axial base located in trans to the NO.

As can be easily observed from the spectra, the two proteins showed a different super-hyperfine interaction, with the 54E showing an almost axial symmetry. The difference was even more pronounced when spectra were recorded under pO_2 = 40 mmHg starting from the aquomet-form (**Figure 58**).

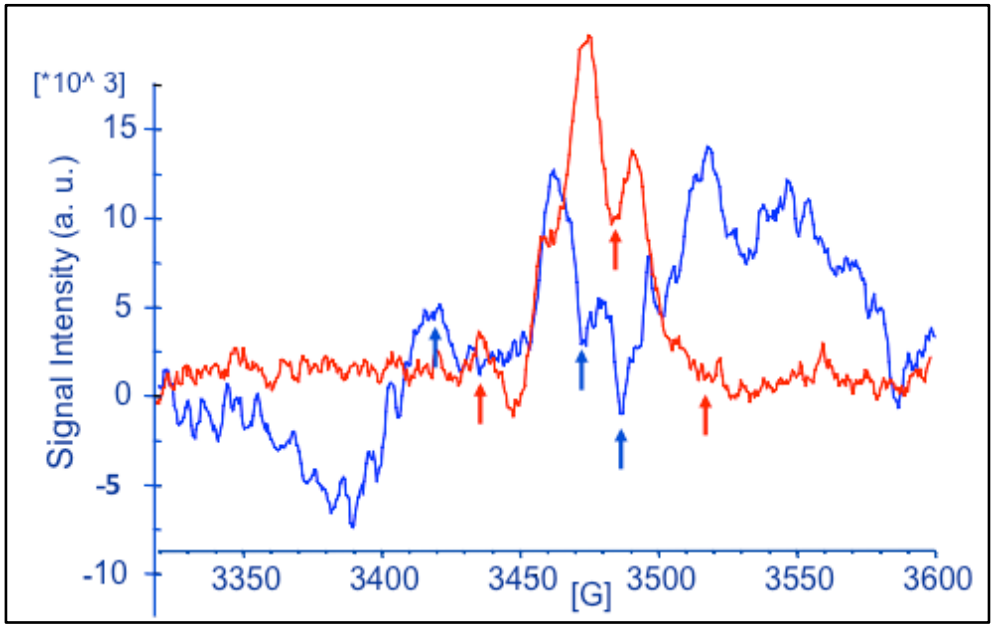

***Figure 58**: Second derivative of the EPR spectra of nitrosyl-54K and 54E isoforms, starting from the corresponding aquomet-form. Spectra were recorded from the aquomet-54K and 54E isoforms (0.05 mM) after incubation with the NO donor (0.05 mM), at pO_2 = 40 mmHg. Spectra have been not normalized to allow for a better comparison.*

The NO binding of the two Mb isoforms is reported in **Figure 59** as the intensity of the EPR signal due to the nitrosyl-Mb generated (the a.u. were determined by double integration of first derivative EPR spectra) as a function of the oxygen concentration. A significantly larger NO binding capacity (more than double; $p < 0.01$) was determined for 54E under deoxygenated conditions, while the two proteins became almost comparable in the presence of oxygen. An exponential decay of the bound NO as a function of pO_2 (R^2 = 0.99) was found by fitting a model curve to the experimental data: NO binding rate (amount of NO (a.u) · pO_2^{-1}) was higher for the 54E than 54K isoform.

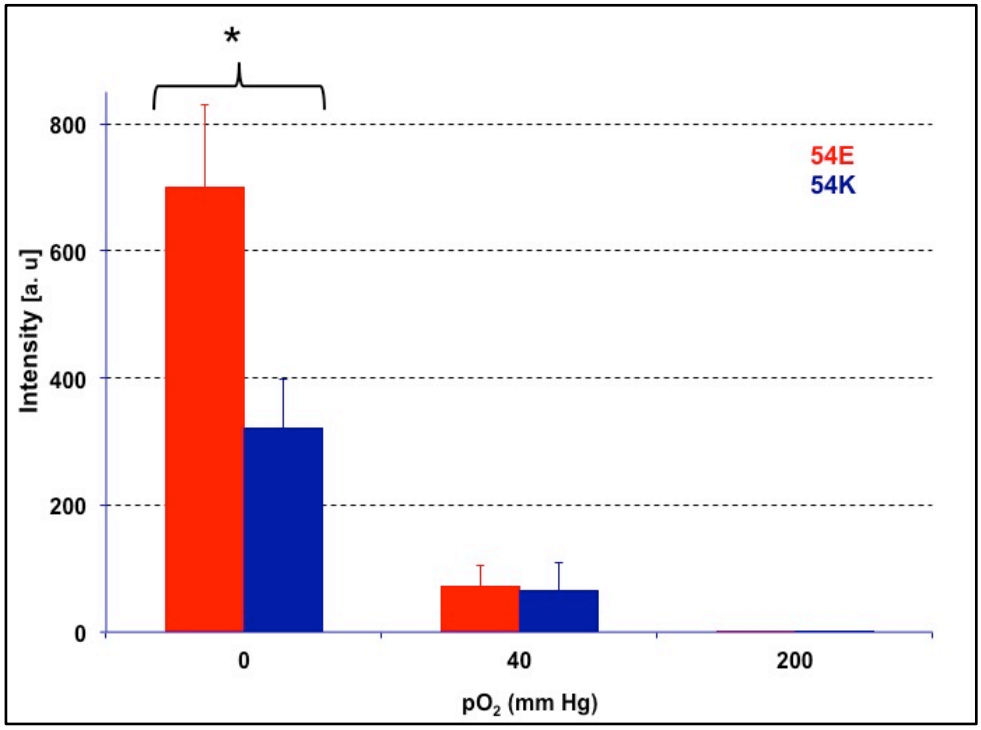

***Figure 59**: NO binding affinity of the two human Mb isoforms. Histogram of double integrated signals of the EPR spectra due to the nitrosyl-Mb formed starting from either 54K or 54E in the aquomet-form (0.05 mM), after incubation with the NO donor (0.05 mM) at different pO_2 levels. The arbitrary concentrations (a.u.) were determined by double integration of first derivative EPR spectra. The exponential decay of NO amount bound to each protein as a function of pO_2 (r^2 = 0.99) is characterized by a different rate constant for the two proteins: 54E: 0.037 and 54K: 0.033 a.u pO_2^{-1}. Standard deviation is also reported, which was calculated from four independent measurements.*

4 DISCUSSION

Aim of our study was to shed light into the mechanisms involved in oxidative stress responses in man at both integrative and molecular levels. Our experimental investigations have been focused to the study of ROS production under various conditions of hypoxic states.
In healthy subjects, the experimental protocols were designed in order to study the effects of: a) exercise (as inducing a transitory hypoxic state) of both short (in hockey players, swimmers) and long duration (in triathletes); b) training (as inducer of an adaptive antioxidant response in swimmers); c) hypoxia, both hypo and normobaric (to study the effect of the assumed model condition itself, in young sedentary subjects); d) antioxidant molecules administration as an external way helping redox balance.
In neurodegenerative pathologies (patients affected by: Mild Cognitive Impairment (MCI), Type II Diabetic Neuropathy (Type II DN) and sporadic Amyotrophic Lateral Sclerosis (sALS)) after checking the expected unbalance throughout a significant increase of ROS under resting conditions, the effect of training on the possibility to restore a normal ROS production level was investigate. Now, hereafter you will find point by point the discussion to simplify the lecture.

EPR, Blood, ROS production and oxidative stress: starting considerations

ROS are highly unstable oxygen molecules characterized by the presence of at least one unpaired electron, which can be stabilized by subtracting electrons to neighboring molecules.
Despite the growing interest in the role played by ROS, reliable quantitative methods for the assessment of oxidative stress in humans are still lacking. Electron Paramagnetic Resonance (EPR) spectroscopy is, without any doubt, the only direct away to detect and measure free radicals [111].
Nevertheless ROS half-life is too short if compared to the EPR time scale so they are EPR-invisible: only when 'trapped' and transformed in a more stable radical species they become EPR detectable [101,102]. In particular, in EPR spectra, signal areas are proportional to the number of the excited electron spins, potentially leading to absolute concentration levels, when adopting a stable radical compound as reference.
Moreover our developed method was found suitable to be applied to a lot of physiological and pathological subjects and conditions. It must be underlined the novelty of the technique so that, as already reported, we completely lacked literature data to be taken as reference.
All together these reasons led biologists to currently use enzymatic assay methods to determine the ROS-induced damage by means of bio-molecules such as proteins, lipids and DNA and as recently reviewed [1] wide literature data can be found using enzymatic methods, in human blood on both plasma serum and red cell samples. Blood interacts with all organs and tissues and, consequently, with many possible sources of reactive species. In addition, a lot of oxidizable substrates are already present in blood so carrying a lot of substances that are considered oxidative stress markers (e.g., TBARS, protein carbonyls).

Changes in blood concentrations of these markers reflect corresponding changes in tissue of interest (mainly skeletal muscle) [112]. As a matter of facts, the vast majority of the relevant human studies have measured the redox status by using plasma or serum. This choice was a probably adopted after considering that plasma reflects tissue redox status together with the ease of plasma collecting procedure. However with this latter choice we cannot exclude potential artefacts generated by in vitro chemistry during the preparation and incubation phase of the spin probe or spin trap used, although this limitation is not exclusive to a particular technique since it has interpretive implications for any reactive metabolite measured ex vivo, especially human plasma.
Moreover, due to classic tests have mainly quantified the ROS levels in human plasma but not those associated with erythrocytes, these studies have not taken into account the role of circulating cells. Ginsburg et al. [113] raised serious doubts whether reports on antioxidant quantifications carried out exclusively in plasma can be trusted to represent true oxidant-scavenging abilities.
Indeed red blood cells may exert both antioxidant and pro-oxidant activity. Because of the high iron concentration (~20 mM), the red blood cell (RBC) can be considered an “iron mine” but, paradoxically, it is also one of the major components of blood antioxidant capacity and one of the most resistant to oxidative stress cell. A very efficient intracellular reducing machinery, coupled with its high cell density makes the erythrocyte an effective “sink” of reactive species. Probably not only the blood per se but, more important, the whole organism can benefit from RBC scavenging ability. The reverse side of RBC antioxidant power is its capability of being, in turn, a source of reactive species. The superoxide radical generated within the RBC by deoxygenated or partially oxygenated hemoglobin, usually found at low levels and likely under physiologic conditions, does not represent a big hazard for the cell. Similarly, the ability of RBC to scavenge or generate nanomolar concentrations of NO• can be easily handled by the methemoglobin reductase/NADH/glycolysis system. Completely different may be the situation when the erythrocyte crosses a tissue where an intense production of reactive oxygen/nitrogen species is occurring. Under these conditions, the RBC may accumulate oxidative damage, in turn reflecting the oxidative stress of other tissues and organs. For this reason, oxidative status of RBCs is potential candidate for monitoring the overall oxidative-stress status.
During exercise, since reactive species are generated by both blood and muscle, it is reasonable to assume that there is a bidirectional movement of reactive species from the muscle to the blood, and vice versa, until equilibrium is reached. The same may hold true for exchanges among blood constituents, namely, plasma, erythrocytes, leukocytes and platelets [1], once that certain basic assumptions are met: reactive species with adequate half-life have the ability to cross membranes and generate reactive species at the vicinity of the compartments considered.
As a matter of facts with respect to spin-trapping EPR, enzymatic assays are ‘a posteriori’ methods

Fresh versus Frozen Blood samples: Protocol Design

Based on all these considerations and aiming at reducing the invasiveness of the method and hence increase its clinical and diagnostic potential, herein, we

investigated the application of the radical-probe approach to the measurement of oxidative stress status in peripheral blood.
Moreover fresh, rather than frozen samples were used for the EPR measurements to be able to gain an estimation of the ROS production rate, instead of a single level, well assuming that this procedure allowed us to attain more precise and reliable results (**Figure 24-25**). The experimental protocol was developed to measure ROS production in human blood and then adopted in all experiments carried out "in vivo" (**Figure 20**). EPR ROS determination by capillary blood samples can be well compared to a finger-prick blood sampling for glycemic test. Therefore the easy of the methods seems to be the dominant factor in the overwhelming use of blood measurement in human study.
Unpaired electron(s) carrying species are, as such, EPR visible. However ROS half-life (superoxide [$O_2^{\bullet -}$] $t_{1/2}$ (s): 10^{-4}; nitric oxide [$NO^{\bullet}$]: 0,4 at ambient temperature) is too short if compared to the EPR time scale. Therefore the species have to be 'trapped' and transformed in a more stable radical species to become EPR detectable. Among spin trapping or probe molecules, suitable for biological utilization, CMH was adopted, since it is a molecule capable of diffusion in all cell compartments, including mitochondria [114]. Indeed, due to its peculiar physical–chemical properties, CMH probe is able to cross biological membranes, thereby detecting ROS both in plasma and intracellular compartments. In this way, EPR measurements allowed us to attain a overall quantitative determination of ROS production rate in human blood samples.
In addition, owing to its high efficiency in radical detection, CMH probe can be used at very low concentrations (0.5 - 1 mM) compared to spin traps (10 – 50 mM), which minimizes side-effects of the probes on the biological samples. Moreover CMH rapidly reacts and allows radical detection in a single chemical reaction, while other probes require at least two reactions, which may cause artefacts [115].

Reproducibility measurement and limit of detection

The high reproducibility of the measurement was demonstrated by performing the experiments two times on the same subject six hours apart. In fact the procedure itself makes impossible to repeat the same experiment several times on the same blood sample. Nevertheless the collected data suggested that repeated experiments from a resting subject gave almost super-imposable results: we can be observed an excellent correlation coefficient ($R^2 = 0.9999$) (**Figure 25**).
The high sensibility EPR instrument was demonstrated by limit of detection (LOD) and quantification (LOQ) of $30 \cdot 10^{-3}$ mM and $100 \cdot 10^{-3}$ mM were calculated respectively.

Starting measurement

After checking the reproducibility of the EPR measurements from the collected data; we tested the ROS production rate in human blood in about one hundred, middle aged, healthy subjects. Different ROS concentrations were obtained when collecting data, on the same resting subject, from different blood fractions. These series of preliminary measurements on a homogeneous group of healthy subjects was firstly carried out for determined the mean measurements in blood.

In peripheral blood ROS production levels were found about 18% greater (1.79 ± 0.12 μmol · min^{-1} vs 1.48 ± 0.2 μmol · min^{-1}) than in venous, owing to the different pO_2 (100 mmHg vs 75 mmHg). An even greater level was found in erythrocytes samples (2.8 ± 0.3 μmol · min^{-1}), due to the increased number of cells in the same volume. On the contrary, significantly lower results (0.16 ± 0.02 μmol · min^{-1}) were found in plasma due to red cells absence, the main ROS producing elements in blood (**Figure 26**). The data well demonstrate the crucial role played by some parameters (e.g. temperature, $PO_{2)}$ on the results, suggesting that great care must be taken to keep all parameters at a constant level during the whole experimental procedure (**Figure 27**).

Exercise: the transitory hypoxic state

Considerable evidence has linked exhaustive exercise with extensive free radical formation. Davies et al. [116] were the firstly to establish exercise-induced free radical formation after exhaustive physical activity by demonstrating a heightened EPR signal (around g=2.004) in muscle and liver homogenates. Other studies [117, 118] have also been able to demonstrate higher EPR signals with exercise. There are numerous reported that provide reasonable support to the notion that exercise increases the production of reactive oxygen species and that mitochondria are important sources of oxidants species [119, 27]. Other sources of oxidative stress during physical exercise are inflammatory responses mediated by neutrophils [120], the release of transition metals, such as iron, that supports Fenton chemistry with formation of hydroxyl radical, the interaction of met-Myoglobin and met-Hemoglobin with lipid peroxides [121], and the activity of xanthine oxidase [122], possibly within an ischemia-reperfusion model [123]. As known, high-intensity physical exercise alters the fragile balance between oxidants and antioxidant defences and that the mitochondrial respiratory chain and other pathways contribute to free radical generation. As above reported, blood plays paramount importance in regulating redox status changes appearing during exercise.

Using ESR spectroscopy, our studies clearly demonstrated in human capillary blood that a short-term constant-load submaximal exercise (CLE) at heavy-intensity in hockey players, and/or incremental test (IT) in swimmers, induced oxidative injuries since a significant ($p<0.01$) increase: +7% and +16% respectability, in ROS production were detected (**Figure 28 and 31**).

As reported elsewhere [124], professional athletes showed a rapid increase in ROS production at the starting of exercise. This was followed by a gradual decrease in the magnitude of the ROS production, reaching the initial value after 20 min. This finding well accords with the idea that adaptive responses to aerobic training programs render athletes' enzymes less responsive over time to further significant activation, and that increased ROS generation caused by physical exercise overwhelms the body capacity to detoxify from ROS.

As expected when using a systemic determination the ROS detected levels are surely lower mainly because part of the produced ROS have been buffered by blood itself. Bailey et al. [125] showed, in typical EPR spectra, a positive veno-arterial concentration of a-phenyl-*tert*-butylnitrone (PBN) adducts, detected in the arterial and venous circulation, at moderate intensity exercise. In the same article

the authors reported an increase in the EPR signal amplitude, according to the exercise intensity both in the arterial and venous circulation.
Parenthetically we would like to underline that first aim of the present thesis was to evaluate the efficacy of ROS generation assessment by adopting a mini invasive procedure. Just for this reason we have been forced to use arterial capillary blood samples even if we are completely aware that arterial blood, because of circulatory system design, is very far from muscles that are the main ROS sources during exercise.
However despite the moderate exercise levels adopted in these studies, the method was found suitable to detect significant differences so demonstrating its sensitivity even under the adopted experimental conditions. On the other side, under the adopted acquisition protocol, the ROS levels measured in the present study resulted in any case many times over the estimated limits of detection and quantification of a few nanomolar order.
Furthermore, long-duration exercise effects were tested in two groups of athletes during Triathlon competition (swimming, cycling and running): the first group performed a short-competition (ShC 7.3): and the second group performed a long-competition (Ironman). In both groups our study demonstrated that long-duration exercise induced a oxidative injuries since a significant ($p<0.01$) increase: +12.5% and +14% respectively, in ROS production were detected in human capillary blood (**Figure 32**).
Increased production of reactive oxygen and nitrogen species may contribute to elevated levels of lipid and protein peroxidation markers also after the end of exercise (**Figure 29A,B, 33 and 34**). The measurement of these latter only in plasma is enough to describe the changes in erythrocyte and muscle redox status because of a strong communication between the different compartments [112]. Indeed results from the present study indicate that lipid peroxidation, as measured by TBARS, was elevated immediately and until 20 min after CLE (**Figure 29A**). Many studies have provided indications for substantial increase in plasma lipid-peroxidation levels after aerobic exercise [126, 127,128].
The delay in TBARS clearance, compared to more rapid ROS production kinetics, is in agreement with the observation of Echtay et al. [129] who proposed that lipid peroxidation products regulate mitochondrial ROS production by inducing the expression of proteins that inhibit mitochondrial O_2• production by inducing uncoupling.
Otherwise, removal of oxidized proteins from blood is, presumably, a time-consuming process, also considering that oxidative modification in proteins can occur by the effect of ROS directly or indirectly through conjugation to lipoxidation end products. For this reasons protein carbonyls concentration remained elevated for a prolonged period (1 h) after CLE (**Figure 29B**). Other studies generally have reported increases similar to ours immediately after exercise, whereas the increases in protein carbonyls mostly disappeared after 0.5 to 6 h of recovery [126, 130-132]. The different life response of protein carbonyls reported may be partly ascribed also to the different intensity and more or less muscle-damaging exercise mode used in the studies and to differences in the physical fitness of the participants [133].
Other aim of the study was to examine whether measuring blood oxidative stress markers, a currently common practice in biomedical research, is indicative of ROS production. Although almost all oxidative stress biomarkers have been criticized for

their reliability (including those used in the present thesis) [134, 135], it is apparent that, at rest, all changes suggesting increased oxidative stress are directly related to ROS production (**Figure 30A - B**). However the time-course changes of the used markers of oxidative stress were delayed (**Figure 29A** - **B**) than ROS production kinetics (**Figure 28**) and no correlation is possible in dynamic conditions. In other words it must be stressed that the good correlation found between EPR and enzymatic assays data do not represent a validation test for the here proposed EPR technique. By principle, the adopted enzymatic methods can quantitate the damage arising from ROS production, while EPR is the only technique capable, by using suitable probes, of quantitating the ROS production itself. These are the reasons why we could not hypothesize an 'a priori' existing relationship between these methods we cannot absolutely affirm that ROS production will at the same time produce damage. On the other hand the data collected in the present study seem to suggest that the practice of the vast majority of the studies to collect one blood sample immediately after exercise can potentially lead to inaccurate deductions [126].

Finally, as mentioned until now, the short and long-duration exercise invoke increased ROS production in human. In agreement with our data, Kanter et al, Liu et al [136, 137] reported significant increases in oxidative stress in response to marathon and ultra-marathon distance running races. Excessive ROS production and consequent oxidative damage induced by intense long-duration exercise, are mainly a response to increased oxygen utilization [138].

It should also be said that in long-exercise, defenses are often not sufficient to eliminate oxidative damage during and after exercise, as demonstrated by significant increased lipid (ShC +38%, Ironman +49%) (TBARS) and protein (ShC +92%, Ironman +128%) (PC) (**Figure 33** and **34**). The increase lipidic peroxidation is associated with the ROS production and that consequently leads to the breakdown of lipid; the PC content is the most general and widely used biomarker of severe oxidative protein damage.

Triathlon is a multi-event sport (swimming, cycling and running). Although the physiological bases for success in a triathlon are not well understood, the ability to maintain minimal alterations in the homeostasis of cardiovascular, hemodynamic, thermal, metabolic and musculoskeletal functions seem to be a crucial point [139].

Triathlon competition causing changes in biochemical parameters (**Table 7**), dehydration, oxidative stress, (**Table 6**) inflammation and the long-duration exercise is associated with an increased risk of infections in the upper respiratory tract [140].

By laboratory analysis, we observed after competition, a significant increased production of leucocytes, neutrophils, lymphocytes and monocytes cells, probably results by inflammatory response (**Table 7**), our data are in accord with those reported by other authors [141].

As reported by YU et al. [142], HDL cholesterol increased significantly immediately after the race. We found a significantly increase of HDL in both triathletes group (+ 13% and + 17% respectively) after competition too (**Table 7**). It could be assumed that HDL would constitute a primarily target for free radicals, thus delaying LDL deleterious oxidative modifications [143]. Furthermore, it has been hypothesized an efficient antioxidant function played by HDL, which could constitute an adaptive response to the increased oxidative stress [143].

Now, we want to examine the correlation between ROS production at rest (pre competition) and blood chemical laboratory test. Platelets, Iron, HDL, MCH, and Corpuscular Volume exhibited a significantly positive correlation with EPR ROS production (mean r^2=0.50) (**Figure 35A-E**). Lymphocytes shows a minimal and not significantly correlation (r^2=0.23) (**Figure 35F**)
After competition, we found a good direct linear relationship between Hemoglobin, MCH and MCHC and ROS production (mean r^2=0.63) (**Figure 36A-C**).
Once again, these correlation data are important because they allow us to confirm that EPR measure follows the trend of other collected parameters.
Thus, physical exercise and some pathological status can be seen as a typical example of an acute, intermittent or long-lasting/chronic hypoxic exposure or condition.
The role of hypoxia was studied in the exercise [144]. It's known that Hypoxia Inducible Factor 1 (HIF-1) play an important role during exercise. Almen et al, [145] reported that 45 minutes of one-leg knee-extension exercise elevated protein level and DNA binding activity of HIF-1α in human skeletal muscle. Furthermore, it was observed that 6 weeks of high and intensity bicycle training under normoxic condition increased HIF-1 and mRNA expression in human skeletal muscle [146] Endurance exercise-related angiogenesis, up to a significant degree, is regulated by ROS-mediated activation HIF-1α.

Summarizing:

- Confirms the increase of ROS production and oxidative stress after exercise
- Data showed a direct correlation between EPR ROS production rate and markers of oxidative stress concentration (TBARS and PC) at rest

Hypoxia: Acute Normobaric, Acute and Prolonged Hypobaric

Hypoxia induces changes in blood composition: increases the concentration of red blood cells (RBC) because of an increase of erythropoietin secretion (EPO), a decrease of plasma volume (dehydration) and mobilization of erythrocytes from the spleen.
The existence of hypoxia-induced ROS production remains controversial [150]. However a number of reports have provided evidence for ROS formation in acute conditions of hypoxia, but there is no general consensus regarding the physiological significance of these observations. ROS are more likely to be produced in hypoxia when there is both a high reductive capacity (e.g. high $NADH/NAD^+$) and sufficient O_2 available for reaction. Hypoxia exposure can lead to altitude mountain sickness (AMS) and sometime to high-altitude pulmonary or cerebral edema when the exposure is severe. There are indirect evidence from cells and tissue experiments that acute hypoxia induces accumulation of ROS [37,38]. As already said, the increase of ROS accumulation during exposure to hypoxia has important systemic implications [39] and more particularly at the brain level with damage of vascular endothelium, neurons, glia, and down-regulation of Na^+-K^+-ATPase, Ca^{2+}-ATPase, Na^+/Ca^{2+} exchanger activities. [37].
Our present study was designed to investigate in healthy volunteers the role of high and middle altitude associated with hypoxia. This is because AMS is a more

common condition, which affects 40-50% of people who go up over 4200m. Typical symptoms are similar to that of a bad hangover: dizziness, headache, nausea, prolonged shortness of breath, prolonged fatigue, vomiting and exhaustion. In extreme cases, subject may experience agitation, anxiety or mental confusion, lack of coordination or imbalance.
ROS production and oxidative stress in Hypoxia was studied in three conditions: i) Acute Normobaric Hypoxia, ii) Acute Hypobaric Hypoxia and iii) Prolonged Hypobaric Hypoxia.
All the hypoxia-exposure procedures induced the increase in ROS production preceding the appearance of oxidative stress-induced damage (measured as increase in TBARS and PC). There are also other important factors, because in perfused systems local changes in blood flow associated with hypoxia or ischemia can induce a rise of the phenomenon [150]. Martinelli et all, [151] have shown that climbers who have been exposed for prolonged periods to extreme altitude exhibit evidence of oxidative stress in skeletal muscles as demonstrated by the presence of increased lipofuscin in muscle biopsy samples and muscle DNA oxidative damage [152]. Lipofuscin is a product of lipid peroxidation and is largely attributed to mitochondrial membrane oxidative break-down products associated with aging and disease. Similar oxidative changes in muscle biopsies have been observed in hypoxic chronic obstructive pulmonary disease [153].
By contrast, our results show that:

i) In healthy sedentary subjects, immediately after the start of the breathing of a normobaric hypoxic mixture (12.5% O_2 in air, simulating about 4100m altitude) a significant ($p<0.001$) turning on of ROS (+38%) is formed because of the transition to low intracellular O_2 tension (**Figure 38**) as attested by a significant ($p< 0.001$) reduction 88-90% (**Figure 39**) in arterialized blood oxygen.
Figure 38 showed that an important, significant and fast elevation of ROS production occurs immediately after 2 minutes breathing of the mixture (+30%). In agreement with the present finding, Steiner et al, observed in isolated systemic vessels, that hypoxia alone can result in rapid elevations in ROS signalling in local vascular beds [154].
After 30 minutes of the return to normoxia, ROS production still showed +3.5%. During normobaric hypoxia, oxidative damage was observed too: TBARS underwent only a 10% increase at 4 hours of hypoxia. By contrast, 1 hour after hypoxia offset plasma concentration of TBARS it was significantly ($p<0.05$) increased returning back to pre-hypoxia control value in the subsequent 2 hours (**Figure 40A**). PC concentration significantly increased, attaining the highest value ($p<0.059$) at 4 hours. At hypoxia offset, PC decreased slowly, being still higher after 2 hours than at 0 hours (**Figure 40B**).
The late onset of oxidative stress damage seems to give evidence that once again the imbalance between antioxidant capacity and antioxidant production, documented by some biomarkers of oxidative damage, is a time consuming process.

ii) When reaching high altitudes, the decrease in barometric pressure results in a reduction in the partial pressure of oxygen in inhaled air. In acute hypobaric hypoxia, at 3480m s.l, ROS production significantly ($p<0.01$) increases at 6 (+42%) and 24 (+47%) hours respectively (**Figure 41A**) according to a reduction of SO_2 (-

11 and -10% respectively) (**Figure 41B**). One of the most detrimental effects of hypobaric hypoxia is oxidative stress, which could be the consequence of an increase in ROS, as demonstrated in our study, and a decrease in antioxidant and free radical-mediated reduction in pulmonary nitric oxide bioavailability [155, 156, 157]. The passive ascent on the high mountain (Plateau Rosa) by cableway may have contributed to the rapid production of ROS, as the time for acclimation had been lacking. Because of this lack of acclimatization we also observed an increase in the ventilatory frequency (at 6 hours +43%: hyperventilation) (**Figure 42A**) and heart frequency (at 6 hours +30%) (**Figure 42B**). Moreover, three subjects showed typical AMS symptoms.

iii) In prolonged hypobaric hypoxia, after two weeks exposure to moderate altitude (1860m sl), ROS production and lipid peroxidation product significantly ($p<0.01$) increased: ROS +33%; (**Figure 43**) TBARS +9% (**Figure 44A**).
Moreover, even if two weeks exposure to moderate hypoxia induced significant increase in both ROS and oxidative marker concentration, one week after return to s.l. both ROS production and TBARS concentration returned to pre-exposure values and even better, PC concentration significantly ($p<0.01$) reduced (-40%) (**Figure 44B**).

From our results, we may conclude that ROS production and oxidative damage were: type (normobaric versus hypobaric) time and altitude dependent but always reversible.
In fact, 30 minutes after the end of simulated normobaric hypoxia exposure, the ROS production returns to basal value (**Figure 39**).

Summarizing:

- The experimental conditions under investigation, even though very different for degree of hypoxia and duration, were both characterized by comparable trends of accumulation of ROS and oxidative damage.
- Taken all together these results must be considered when altitude exposure is used as endurance training procedure to increase the oxygen transport capacity.
- Our EPR methods can be applied as routinary procedure in mountain medicine for studying pathologies induced by hypoxia following high altitude acute and chronic staying.

Training: Balance Restore

Regular physical exercise increased the level of antioxidant defence and decreased the rate of ROS production [35]. Many data indicate that exercise with moderate intensity has systemic and complex health promoting effects, which undoubtedly involve regulation of redox homeostasis and signaling.
Overload is a primary key of physical training required for peak performance, but overtraining can result in performance decrements, profound fatigue and oxidative damage. Margonis et al [147] examined whether progressively increasing and decreasing training volume and intensity induced oxidative damage to lipids and

proteins. They concluded that over-training induced changes in oxidative stress biomarkers proportional to training load.
Otherwise good training, that is a moderate training, can have a positive effect on ROS production, leading to decrease ROS and increase the antioxidant capacity in whole body.
In triathletes, we found a good linear relationship between ROS productions at rest and years of training (r^2= 0.60) (**Figure 37**). Increasing years of training also increases the production of ROS, even if the ROS production values were always low compared to sedentary subjects.
In master swimmers after a high-volume/low intensity training, moderate daily exercise for eight weeks, induces a significant (p = 0.0001) reduction of ROS production at rest (-20% in POST) and after incremental exhaustive exercise (-25% referred to end exercise in PRE) (**Figure 45**).
Besides an inverse correlation between ROS production at the end of exercise and VO_2max was found (r^2=0.58) (**Figure 46**): a low index of ROS production corresponds to a higher VO_2max. level
Based on our data observed at rest in sedentary subjects, this phenomenon can also be interpreted in another way: physical inactivity decreases the adaptive subject oxidant capacity, including redox processes and the increase of ROS production, which can be transformed into high risk of diseases and into a worsening of life quality [148].
There is a great deal of evidence which indicates that higher VO_2max is associated with a decreased risk in the incidence of a number of life-style related diseases, including breast, colon and prostate cancer, cardiovascular disease, type II diabetes and Alzheimer Disease [148, 149].

Summarizing:

- At rest, in trained versus untrained athletes a lower value of ROS production was found
- "Over training" is dangerous! It increases ROS production
- "Good training" or regular physical exercise decreases ROS production and oxidative stress
- An inverse correlation between ROS production, at the end of exercise, and VO_2max
- Our method was demonstrated rentable to be applied to sport medicine, as an effective /available help in sports centers to set up and adjust training protocols by monitoring training effects on oxidative stress.

Antioxidant supply

Some starting considerations need to be expressed for the analysis of the effects of antioxidant supplementation. Thioctic acid (a-lipoic acid) was adopted as an endogenous antioxidant molecule which, in its reduced form, i.e. dihydrolipoic acid, forms a thiol-disulphide redoxing system [158, 159]. At the same time this moiety can also succeed in restoring intracellular GSH levels [160.] also resulting an essential cofactor in multienzyme complexes and pyruvate dehydrogenase activity.
Indeed, in our study, the time corresponding to the peak activity of R-thioctic acid is delayed well after supplementation (**Figure 47**), as reported by other authors too

[161]. We found that after 90 minutes of supplementation of R-thioctic acid, ROS production level significantly decrease ($p<0.01$).
Antioxidants may be defined as molecules preventing cell damage due to free radicals and are critical in maintaining health at its optimum, both in animals and humans. In living systems, cells require adequate antioxidant defences levels in order to avoid the harmful effect of an excessive ROS production, and so preventing the associated damage. Indeed excess of ROS production might play a role in pathophysiology of many disease conditions. Many basic researching as well as observational epidemiologic studies in humans suggest that antioxidants can prevent oxidative damage. However, this is still a controversial issue because clinical trials have often been produced conflicting results [163]. Indeed there is a need for the design of large multicentre randomized controlled trials to investigate the effects of different types and doses of antioxidant supplementation in selected groups of subjects.
Nevertheless the here adopted methodological EPR approach was found an efficient and practical tool to respond to the question both in acute or chronic conditions. In particular, in the present study, the R-thioctic acid effects in type II diabetic /neuropathic patients were investigated.

Under diseases: Unbalance of ROS production rate

Oxidative stress is a very fashionable topic to take into account in defining etiology of pathologies since ROS play a major role in many diseases. Oxidative damage within cells has been linked to a wide range of diseases including arthritis, cancer, arteriosclerosis, AD, diabetes and ALS [163, 164, 165]. Unfortunately, many of these diseases have no treatment, show rapidly progressive disabilities, in some cases (depending on pathology) up to death. A significant ROS production increment was found in resting subjects affected by neurodegenerative pathologies, suffering of sure homeostasis unbalance condition: Mild Cognitive Impairment (MCI) +2%, sporadic Amyotrophic Lateral Sclerosis (sALS) +20% (**Figure 48**). As reported in the literature, neurodegenerative diseases (e.g. AD, and MCI frequently seen as a prodromal stage of Alzheimer's disease) are generally age-related disorders characterized by the deposition of abnormal form of a specific protein (e.g. the beta-amyloid in AD), while ALS patients displayed lipid and protein oxidative lesions. On the other side, there was substantial evidence to support the hypothesis that oxidative stress is one mechanism producing motor neuron death. This theory gained a better impact with the discovery that in few cases anti-oxidant enzyme, superoxide dismutase 1 (SOD1) mutation is at the basis of the diseases onset [165]
The two here presented studies have to be taken as ‘in fieri’ and were carried out on two groups of patients: A) Type 2 diabetes mellitus neuropathic patients: antioxidant supply; B) sALS patients: exercise and training effects

A) Type 2 diabetes mellitus neuropathic patients

Diabetic neuropathies are diabetes mellitus associated disorders. Patients may develop nerve damage; symptoms such as pain, tingling or numbness, loss of feeling-in hands, arms, feet, and legs are reported. The causes are probably different and researchers are studying how prolonged exposure to high blood

glucose levels can produce nerve damage. Excessive ROS levels or reduction in the antioxidant defenses, such as SODs, Heme Oxygenase-1 (HO-1), NAD(P)H, Quinone Oxidoreductase-1 (NQO-1), catalase, causes oxidative stress, as it has been widely described in a number of various diseases, including type 2 diabetes mellitus.
Major sources of oxidative stress in diabetes include glucose autooxidation, overproduction of ROS by mitochondria and non-enzymatic glycation process [166] Dietary supplementation with α-lipoic acid, evening primrose oil or sunflower oil was found to lower plasma lipids and risk factors [167].
Starting from these considerations, our study aimed at investigating the possible effects in diabetic neuropathy in this kind of patients as a consequence of antioxidant supplementation (1.6g/die R(+) Thyoctic acid): EPR detectable changes in formation of in-vivo ROS in capillary blood were calculated (**Figure 49**). Indeed ROS production significantly ($p<0.01$; -7%) decreased mainly after 1 hour from supplementation. These acute decremental effects of the supply persisted even after 15 days and 30 days of daily supplementation, inducing changes in oxidative markers' levels: TBARS (**Figure 50A**) and PC significantly ($p<0.01$) decreased (-18% respectively) at 30 days (**Figure 50B).** In agreement with literature data, high levels of oxidative damage before antioxidant supply were found. Accordingly it was previously reported, even after diabetes pathology is established, TBARS increasing trend may be reversed by combined treatment with vitamins C, E, and ß-carotene [168]

Summarizing:

- R(+) Thyoctic acid) induced EPR detectable changes in formation of in-vivo ROS in capillary blood
- Changed in oxidative stress biomarker (TBARS and PC)
- Effects of exogenously administered antioxidants have been observed until 30 days
- Necessary to assess the effects on neuropathy

B) sALS patients: exercise and training effects

sALS is as a neurodegenerative disorder whose cause, unfortunately, remains up to now unknown, characterized by rapidly progressive skeletal muscular paralysis reflecting selective death of both upper and lower motoneurons in the primary cortex, brainsterm and spinal cord. Based on the region where motoneurons are primarily degenerated, strictly related to the afore mentioned symptoms, ALS is classified in two different forms: the bulbar-onset and the spinal-onset (25 and 75% of cases respectively). Bulbar onset firstly involves lip, tongue and throat muscles thereby resulting in progressive dysarthria and dysphagia. By contrast limbs and/or trunk muscles are firstly affected in the Spinal form together with muscular weakness and atrophy, cramps and fasciculation. The initial localization of the degenerative process is a known predictor of progression: indeed bulbar forms are characterized by a shorter life survival.
All these observations led us to divide sALS patients in two groups according to symptoms: bulbar and spinal. Exercise (t0) and training (t1 – 20 weeks; 30 min/day cycling) effects has been tested in both of them.

In **bulbars**: at (t0) a significant decrease ($p<0.05$) of ROS production rate was found both immediately at the end (-17%) of an incremental test (IT) and 15 minutes after the end of the exercise (recovery) (-17%). By contrast, at t1, no significant modification in the ROS production rate was found (**Figure 51A**).
The t1 decrement can probably be attributed to an oxygen supply impaired (intermittent hypoxia). Otherwise other factors can possible produce episodic glucose deficit (hypoglycemia). These hypotheses are supported by Zhang et al Hypoxia Inducible Factor-1 as a target for neurodegenerative diseases [169], who reported HIF-1 as a target for ALS and then hypoxia as a typical factor leading to intermittent and topical suppression of blood flow around motor neuron axon and at tissue levels. In addition age related hypoxia or other factors can produce either chronic or episodic deficits in glucose chronically-reducing vascular perfusion.
Other authors focus their attention in the role of genetic expression of vascular endothelial growth factors (VEGF) reactive to hypoxia: VEGF is in fact known by the critical role playing in the growth and control of vascular permeability.
At t0, the here reported oxidative damage results indicated lipid peroxidation: (TBARS) and Protein Carbonyl (PC) concentrations slightly decreased at the end the exercise. Conversely, at t1 TBARS and PC concentrations increased (+8% vs 22%) at the exercise end (**Figure 52A**-**B**).
By contrast in **spinal** patients: at t0 an increase (+7%, $p>0.05$) of ROS production rate was found immediately at the end of exercise followed by a progressive returning to the basal level after 15 minutes.
At t1 an increase (+4%, $p>0.05$) of ROS production rate was observed progressively returning to the basal level after 15 minutes (**Figure 51B**).
The observed trend was comparable to the exercise response found in healthy subject, characterized by an increase of ROS immediately after exercise.
We can argue that in spinal patients antioxidant defenses are often not able to scavenge oxidative damage during and after exercise, as demonstrated by the significantly increased lipid (t0 and t1 +8%) (TBARS) and protein (t0 +14% and t1 +13%) (PC) levels (**Figure 53A**-**B**).
As reported in the literature [170] oxidative stress reflected by elevated lipid peroxidation is attributable to enzyme SOD1 mutation (in ALS familiar cases) or non SOD 1 (sporadic ALS cases). Our data confirmed the high oxidative damage by plasma TBARS and PC data, as previously reported [171].
No evidence of an improvement between t0 and t1 was found in ALS control group as concerning ROS production.
Finally, the positive training effects are highlighted in **Figures 54** and **55**. Although preliminary data, once again, we have found a match between EPR data, oxidative markers (TBARS and PC) and data collected by NIRS. After training, the ability of O_2 muscle extraction was found improved (+85%) in sALS patients versus Ctrl groups.
Even if ALS studies of the exercise effects are very controversial [172] from our data exercise does not seem to play deleterious effects on the investigated patients.

Summarizing:

- In neurodegenerative disorders an over production of ROS was observed.
- Spinal and bulbar sALS showed a different behavior as a consequence of exercise

- The presence of oxidative damage (TBARS and PC) is confirmed
- Regular moderate exercise can improve the performance in spinal sALS patients, but not in bulbars.

Myoglobin and NO

Interest in human Mbs originated from the observation, in the literature, of different isoforms. Among them, 54K is the most expressed one in the skeletal muscle of populations born and living at low altitude. On the other hand, Mb over-expression has been reported for Tibet natives, totally attributable to the second main isoform 54E, together with a better working and running efficiency [54, 169, 173]. Compared to lowlanders, Tibetans have been found to offset physiological hypoxia with more than double blood flow and more than six fold higher concentration of bioactive NO products, including plasma and red blood cell nitrate and nitroso proteins and plasma nitrite. [174, 175] Thus, a possible role for the latter in hypoxia adaptation of these high-altitude populations has been put forward, with particular emphasis on a different NO scavenging and/or nitrite reductase activity of the two human Mb isoforms. However, neither experimental nor computational data supporting this hypothesis are available so far, since, generally speaking, human Mb is rarely investigated when compared to those from other species

As already indicated, NO is a highly diffusive and reactive molecule, produced, in the cells, by the NO synthases enzymes (NOS), using L-arginine and O_2 as substrates. Among many different and fundamental roles as a signaling molecule, NO is a well-known inhibitor of the mitochondrial respiratory chain, having the cytochrome-c-oxidase as its primary target. Under hypoxia, the low O_2 availability leads to NOS inactivation (being substrate limited). The NO produced by Mb down-regulates mitochondria O_2 consumption, contributing to elongate the intracellular oxygen gradient [176, 177] and limiting the formation of deleterious reactive oxygen species [63].

EPR was the other technique of choice, being considered particularly suitable to investigate NO binding to Mb. Indeed, nitrosyl-heme is characterized by an unpaired electron, such that, from the very beginning, NO was used as a spin-labeled ligand for probing the electronic structure of the heme group and its environment, also in the light of the fact that the O_2 Hb/Mb complex is diamagnetic, thus EPR invisible. [85] NO binding to the metallo-heme protein's center can be directly measured in vitro and in vivo. In fact, by virtue of differences in the line shape and position of the magnetic field (g values) of the EPR absorption, spectra are sensitive to conformational changes of the protein's moiety, which, in turn, produce geometrical changes at the metal site. The binding of NO to these proteins gives rise to a unique EPR spectrum, with characteristic symmetry and hyperfine coupling [178].

Under conditions as physiologic as possible, in the present study, the NO binding capacity of the two more expressed human Mb isoforms was compared, to the best of authors' knowledge, for the first time in the literature. Our results suggest a different unpaired electron interaction with the axial base nitrogen for the two proteins, with, possibly, a stronger bond between the H93 and the iron for 54E than 54K. In turn, these observations support the differences found in DP dynamics of the two isoforms with the MD simulations. Indeed, in the 54E, the distal histidine was found to move relatively far from the heme much more often than observed in

the 54K. This might be probably reflected by a slightly weaker coordination of the ligand bound to the iron at the heme distal side, leading, in turn, to a relatively stronger interaction between the iron and the proximal histdine.
Particular attention was paid to establish the NO donor concentration to be adopted. The necessity of avoiding the use of a large excess of the NO (e.g. 10-fold greater) has been previously pointed out as one of the main aspects to be taken into account to model, in vitro, a physiological environment.
From the spectra, the two proteins showed a different super-hyperfine interaction, with the 54E showing an almost axial symmetry. The difference could be also observed when spectra were recorded under pO_2 = 40 mmHg starting from the aquomet-form [**Figure 58**]. These results suggest a different unpaired electron interaction with the axial base nitrogen for the two proteins, with, possibly, a stronger bond between the H93 and the iron for 54E than 54K The pO_2 levels were in turn chosen to mirror three well known physiological conditions: the extreme hypoxia (pO_2 = 0), the resting O_2 partial pressure in venous blood and interstitial space of peripheral tissues (pO_2 = 40 mmHg) and the "maximum" O_2 concentration reached on air-exposure, respectively. Moreover, it is important to stress here, that pO_2 = 40 mmHg was also found to correspond to the maximum efficiency of the NO donor employed, when both NO generation and its oxidation to NO^{2-} in the presence of O_2 are taken into account.
The NO binding of the two Mb isoforms is reported in **Figure 59** as the intensity of the EPR signal due to the nitrosyl-Mb generated as a function of the oxygen concentration. A significantly larger NO binding capacity (more than double; $p < 0.01$) was determined for 54E under deoxygenated conditions, while the two proteins became almost comparable in the presence of oxygen. An exponential decay of the bound NO as a function of pO_2 (R^2 = 0.99) was found by fitting a model curve to the experimental data: NO binding rate (amount of NO (a.u) $\cdot$ pO_2^{-1}) was higher for the 54E than 54K isoform.
The results obtained by EPR showed a significantly larger NO binding capacity for the 54E isoform with respect to the 54K, but, very interestingly, this difference was circumscribed to the deoxygenate state

Summarizing:

- Very interesting differences emerged into 54 K and 54E.
- The two isoforms resulted to have a intriguingly different behavior tuned by the presence of oxygen, such that their differences became strikingly evident at a very low pO_2 level.
- Presence of oxygen at a pO_2 of both 40 and 200 mmHg, the binding capacity became significantly lower and almost comparable for the two proteins

5 CONCLUDING REMARKS

The here presented study aimed at highlighting mechanisms involved in Oxidative Stress responses in man at both integrative and molecular levels. We believe we succeeded in elucidate some points in particular to underline the following:

- The EPR method herein presented allowed reliable, rapid and non-invasive absolute measurement of ROS production rate in human peripheral blood. Due to its simplicity coupled with the high sensitivity and specificity seems to us the most suitable, when compared to the other currently available methods, generally applied to evaluate ROS production/damage. Indeed the method was found suitable to be applied to a lot of physiological and pathological subjects and conditions.
- The obtained results offered a contribute into different medical fields: sport and mountain medicine, clinical trials, helping in evaluating the efficiency of training protocols, in monitoring pathologies progression and/or therapies effects. Indeed some of the here presented studies, especially when concerning disease conditions, have to be considered 'in progress', nevertheless an extremely interesting road to be taken was marked, so calling for further investigation.
- Also in 'in vitro' experiments EPR technique gave experimental evidence to the relevant role played by Mb isoforms as NO scavenger especially under hypoxic conditions also confirming MD simulation analysis data.
- Finally we are confident that all these studies do provide a firm basis for future researching activity.

BIBLIOGRAPHY

1. Nikolaidis MG, Jamurtas AZ. Blood as a reactive species generator and redox status regulator during exercise. Arch Biochem Biophys. (2009) Oct 15; 490(2): 77-84.
2. Gutteridge JM, Halliwell B. Free radicals and antioxidants in the year 2000. A historical look to the future. Ann N Y Acad Sci. 2000; 899:136-47. Review.
3. Beckman KB, Ames BN. The free radical theory of aging matures. Physiol Rev. 1998 Apr; 78(2): 547-81.
4. Devasagayam TP, Tilak JC, Boloor KK, Sane KS, Ghaskadbi SS, Lele RD. Free radicals and antioxidants in human health: current status and future prospects. J Assoc Physicians India. 2004 Oct; 52:794-804.
5. Gille L, Nohl H. The ubiquinol/bc1 redox couple regulates mitochondrial oxygen radical formation. Arch Biochem Biophys. 2001 Apr 1; 388(1): 34-8.
6. Freitas M, Gomes A, Porto G, Fernandes E Nickel induces oxidative burst, NF-κB activation and interleukin- 8 production in human neutrophils. Journal of Biological Inorganic Chemistry, vol. 15, no. 8, pp. 1275–1283, 2010.
7. Dowling DK, Simmons LW. Reactive oxygen species as universal constraints in life-history evolution. Proc Biol Sci. 2009 May 22; 276(1663): 1737-45.
8. Harman D. Aging: a theory based on free radical and radiation chemistry. J Gerontol. 1956 Jul; 11(3): 298-300.
9. Beckman KB, Ames BN. The free radical theory of aging matures. Physiol Rev. 1998 Apr; 78(2): 547-81.
10. Farr SB, Kogoma T.Oxidative stress responses in Escherichia coli and Salmonella typhimurium. Microbiol Rev. 1991 Dec; 5 5(4): 561-85.
11. Reed TT. Lipid peroxidation and neurodegenerative disease. Free Radic Biol Med. 2011 Oct 1; 51 (7): 1302-19.
12. Dizdaroglu M, Jaruga P. Mechanisms of free radical-induced damage to DNA. Free Radic Res. 2012 Apr;46(4):382-419.
13. Cadenas E, Davies KJ. Mitochondrial free radical generation, oxidative stress, and aging. Free Radic Biol Med. 2000 Aug; 29(3-4): 222-30.
14. Handy DE, Loscalzo J. Redox regulation of mitochondrial function. Antioxid Redox Signal. 2012 Jun 1;16 (11):1323-67.
15. Kuznetsov AV, Kehrer I, Kozlov AV, Haller M, Redl H, Hermann M, Grimm M, Troppmair J. Mitochondrial ROS production under cellular stress: comparison of different detection methods. Anal Bioanal Chem. 2011 Jun; 400(8): 2383-90.
16. Bellance N, Lestienne P, Rossignol R. Mitochondria: from bioenergetics to the metabolic regulation of carcinogenesis. Front Biosci. 2009 Jan 1; 14:4015-34.
17. Karbowski M, Neutzner A. Neurodegeneration as a consequence of failed mitochondrial maintenance. Acta Neuropathol. 2012 Feb; 123(2): 157-71.
18. Ago T, Kuroda J, Kamouchi M, Sadoshima J, Kitazono T. Pathophysiological roles of NADPH oxidase/nox family proteins in the vascular system. -Review and perspective. Circ J. 2011; 75(8):1791-800.
19. Apel K, Hirt H. Reactive oxygen species: metabolism, oxidative stress, and signal transduction. Annu Rev Plant Biol. 2004; 55:373-99.
20. Fuhua P, Xuhui D, Zhiyang Z, Ying J, Yu Y, Feng T, Jia L, Lijia G, Xueqiang H. Antioxidant status of bilirubin and uric acid in patients with myasthenia gravis. Neuroimmunomodulation. 2012; 19(1): 43-9.

21. Floyd RA. Neuroinflammatory processes are important in neurodegenerative diseases: an hypothesis to explain the increased formation of reactive oxygen and nitrogen species as major factors involved in neurodegenerative disease development. Free Radic Biol Med. 1999 May; 26(9-10): 1346-55.
22. Weisel RD, Mickle DA, Finkle CD, Tumiati LC, Madonik MM, Ivanov J, Burton GW, Ingold KU. Myocardial free-radical injury after cardioplegia. Circulation. 1989 Nov; 80(5 Pt 2):III14-8.
23. Kehrer JP. Free radicals as mediators of tissue injury and disease. Crit Rev Toxicol. 1993; 23(1): 21-48. Review.
24. Dröge W. Aging-related changes in the thiol/disulfide redox state: implications for the use of thiol antioxidants. Exp Gerontol. 2002 Dec; 37(12): 1333-45. Review.
25. M. G. Nikolaidis, A. Z. Jamurtas, "Blood as a reactive species generator and redox status regulator during exercise," Archives of Biochemistry and Biophysics, vol. 490, pp. 77–84, 2009.
26. Banerjee AK, Mandal A, Chanda D, Chakraborti S. Oxidant, antioxidant and physical exercise. Mol Cell Biochem. 2003 Nov; 253(1-2):307-12.
27. Sen CK. Oxidants and antioxidants in exercise. J Appl Physiol. 1995 Sep; 79(3): 675-86.
28. Powers SK, Jackson MJ. Exercise-induced oxidative stress: cellular mechanisms and impact on muscle force production. Physiol Rev. 2008 Oct; 88(4):1243-76. Review.
29. Blennow G, Nilsson B, Siesjö BK. Influence of reduced oxygen availability on cerebral metabolic changes during bicuculline-induced seizures in rats. J Cereb Blood Flow Metab. 1985 Sep; 5(3): 439-45.
30. Quindry JC, Stone WL, King J, Broeder CE. The effects of acute exercise on neutrophils and plasma oxidative stress. Med Sci Sports Exerc. 2003 Jul; 35(7): 1139-45.
31.Tauler P, Aguiló A, Guix P, Jiménez F, Villa G, Tur JA, Córdova A, Pons A. Pre-exercise antioxidant enzyme activities determine the antioxidant enzyme erythrocyte response to exercise. J Sports Sci. 2005 Jan; 23(1): 5-13.
32. Sureda A, Ferrer MD, Tauler P, Maestre I, Aguiló A, Córdova A, Tur JA, Roche E, Pons A. Intense physical activity enhances neutrophil antioxidant enzyme gene expression. Immunocytochemistry evidence for catalase secretion. Free Radic Res. 2007 Aug; 41(8): 874-83.
33. Sureda A, Ferrer MD, Tauler P, Romaguera D, Drobnic F, Pujol P, Tur JA, Pons A. Effects of exercise intensity on lymphocyte H2O2 production and antioxidant defences in soccer players. Br J Sports Med. 2009 Mar; 43(3): 186-90.
34. Kasuya N, Kishi Y, Sakita SY, Numano F, Isobe M. Acute vigorous exercise primes enhanced NO release in human platelets. Atherosclerosis. 2002 Mar, 161(1): 225-32.
35. Radak Z, Bori Z, Koltai E, Fatouros IG, Jamurtas AZ, Douroudos II, Terzis G, Nikolaidis MG, Chatzinikolaou A, Sovatzidis A, Kumagai S, Naito H, Boldogh I. Age-dependent changes in 8-oxoguanine-DNA glycosylase activity are modulated by adaptive responses to physical exercise in human skeletal muscle. Free Radic Biol Med. 2011 Jul 15; 51(2): 417-23.
36. Gautier E, Arnaud C, Bäck M, Pépin JL, Petri MH, Baguet JP, Tamisier R, Lévy P, Stanke-Labesque F. Intermittent hypoxia activated cyclooxygenase pathway: role in atherosclerosis. Eur Respir J. 2012 Oct 11.

37. Bailey DM, Taudorf S, Berg RM, Lundby C, McEneny J, Young IS, Evans KA, James PE, Shore A, Hullin DA, McCord JM, Pedersen BK, Möller K. Increased cerebral output of free radicals during hypoxia: implications for acute mountain sickness? Am J Physiol Regul Integr Comp Physiol. 2009 Nov; 297(5): R1283-92.
38. Faoro V, Fink B, Taudorf S, Dehnert C, Berger MM, Swenson ER, Bailey DM, Bärtsch P, Mairbäurl H. Acute in vitro hypoxia and high-altitude (4,559 m) exposure decreases leukocyte oxygen consumption. Am J Physiol Regul Integr Comp Physiol. 2011 Jan; 300(1): R32-9.
39. Bailey DM, Ainslie PN, Jackson SK, Richardson RS, Ghatei M. Evidence against redox regulation of energy homoeostasis in humans at high altitude. Clin Sci (Lond). 2004 Dec; 107(6): 589-600.
40. Cerretelli P, Gelfi C. Energy metabolism in hypoxia: reinterpreting some features of muscle physiology on molecular grounds. Eur J Appl Physiol. 2011 Mar; 111(3):421-32. Review.
41. Gelfi C, Vasso M, Cerretelli P. Diversity of human skeletal muscle in health and disease: contribution of proteomics. J Proteomics. 2011 May 16; 74(6): 774-95. Review.
42. DeLorey DS, Kowalchuk JM, Paterson DH. Relationship between pulmonary O2 uptake kinetics and muscle deoxygenation during moderate-intensity exercise. J Appl Physiol. 2003 Jul; 95(1): 113-20.
43. Hendgen-Cotta UB, Kelm M, Rassaf T. A highlight of myoglobin diversity: the nitrite reductase activity during myocardial ischemia-reperfusion. Nitric Oxide. 2010 Feb 15; 22(2): 75-82.
44. Ordway GA, Garry DJ. Myoglobin: an essential hemoprotein in striated muscle. J Exp Biol. 2004 Sep; 207(Pt 20): 3441-6.
45. Pellam JR, Harker D.Nobel Awards--Physics and Chemistry. Science. 1962 Nov 9; 138(3541): 667-9.
46. Brunori M, Bourgeois D, Vallone B. The structural dynamics of myoglobin. J Struct Biol. 2004 Sep; 147(3): 223-34.
47. Frauenfelder H, McMahon BH, Fenimore PW. Myoglobin: the hydrogen atom of biology and a paradigm of complexity. Proc Natl Acad Sci U S A. 2003 Jul 22; 100(15):8615-7. Review.
48. Kendrew JC, Dickerson RE, Strandberg BE, Hart RG, Davies DR, Phillips Dc, Shore VC.Structure of myoglobin: A three-dimensional Fourier synthesis at 2 A. resolution. Nature. 1960 Feb 13; 185(4711): 422-7.
49. John C Kendrew. Myoglobin and the structure of proteins. Nobel Lecture, December 11, 1962.
50. Wittenberg BA, Wittenberg JB. Transport of oxygen in muscle. Annu Rev Physiol. 1989; 51:857-78.
51. Kooyman GL, Ponganis PJ. The physiological basis of diving to depth: birds and mammals. Annu Rev Physiol. 1998; 60:19-32.
52. http://www.uniprot.org
53. Cossins AR, Williams DR, Foulkes NS, Berenbrink M, Kipar. A Diverse cell-specific expression of myoglobin isoforms in brain, kidney, gill and liver of the hypoxia-tolerant carp and zebrafish. J Exp Biol. 2009 Mar; 212(Pt 5): 627-38.
54. Gelfi C, De Palma S, Ripamonti M, Eberini I, Wait R, Bajracharya A, Marconi C, Schneider A, Hoppeler H, Cerretelli P.New aspects of altitude adaptation in Tibetans: a proteomic approach. FASEB J. 2004 Mar;18(3):612-4.

55. Kristiansen G, Hu J, Wichmann D, Stiehl DP, Rose M, Gerhardt J, Bohnert A, ten Haaf A, Moch H, Raleigh J, Varia MA, Subarsky P, Scandurra FM, Gnaiger E, Gleixner E, Bicker A, Gassmann M, Hankeln T, Dahl E, Gorr TA.Endogenous myoglobin in breast cancer is hypoxia-inducible by alternative transcription and functions to impair mitochondrial activity: a role in tumor suppression? J Biol Chem. 2011 Dec 16; 286 (50): 43417-28.
56. Techdoc Rep SAN TDR USAF Sch Aerosp Med. 1962 Nov; SAM-TDR-62-89: 8p.
57. Brunori M. Nitric oxide, cytochrome-c oxidase and myoglobin. Trends Biochem Sci. 2001Jan; 26(1): 21-3.
58. Shiva S, Huang Z, Grubina R, Sun J, Ringwood LA, MacArthur PH, Xu X, Murphy E, Darley-Usmar VM, Gladwin MT. Deoxymyoglobin is a nitrite reductase that generates nitric oxide and regulates mitochondrial respiration. Circ Res. 2007 Mar 16; 100(5): 654-61.
59. Liu Q, Gross SS. Binding sites of nitric oxide synthases. Methods Enzymol.1996; 268:311-24.
60. Knowles RG, Moncada S. Nitric oxide synthases in mammals. Biochem J. 1994 Mar 1; 2 98 (Pt 2): 249-58.
61. S. Mitochondria as metabolizers and targets of nitrite. Nitric Oxide. 2010 Feb 15; 22(2): 64-74.
62. Totzeck M, Hendgen-Cotta UB, Rammos C, Petrescu AM, Meyer C, Balzer J, Kelm M, Rassaf T. Assessment of the functional diversity of human myoglobin. Nitric Oxide. 2012 May 15; 26(4): 211-6.
63. Chen Q, Moghaddas S, Hoppel CL, Lesnefsky EJ. Reversible blockade of electron transport during ischemia protects mitochondria and decreases myocardial injury following reperfusion. J Pharmacol Exp Ther. 2006 Dec; 319(3): 1405-12.
64. Rassaf T, Flögel U, Drexhage C, Hendgen-Cotta U, Kelm M, Schrader J. Nitrite reductase function of deoxymyoglobin: oxygen sensor and regulator of cardiac energetics and function. Circ Res. 2007 Jun 22; 100(12): 1749-54.
65. Huang Z, Shiva S, Kim-Shapiro DB, Patel RP, Ringwood LA, Irby CE, Huang KT, Ho C, Hogg N, Schechter AN, Gladwin MT. Enzymatic function of hemoglobin as a nitrite reductase that produces NO under allosteric control. J Clin Invest. 2005 Aug; 115(8): 2099-107.
66. Antonini E, Rossi-Fanelli A. Heterogeneity of human myoglobin. Arch Biochem Biophys. 1956 Dec; 65(2): 587-90.
67. Rossi-Fanelli A, Antonini E. Studies on the oxygen and carbon monoxide equilibria of human myoglobin. Arch Biochem Biophys. 1958 Oct; 77(2): 478-92.
68. Boulton FE, Huntsman RG, Lorkin PA, Lehmann H. Abnormal human myoglobin: 53 (D4) glutamic acid--lysine. Nature. 1969 Aug 23; 223(5208): 832-3.
69. Boulton FE, Huntsman RG, Romero Herrera AE, Lorkin PA, Lehmann H. A human myoglobin variant 133 (H-10) lysine--asparagine. Biochim Biophys Acta. 1971 Mar 23; 229(3): 871-6.
70. Boulton FE, Huntsman RG, Yawson GI, Romero Herrera AE, Lorkin PA, Lehmann H. The second variant of human myoglobin; 138 (H16) arginine leads to glutamine. Br J Haematol. 1971 Jan; 20(1): 69-74.
71. Boulton FE, Huntsman RG, Romero Herrera A, Lorkin PA, Lehmann H. The third variant of human myoglobin showing an unusual amino acid substitution: 138 (H16) arginine--tryptophan. Biochim Biophys Acta. 1971 Mar 23; 229(3): 716-9.

72. Reynafarje B. Myoglobin content and enzymatic activity of muscle and altitude adaptation. J Appl Physiol. 1962 Mar; 17:301-5.
73. Beall CM. Two routes to functional adaptation: Tibetan and Andean high-altitude natives. Proc Natl Acad Sci U S A. 2007 May 15; 104 Suppl 1:8655-60.
74. Bourgeois D, Vallone B, Arcovito A, Sciara G, Schotte F, Anfinrud PA, Brunori M.Extended subnanosecond structural dynamics of myoglobin revealed by Laue crystallography. Proc Natl Acad Sci U S A. 2006 Mar 28; 103(13): 4924-9.
75. Elber R. Ligand diffusion in globins: simulations versus experiment. Curr Opin Struct Biol. 2010 Apr; 20(2): 162-7.
76. Ceccarelli M, Anedda R, Casu M, Ruggerone P. CO escape from myoglobin with metadynamics simulations. Proteins. 2008 May 15; 71(3): 1231-6.
77. Olson JS, Soman J, Phillips GN Jr. Ligand pathways in myoglobin: a review of Trp cavity mutations. IUBMB Life. 2007 Aug-Sep; 59(8-9): 552-62.
78. Perutz MF, Mathews FS. An x-ray study of azide methaemoglobin. J Mol Biol. 1966 Oct 28; 21(1): 199-202.
79. Whitaker TL, Berry MB, Ho EL, Hargrove MS, Phillips GN Jr, Komiyama NH, Nagai K, Olson JS. The D-helix in myoglobin and in the beta subunit of hemoglobin is required for the retention of heme. Biochemistry. 1995 Jul 4; 34(26): 8221-6.
80. Dasmeh P, Kepp KP. Bridging the gap between chemistry, physiology, and evolution: quantifying the functionality of sperm whale myoglobin mutants. Comp Biochem Physiol A Mol Integr Physiol. 2012 Jan; 161(1): 9-17.
81. Gussoni M, MA, Vezzoli A, Anedda R, Greco F, Ceccarelli M, Casu M.Structural characterization of recombinant human myoglobin isoforms by (1)H and (129)Xe NMR and molecular dynamics simulations. Biochim Biophys Acta. 2011 Dec; 1814(12): 1919-29.
82. Scorciapino MA, Robertazzi A, Casu M, Ruggerone P, Ceccarelli M. Breathing motions of a respiratory protein revealed by molecular dynamics simulations. J Am Chem Soc. 2009 Aug 26; 131(33): 11825-32.
83. Scorciapino MA, Robertazzi A, Casu M, Ruggerone P, Ceccarelli M. Heme proteins: the role of solvent in the dynamics of gates and portals. J Am Chem Soc. 2010 Apr 14; 132(14): 5156-63.
84. Ingram DJ, Kendrew JC. Orientation of the haem group in myoglobin and its relation to the polypeptide chain direction. Nature. 1956 Oct 27; 178(4539): 905-6.
85. Kon H. Paramagnetic resonance study of Nitric Oxide hemoglobin. J Biol Chem. 1968 Aug 25; 243(16): 4350-7.
86. Yonetani T, Drott HR, Leigh JS Jr, Reed GH, Waterman MR, Asakura T. Electromagnetic properties of hemoproteins. 3. Electron paramagnetic resonance characteristics of iron (III) and manganese (II) protoporphyrins IX and their apohemoprotein complexes in high spin states. J Biol Chem. 1970 Jun 10; 245(11): 2998-3003.
87. Gerschman R, Gilbert DL, Nye SW, Dwyer P, Fenn WO. Oxygen poisoning and x-irradiation: a mechanism in common. Science. 1954 May 7; 119(3097): 623-6
88. Harman D. The aging process. Proc Natl Acad Sci U S A. 1981 Nov; 78(11): 7124-8.
89. Lorgis L, Zeller M, Dentan G, Sicard P, Richard C, Buffet P, L'Huillier I, Beer JC, Cottin Y, Rochette L, Vergely C. The free oxygen radicals test (FORT) to assess circulating oxidative stress in patients with acute myocardial infarction. Atherosclerosis. 2010 Dec; 213(2): 616-21.

90. Harma MI, Harma M, Erel O. d-ROMs test detects ceruloplasmin, not oxidative stress. Chest. 2006 Oct; 130(4): 1276; author reply 1276-7.
91. Han JY, Takeshita K, Utsumi H. Noninvasive detection of hydroxyl radical generation in lung by diesel exhaust particles. Free Radic Biol Med. 2001 Mar 1; 30(5): 516-25.
92. Berliner LJ, Khramtsov V, Fujii H, Clanton TL. Unique in vivo applications of spin traps. Free Radic Biol Med. 2001 Mar 1; 30(5): 489-99.
93. Holley AE, Cheeseman KH. Measuring free radical reactions in vivo. Br Med Bull. 1993 Jul; 49(3): 494-505.
94. Kohen R, Nyska A. Oxidation of biological systems: oxidative stress phenomena, antioxidants, redox reactions, and methods for their quantification. Toxicol Pathol. 2002 Nov-Dec; 30(6): 620-50.
95. Dalle-Donne I, Rossi R, Colombo R, Giustarini D, Milzani A. Biomarkers of oxidative damage in human disease. Clin Chem. 2006 Apr; 52(4): 601-23.
96. Dalle-Donne I, Rossi R, Giustarini D, Milzani A, Colombo R. Protein carbonyl groups as biomarkers of oxidative stress. Clin Chim Acta. 2003 Mar; 329 (1-2): 23-38.
97. Armstrong D, Browne R. The analysis of free radicals, lipid peroxides, antioxidant enzymes and compounds related to oxidative stress as applied to the clinical chemistry laboratory. Adv Exp Med Biol. 1994; 366:43-58.
98. Nikolaidis MG, Jamurtas AZ. Blood as a reactive species generator and redox status regulator during exercise. Arch Biochem Biophys. 2009 Oct 15; 490(2): 77-84.
99. Singh RK, Tripathi AK, Tripathi P, Singh S, Singh R, Ahmad R. Studies on biomarkers for oxidative stress in patients with chronic myeloid leukemia. Hematol Oncol Stem Cell Ther. 2009; 2(1): 285-8.
100. Bailey DM, Lawrenson L, McEneny J, Young IS, James PE, Jackson SK, Henry RR, Mathieu-Costello O, McCord JM, Richardson RS.Electron paramagnetic spectroscopic evidence of exercise-induced free radical accumulation in human skeletal muscle. Free Radic Res. 2007 Feb; 41(2): 182-90.
101. Sajfutdinov RG, Larina LI, Vakul'skaya TI, Voronkov MG. Electron Paramagnetic Resonance in Biochemistry and Medicine. (2001) New York: Kluwer Academic /Plenum Publishers.
102. Dikalov SI, Dikalova AE, Mason RP. Non invasive diagnostic tool for inflammation-induced oxidative stress using electron spin resonance spectroscopy and an extracellular cyclic hydroxylamine. *Arch Biochem Biophys*. (2002) Jun 15; 402(2): 218-26.
103. Spasojević I. Free radicals and antioxidants at a glance using EPR spectroscopy. Crit Rev Clin Lab Sci. 2011 May-Jun; 48(3): 114-42. Review.
104. Beaver WL, Wasserman K, Whipp BJ. A new method for detecting anaerobic threshold by gas exchange. J Appl Physiol. 1986 Jun; 60(6): 2020-7.
105. Grassi B, Marzorati M, Lanfranconi F, Ferri A, Longaretti M, Stucchi A, Vago P, Marconi C, Morandi L. Impaired oxygen extraction in metabolic myopathies: detection and quantification by near-infrared spectroscopy. Muscle Nerve. 2007 Apr; 35(4): 510-20.
106. Grassi B, Pogliaghi S, Rampichini S, Quaresima V, Ferrari M, Marconi C, Cerretelli P. Muscle oxygenation and pulmonary gas exchange kinetics during cycling exercise on-transitions in humans. J Appl Physiol. 2003 Jul; 95(1): 149-58.

107. Porcelli S, Marzorati M, Lanfranconi F, Vago P, Pisot R, Grassi B. Role of skeletal muscles impairment and brain oxygenation in limiting oxidative metabolism during exercise after bed rest. J Appl Physiol. 2010 Jul; 109(1): 101-11.
108. Kowalchuk JM, Rossiter HB, Ward SA, Whipp BJ. The effect of resistive breathing on leg muscle oxygenation using near-infrared spectroscopy during exercise in men. Exp Physiol. 2002 Sep; 87(5): 601-11.
109. Borg GA. Perceived exertion: a note on "history" and methods. Med Sci Sports. 1973 Summer; 5(2): 90-3.
110. ICH Harmonised Tripartite Guideline: “Validation on Analytical Procedures: Text and [Methodology”, (R1), Step 4, 2005.
111. Sachdev S, Davies KJ. Production, detection, and adaptive responses to free radicals in exercise. Free Radic Biol Med. 2008 Jan 15;44(2): 215-23.
112. A. S. Veskoukis, M. G. Nikolaidis, A. Kyparos, D. Kouretas, “Blood reflects tissue oxidative stress depending on biomarker and tissue studied,” Free Radical Biology and Medicine, vol. 47, pp. 1371–1374, 2009.
113. I. Ginsburg, R. Kohen, E. Koren, “Quantifying Oxidant-Scavenging Ability of Blood,” New England Journal of Medicine, vol. 364, p. 9, 2011.
114. Dikalov SI, Kirilyuk IA, Voinov M, Grigor'ev IA. EPR detection of cellular and mitochondrial superoxide using cyclic hydroxylamines. Free Radic Res. 2011 Apr; 45(4): 417-30.
115. Zielonka J, Zhao H, Xu Y, Kalyanaraman B. Mechanistic similarities between oxidation of hydroethidine by Fremy's salt and superoxide: stopped-flow optical and EPR studies. Free Radic Biol Med. 2005 Oct 1; 39(7):853-63.
116. Davies KJ, Quintanilha AT, Brooks GA, Packer L. Free radicals and tissue damage produced by exercise. Biochem Biophys Res Commun. 1982 Aug 31; 107(4): 1198-205
117. Jackson MJ, Edwards RH, Symons MC. Electron spin resonance studies of intact mammalian skeletal muscle. Biochim Biophys Acta. 1985 Nov 20; 847(2): 185-90
118. Richardson RS, Donato AJ, Uberoi A, Wray DW, Lawrenson L, Nishiyama S, Bailey DM. Exercise-induced brachial artery vasodilation: role of free radicals. Am J Physiol Heart Circ Physiol. 2007 Mar; 292(3): H1516-22.
119. Ji LL. Antioxidants and oxidative stress in exercise. Proc Soc Exp Biol Med. 1999 Dec; 222(3): 283-92.
120. Jenkins RR.Free radical chemistry. Relationship to exercise. Sports Med. 1988 Mar; 5(3): 156-70.
121. Cooper CE, Vollaard NB, Choueiri T, Wilson MT.Exercise, free radicals and oxidative stress. Biochem Soc Trans. 2002 Apr; 30(2): 280-5
122. Heunks LM, Viña J, van Herwaarden CL, Folgering HT, Gimeno A, Dekhuijzen PN. Xanthine oxidase is involved in exercise-induced oxidative stress in chronic obstructive pulmonary disease. Am J Physiol. 1999 Dec; 277(6 Pt 2): R1697-704.
123. Hellsten Y. Xanthine dehydrogenase and purine metabolism in man. With special reference to exercise. Acta Physiol Scand Suppl. 1994; 621:1-73.
124.Paolini M, Valgimigli L, Marchesi E, Trespidi S, Pedulli GF Taking EPR "snapshots" of the oxidative stress status in human blood. Free Radic Res. 2003 May; 37(5): 503-8.

125. Bailey DM, Young IS, McEneny J, Lawrenson L, Kim J, Barden J, Richardson RS.Regulation of free radical outflow from an isolated muscle bed in exercising humans. Am J Physiol Heart Circ Physiol. 2004 Oct; 287(4): H1689-99.
126. Michailidis Y, Jamurtas AZ, Nikolaidis MG, Fatouros IG, Koutedakis Y, Papassotiriou I, Kouretas D. Sampling time is crucial for measurement of aerobic exercise-induced oxidative stress. Med Sci Sports Exerc. 2007 Jul; 39(7): 1107-13.
127. Waring WS, Convery A, Mishra V, Shenkin A, Webb DJ, Maxwell SR. Uric acid reduces exercise-induced oxidative stress in healthy adults. Clin Sci (Lond). 2003 Oct; 105(4): 425-30.
128. Watson TA, Callister R, Taylor RD, Sibbritt DW, MacDonald-Wicks LK, Garg ML. Antioxidant restriction and oxidative stress in short-duration exhaustive exercise. Med Sci Sports Exerc. 2005 Jan; 37(1): 63-71.
129. Echtay KS, Esteves TC, Pakay JL, Jekabsons MB, Lambert AJ, Portero-Otín M, Pamplona R, Vidal-Puig AJ, Wang S, Roebuck SJ, Brand MD. A signalling role for 4-hydroxy-2-nonenal in regulation of mitochondrial uncoupling. EMBO J. 2003 Aug 15; 22(16): 4103-10.
130. Alessio HM, Hagerman AE, Fulkerson BK, Ambrose J, Rice RE, Wiley RL.Generation of reactive oxygen species after exhaustive aerobic and isometric exercise. Med Sci Sports Exerc. 2000 Sep;32(9):1576-81.
131. Bloomer RJ, Davis PG, Consitt LA, Wideman L. Plasma protein carbonyl response to increasing exercise duration in aerobically trained men and women. Int J Sports Med. 2007 Jan; 28(1): 21-5.
132. Bloomer RJ, Goldfarb AH, McKenzie MJ.Oxidative stress response to aerobic exercise: comparison of antioxidant supplements. Med Sci Sports Exerc. 2006 Jun; 38(6): 1098-105.
133. Groussard C, Rannou-Bekono F, Machefer G, Chevanne M, Vincent S, Sergent O, Cillard J, Gratas-Delamarche A. Changes in blood lipid peroxidation markers and antioxidants after a single sprint anaerobic exercise. Eur J Appl Physiol. 2003 Mar; 89(1): 14-20.
134. Jenkins RR. Exercise and oxidative stress methodology: a critique. Am J Clin Nutr. 2000 Aug; 72(2 Suppl): 670S-4S.
135. Vollaard NB, Shearman JP, Cooper CE. Exercise-induced oxidative stress:myths, realities and physiological relevance. Sports Med. 2005; 35(12):1045-62.
136. Kanter M. Free radicals, exercise and antioxidant supplementation. Proc Nutr Soc. 1998 Feb; 57(1): 9-13. Review.
137. Liu JF, Chang WY, Chan KH, Tsai WY, Lin CL, Hsu MC. Blood lipid peroxides and muscle damage increased following intensive resistance training of female weightlifters. Ann N Y Acad Sci. 2005 May; 1042:255-61
138. Carmeli E, Coleman R, Reznick AZ. The biochemistry of aging muscle. Exp Gerontol. 2002 Apr; 37(4):477-89. Review.
139. Bentley DJ, Millet GP, Vleck VE, McNaughton LR. Specific aspects of contemporary triathlon: implications for physiological analysis and performance. Sports Med. 2002; 32(6):345-59. Review.
140. Nieman DC. Exercise, upper respiratory tract infection, and the immune system. Med Sci Sports Exerc. 1994 Feb; 26(2): 128-39.
141. Purvis D, Gonsalves S, Deuster PA.Physiological and psychological fatigue in extreme conditions: overtraining and elite athletes. PM R. 2010 May;2(5):442-50. Review.

142. Yu HH, Ginsburg GS, O'Toole ML, Otvos JD, Douglas PS, Rifai N. Acute changes in serum lipids and lipoprotein subclasses in triathletes as assessed by proton nuclear magnetic resonance spectroscopy. Arterioscler Thromb Vasc Biol. 1999 Aug; 19(8): 1945-9.
143. Brites F, Zago V, Verona J, Muzzio ML, Wikinski R, Schreier L. HDL capacity to inhibit LDL oxidation in well-trained triathletes. Life Sci. 2006 May 22; 78(26): 3074-81.
144. Clanton TL, Klawitter PF. Invited review: Adaptive responses of skeletal muscle to intermittent hypoxia: the known and the unknown. J Appl Physiol. 2001 Jun; 90(6): 2476-87.
145. Ameln H, Gustafsson T, Sundberg CJ, Okamoto K, Jansson E, Poellinger L, Makino Y.Physiological activation of hypoxia inducible factor-1 in human skeletal muscle. FASEB J. 2005 Jun; 19(8): 1009-11.
146. Vogt M, Puntschart A, Geiser J, Zuleger C, Billeter R, Hoppeler H. Molecular adaptations in human skeletal muscle to endurance training under simulated hypoxic conditions. J Appl Physiol. 2001 Jul; 91(1): 173-82.
147. Margonis K, Fatouros IG, Jamurtas AZ, Nikolaidis MG, Douroudos I, Chatzinikolaou A, Mitrakou A, Mastorakos G, Papassotiriou I, Taxildaris K, Kouretas D. Oxidative stress biomarkers responses to physical overtraining: implications for diagnosis. Free Radic Biol Med. 2007 Sep 15; 43(6): 901-10.
148. Radak Z, Zhao Z, Koltai E, Ohno H, Atalay M. Oxygen Consumption and Usage During Physical Exercise: The Balance Between Oxidative Stress and ROS-Dependent Adaptive Signaling. Antioxid Redox Signal. 2012 Nov 16.
149. Gulati M, Pandey DK, Arnsdorf MF, Lauderdale DS, Thisted RA, Wicklund RH, Al-Hani AJ, Black HR. Exercise capacity and the risk of death in women: the St James Women Take Heart Project. Circulation. 2003 Sep 30; 108(13): 1554-9.
150. Clanton TL. Hypoxia-induced reactive oxygen species formation in skeletal muscle. J Appl Physiol. 2007 Jun; 102(6): 2379-88. Review.
151. Martinelli M, Winterhalder R, Cerretelli P, Howald H, Hoppeler H. Muscle lipofuscin content and satellite cell volume is increased after high altitude exposure in humans. Experientia. 1990 Jul 15; 46(7): 672-6.
152. Magalhães J, Ascensão A, Soares JM, Ferreira R, Neuparth MJ, Marques F, Duarte JA. Acute and severe hypobaric hypoxia increases oxidative stress and impairs mitochondrial function in mouse skeletal muscle. J Appl Physiol. 2005 Oct; 99(4): 1247-53.
153. Koechlin C, Maltais F, Saey D, Michaud A, LeBlanc P, Hayot M, Préfaut C. Hypoxaemia enhances peripheral muscle oxidative stress in chronic obstructive pulmonary disease. Thorax. 2005 Oct; 60(10): 834-41.
154. Steiner DR, Gonzalez NC, Wood JG. Interaction between reactive oxygen species and nitric oxide in the microvascular response to systemic hypoxia. J Appl Physiol. 2002 Oct; 93(4): 1411-8.
155. Mishra A, Ali Z, Vibhuti A, Kumar R, Alam P, Ram R, Thinlas T, Mohammad G, Pasha MA.CYBA and GSTP1 variants associate with oxidative stress under hypobaric hypoxia as observed in high-altitude pulmonary oedema. Clin Sci (Lond). 2012 Mar; 122(6): 299-309.
156. Jefferson JA, Simoni J, Escudero E, Hurtado ME, Swenson ER, Wesson DE, Schreiner GF, Schoene RB, Johnson RJ, Hurtado A.Increased oxidative stress following acute and chronic high altitude exposure. High Alt Med Biol. 2004 Spring; 5(1): 61-9.

157: Bailey DM, Dehnert C, Luks AM, Menold E, Castell C, Schendler G, Faoro V, Gutowski M, Evans KA, Taudorf S, James PE, McEneny J, Young IS, Swenson ER, Mairbäurl H, Bärtsch P, Berger MM. High-altitude pulmonary hypertension is associated with a free radical-mediated reduction in pulmonary nitric oxide bioavailability. J Physiol. 2010 Dec 1; 588(Pt 23): 4837-47.
158. Suzuki YJ, Tsuchiya M, Packer L. Thioctic acid and dihydrolipoic acid are novel antioxidants which interact with reactive oxygen species. Free Radic Res Commun. 1991; 15(5): 255-63.
159. Scott BC, Aruoma OI, Evans PJ, O'Neill C, Van der Vliet A, Cross CE, Tritschler H, Halliwell B. Lipoic and dihydrolipoic acids as antioxidants. A critical evaluation. Free Radic Res. 1994 Feb; 20(2):119-33.
160. Busse E, Zimmer G, Schopohl B, Kornhuber B. Influence of alpha-lipoic acid on intracellular glutathione in vitro and in vivo. Arzneimittelforschung. 1992 Jun; 42(6): 829-31.
161. Seaton TA, Jenner P, Marsden CD. The isomers of thioctic acid alter C-deoxyglucose incorporation in rat basal ganglia. Biochem Pharmacol. 1996 Apr 12; 51(7): 983-6.
162. Yoshihara D, Fujiwara N, Suzuki K. Antioxidants: benefits and risks for long-term health. Maturitas. 2010 Oct; 67(2): 103-7.
163. Davison GW, Ashton T, George L, Young IS, McEneny J, Davies B, Jackson SK, Peters JR, Bailey DM. Molecular detection of exercise-induced free radicals following ascorbate prophylaxis in type 1 diabetes mellitus: a randomised controlled trial. Diabetologia. 2008 Nov; 51(11):2049-59.
164. Lee DH, Gold R, Linker RA. Mechanisms of Oxidative Damage in Multiple Sclerosis and Neurodegenerative Diseases: Therapeutic Modulation via Fumaric Acid Esters. Int J Mol Sci. 2012; 13(9): 11783-803. doi: 10.3390/ijms130911783
165. Barber SC, Mead RJ, Shaw PJ.Oxidative stress in ALS: a mechanism of neurodegeneration and a therapeutic target. Biochim Biophys Acta. 2006 Nov-Dec; 1762(11-12): 1051-67.
166. de Lemos ET, Oliveira J, Pinheiro JP, Reis F. Regular physical exercise as a strategy to improve antioxidant and anti-inflammatory status: benefits in type 2 diabetes mellitus. Oxid Med Cell Longev. 2012; 2012:741545. doi: 10.1155/2012/741545.
167. Ford I, Cotter MA, Cameron NE, Greaves M. The effects of treatment with alpha-lipoic acid or evening primrose oil on vascular hemostatic and lipid risk factors, blood flow, and peripheral nerve conduction in the streptozotocin-diabetic rat. Metabolism. 2001 Aug; 50(8): 868-75.
168. Altavilla D, Saitta A, Cucinotta D, Galeano M, Deodato B, Colonna M, Torre V, Russo G, Sardella A, Urna G, Campo GM, Cavallari V, Squadrito G, Squadrito F. Inhibition of lipid peroxidation restores impaired vascular endothelial growth factor expression and stimulates wound healing and angiogenesis in the genetically diabetic mouse. Diabetes. 2001 Mar; 50(3): 667-74.
169. Zhang Z, Yan J, Chang Y, ShiDu Yan S, Shi H.Hypoxia inducible factor-1 as a target for neurodegenerative diseases. Curr Med Chem. 2011; 18(28): 4335-43.
170. Barber SC, Shaw PJ.Oxidative stress in ALS: key role in motor neuron injury and therapeutic target. Free Radic Biol Med. 2010 Mar 1; 48(5): 629-41.
171. Bonnefont-Rousselot D, Lacomblez L, Jaudon M, Lepage S, Salachas F, Bensimon G, Bizard C, Doppler V, Delattre J, Meininger V.Blood oxidative stress in amyotrophic lateral sclerosis. J Neurol Sci. 2000 Sep 1; 178(1): 57-62.

172. de Almeida JP, Silvestre R, Pinto AC, de Carvalho M. Exercise and amyotrophic lateral sclerosis. Neurol Sci. 2012 Feb; 33(1): 9-15. doi: 10.1007/s10072-011-0921-9. Review.
173. Marconi C, Marzorati M, Sciuto D, Ferri A, Cerretelli P.Economy of locomotion in high-altitude Tibetan migrants exposed to normoxia. J Physiol. 2005 Dec 1; 569(Pt 2): 667-75.
174. Erzurum SC, Ghosh S, Janocha AJ, Xu W, Bauer S, Bryan NS, Tejero J, Hemann C, Hille R, Stuehr DJ, Feelisch M, Beall CM.Higher blood flow and circulating NO products offset high-altitude hypoxia among Tibetans. Proc Natl Acad Sci U S A. 2007 Nov 6; 104(45): 17593-8.
175. Kayser B, Hoppeler H, Desplanches D, Marconi C, Broers B, Cerretelli P. Muscle ultrastructure and biochemistry of lowland Tibetans. J Appl Physiol. 1996 Jul; 81(1): 419-25.
176. Shiva S. Mitochondria as metabolizers and targets of nitrite. Nitric Oxide. 2010 Feb 15; 22(2): 64-74.
177. Hendgen-Cotta UB, Flögel U, Kelm M, Rassaf T. Unmasking the Janus face of myoglobin in health and disease. J Exp Biol. 2010 Aug 15; 213(Pt 16): 2734-40.
178. Yonetani T, Yamamoto H, Erman JE, Leigh JS Jr, Reed GH. Electromagnetic properties of hemoproteins. V. Optical and electron paramagnetic resonance characteristics of nitric oxide derivatives of metalloporphyrin-apohemoprotein complexes. J Biol Chem. 1972 Apr 25; 247(8): 2447-55.

SCIENTIFIC PRODUCTION RELATIVE TO THE PRESENT WORK

1. Scorciapino MA, Spiga E, Vezzoli A, Mrakic-Sposta S, Russo R, Fink B, Mariano Casu M, Gussoni M, Matteo Ceccarelli M. STRUCTURE-FUNCTION PARADIGM IN HUMAN MYOGLOBIN: HOW A SINGLE-RESIDUE SUBSTITUTION MODULATES NO AFFINITY AT LOW PO_2. Submitted, December 2012

2. Mrakic Sposta S, Porcelli S, Bellistri G, Montorsi M, Gussoni M, Vezzoli A. EXERCISE AND TRAINING EFFECTS IN SWIMMERS: ROS PRODUCTION PROFILE BY ELECTRON PARAMAGNETIC RESONANCE (EPR). Acta Physiologica 2012 Sep (206) Suppl 692: 141. IF: 3.09

3. Vezzoli A, Mrakic Sposta S, Montorsi M, Russo R, Casu M, Scorciapino MA, Ceccarelli M, Gussoni M. THE ROLE OF HUMAN MYOGLOBIN ISOFORMS AS NITRIC OXIDE SCAVENGER UNDER HYPOXIA THROUGHOUT AN ELECTRON PARAMAGNETIC RESONANCE STUDY. Acta Physiologica 2012 Sep (206) Suppl 692: 204. IF: 3.09

4. Mrakic-Sposta S, Gussoni G, Montorsi M, Porcelli S, Vezzoli A, Marconi C, Cerretelli P. EFFECTS OF ACUTE OR CHRONIC HYPOXIA ON REACTIVE OXYGEN SPECIES PRODUCTION ASSESSED BY ELECTRON PARAMAGNETIC RESONANCE Atti del congresso – XXIII World Congress of Sports Medicine. 27-30 Settembre 2012

5. Mrakic-Sposta S, Gussoni M, Montorsi M, Porcelli S, Vezzoli A. ASSESSMENT OF A STANDARDIZED ROS PRODUCTION PROFILE IN HUMANS BY ELECTRON PARAMAGNETIC RESONANCE. Oxid Med Cell Longev. 2012;2012:973927. IF: 2.841

6. Vezzoli A, Gussoni M, Mrakic-Sposta S, Porcelli S, Montorsi M, Marconi C, Cerretelli P. ASSESSMENT OF A STANDARDIZED ROS PRODUCTION PROFILE IN HUMANS BY ELECTRON PARAMAGNETIC RESONANCE (EPR). Acta Physiologica 2011 Sept (203) Suppl 688: 69. IF: 3.09

ACKNOWLEDGMENTS

This presents an opportunity to show my deepest appreciation to various individuals who have guided, encouraged and inspired me throughout the course of this PhD studies.

Firstly, I would like to express my gratitude to my Tutor of Studies, ***Dott.ssa Maristella Gussoni***, for initially giving me the opportunity to undertake a PhD and more importantly for always believing in my capabilities. Her "global view" of science and life helped me to approach my job with a different and better mental outlook. Thank you also for whose encouragement, personal guidance, your enthusiastic supervision and support from the initial to the final level of this PhD Thesis.

Secondly, I wish to thank to my Co-Tutor of studies ***Dott.ssa Alessandra Vezzoli*** for her detailed and constructive comments and for her important support throughout this work.

Now, I want to thank the members of the CNR-IBFM of Milan: Prof. Paolo Cerretelli, Dott. Claudio Marconi, Dott. Mauro Marzorati, Dott. Simone Porcelli and Dott.ssa Michela Montorsi. who accepted me into their laboratories.

My sincere thanks are due to:

- Dott. Luca Maderna and Dott.ssa Francesca Gregorini (Istituto Auxologico Milano)
- Dott. Alessandro Mezzani (Fondazione Maugeri Veruno – Novara)
- Dott.ssa Lorenza Pratali (CNR-IFC Pisa)

for our collaboration in the projects.

I would you like to thank Dott. Bruno Fink, Dott.ssa. Manuela Liberi and Dott. Roberto Melzi of Bruker Biospin for their kind technical support

I want thank the Italian Federation of Sport Medicine

My special acknowledgements go to all those people who made the studies possible: all subjects, all athletes and in particular all patients.

This thesis would not have been possible without the support, critiques, the questions and the remarkable patience of the above. Thank you all once again.